



저작자표시-비영리-변경금지 2.0 대한민국

이용자는 아래의 조건을 따르는 경우에 한하여 자유롭게

- 이 저작물을 복제, 배포, 전송, 전시, 공연 및 방송할 수 있습니다.

다음과 같은 조건을 따라야 합니다:



저작자표시. 귀하는 원저작자를 표시하여야 합니다.



비영리. 귀하는 이 저작물을 영리 목적으로 이용할 수 없습니다.



변경금지. 귀하는 이 저작물을 개작, 변형 또는 가공할 수 없습니다.

- 귀하는, 이 저작물의 재이용이나 배포의 경우, 이 저작물에 적용된 이용허락조건을 명확하게 나타내어야 합니다.
- 저작권자로부터 별도의 허가를 받으면 이러한 조건들은 적용되지 않습니다.

저작권법에 따른 이용자의 권리는 위의 내용에 의하여 영향을 받지 않습니다.

이것은 [이용허락규약\(Legal Code\)](#)을 이해하기 쉽게 요약한 것입니다.

[Disclaimer](#)



A Doctoral Dissertation

Cause and Cure for unusual p22phox deficient Chronic Granulomatous Disease on Jeju Island : Therapeutic vector design and New mechanism for superoxide mediated EMT

Department of Medicine

GRADUATE SCHOOL

JEJU NATIONAL UNIVERSITY

Young Mee Kim

February, 2012








제주도내 p22phox관련 만성육아종질환 원인과 치료에 따른 therapeutic virus 디자인 그리고 superoxide에 의한 EMT 유도연구

지도교수 조 문 제
김 영 미

이 논문을 의학 박사학위 논문으로 제출함

2012년 2월

김영미의 의학 박사학위 논문을 인준함

심사위원장	<u>박 덕 배</u>	
위 원	<u>이 정 원</u>	
위 원	<u>고 영 상</u>	
위 원	<u>신 경 수</u>	
위 원	<u>조 문 제</u>	

제주대학교 대학원

2012년 2월



Cause and Cure for unusual p22phox deficient Chronic Granulomatous Disease on Jeju Island : Therapeutic vector design and New mechanism for superoxide mediated EMT

Young Mee Kim
(Supervised by Professor **Moon Jae Cho**)

A thesis submitted in partial fulfillment of the requirement for degree of doctor of philosophy in Medicine

Date Approved:

2012.2

DeokAE PARK
[Signature]
[Signature]
[Signature]
[Signature]

Department of Medicine
Graduate School, Jeju National University
February, 2012



CONTENTS

CONTENS	i
LIST OF TABLES	v
LIST OF FIGURES	vi

I . PART I. NADPH oxidase NOX 2 is responsible for mediated EMT signaling in HeLa cells	1
1. ABSTRACT	2
2. INTRODUCTION	3
3. MATERIALS AND METHODS	7
3.1. Cell culture and transfection	7
3.2. Western blots and antibodies	7
3.3. RT-PCR analysis	8
3.4. Plasmid construction	8
3.5. NADPH Oxidase Assay	9
3.6. Gelatin Zymography	10
3.7. In vitro wound healing assay	10
4. RESULTS	13
4.1. p40phox expression and ROS generation during TGF- β 1-induced EMT	
4.2. Localization of the full-length p40phox in transfected cells	18
4.3. Introduction of p40phox gene induced NADPH oxidase 2 (NOX 2) subunits and enzymes involved in homeosis of creative oxygen sepsis (ROS)	
.....	23



4.4. Overexpression of p40phox induced cell growth rate increase and reduced of p21 and p27	26
4.5. Activation of matrix metalloproteinase by over-expression of p40phox in HeLa cells involved reactive oxygen species	29
4.6. ROS mediate p40phox induced EMT	33
4.7. p40phox mediated YB-1 increase through ROS generation	36
4.8. ROS generation induced EMT blocked by inhibitors	37
5. DISCUSSION	41

II. PART II. Genetic Analysis of 10 Unrelated Korean Families with p22-phox deficient Chronic Granulomatous Disease: An Unusually Identical Mutation of the CYBA Gene on Jeju Island, Korea

1. ABSTRACT	2
2. INTRODUCTION.....	53
3. MATERIALS AND METHODS	55
3.1. Patients.....	55
3.2. DHR flow cytometry.....	55
3.3. Western blot analysis of the NADPH oxidase components	56
3.4. Isolation of total RNA and RT-PCR.....	56
3.5. Isolation and amplification of genomic DNA of <i>CYBA</i>	57
3.6. Sequence analysis.....	58
4. RESULTS	59
5. DISCUSSION	65

III. PART III. Survey on the present condition of heterozygote carriers with p22-phox-deficient CGD on Jeju Island, Korea	69
1. ABSTRACT	70
2. INTRODUCTION	72
3. MATERIALS AND METHODS	74
3.1. Study population	74
3.2. Nested PCR amplification of a specific region on p22phox exon 1	74
3.3. Sequence analysis for precision test of heterozygote-specific primers	75
3.4. Data analysis	76
4. RESULTS	77
5. DISCUSSION	86
IV. PART IV. Development of Lentiviral vector and efficient infection method for the gene therapy of p22phox defective CGD	88
1. ABSTRACT	89
2. INTRODUCTION	90
3. MATERIALS AND METHODS	94
3.1. Construction of vectors encoding p22phox	94
3.2. Maintenance of cell culture and transfection	94
3.3. Vector production	94
3.4. Virus titration	95
3.5. Transduction and calculation of the titer in transducing units	95
3.6. Infection of hTERT and Bmi-1 constructs	96
3.7. Induction of differentiation	97
3.8. Dihydrorhodamine 123 FACS quantitation of superoxide production	98
3.9. Isolated WBC (white blood cell)	98



4. RESULTS	100
5. DISCUSSION	116
V. REFERENCES	120
VI. ABSTRACT IN KOREAN	134



LIST OF TABLES

Table 1. Primers used in the study	11
Table 2. Characteristics of CGD patients in <i>Jeju, Korea</i>	60
Table 3. Single nucleotide substitution within the <i>CYBA</i> gene in CGD patients.....	63
Table 4. Characteristics of study population.....	78
Table 5. List of primers used in this study.....	83
Table 6. District distribution of heterozygote carriers and CGD patients.....	84
Table 7. Age distribution of heterozygote carriers.....	85

LIST OF FIGURES

Figure 1.	NOX 2 is involved in ROS production in EMT by TGF-β1	17
Figure 2.	p40phox expression and ROS generation in HeLa and HEK 293T cells	21
Figure 3.	NADPH oxidase 2 subunits and antioxidant enzymes expressed in HeLa-p40phox cells	24
Figure 4.	The effects of p40phox on proliferation of HeLa cell	28
Figure 5.	Regulation of matrix metalloproteinase expression in HeLa-p40phox cells	32
Figure 6.	ROS generation by p40phox induced EMT in HeLa-p40phox cells	35
Figure 7.	Over-expression of superoxide in HeLa cells increased YB-1 expression	38
Figure 8.	Inhibition of MEK/ERK, JNK/p38 MAP kinases and PI3K/AKT pathways ROS induced EMT	40
S1.	Down-regulation of YB-1 by shSLUG	46
S2.	ROS generation at different DNA concentrations in HeLa-p40phox cells	48
S3.	Activation of NADPH oxidase stimulates AA	49
S4.	TGF-β1-induced expression of Nox-2 in different nonphagocytic cells	50
Figure 9.	Dihydrorhodamine-1,2,3 (DHR) flow cytometric analysis of granulocyte oxidative activity in family III	61

Figure 10.	Western blot analysis of NADPH oxidase components in family III.....	62
Figure 11.	RT-PCR of <i>CYBA</i> cDNA from family III.....	63
Figure 12.	Sequence analysis of the <i>CYBA</i> gene from family III.....	64
Figure 13.	Identification of the mutant site by nested PCR for the determination of the p22phox heterozygous carrier.....	80
Figure 14.	We found that the CGD patients the results of sequence analysis of two patients with p22-phox-deficient CGD.....	101
Figure 15.	Schematic diagram of lentiviral vector construction and transduction.....	103
Figure 16.	Transducing efficiency in HeLa cells.....	106
Figure 17.	Transduction efficiency of pLL3.7 EF1a and pLL3.7 EF1a p22phox lentiviral vector in promyelocytic HL60 cells.....	108
Figure 18.	Comparison of transgene expression in WBC (white blood cell) and WBC ^{hTERT+Bmi-1} cells.....	111
Figure 19.	Analysis of superoxide generation before and after differentiation HL 60 with a pLL3.7 EF1a and pLL3.7 EF1a -p22phox.....	115



PART I

NADPH oxidase NOX 2 is responsible for mediated EMT

signaling in HeLa cells

1. ABSTRACT

Epithelium-to-mesenchyme transitions (EMTs) are characterized by morphological and behavioral changes in cells. During an EMT, E-cadherin is down-regulated while snail, slug and vimentin are up-regulated. The goal of this study was to understand the role ROS plays in EMT using a HeLa-p40phox model system: ROS mediated EMT in mammary epithelial cells. We showed that mRNA of NOX 2 and NOX 5 are increased, and with the increased expression of several matrix metalloproteinase (MMPs) in response to ROS. Moreover, these changes were reversible upon removal of ROS. Down-regulation of E-cadherin and up-regulation of snail, slug and vimentin occurred in transcriptional level. Interestingly, TGF- β 1-induced EMT in HeLa cells was significantly increased ROS. Together, these data suggest that ROS switching is necessary for increased EMT but is not required for the morphological changes that accompany EMT.

Key words: TGF- β 1, NADPH oxidase 2 (NOX 2), ROS, EMT

2. INTRODUCTION

Superoxide production by the phagocyte NADPH oxidase during the respiratory burst is an essential component of the innate immune response. The active enzyme is assembled from a membrane-bound flavocytochrome b, a heterodimer composed of gp91phox and p22phox subunits, and cytosolic regulatory components p47phox, p67phox, p40phox, and the Rac GTPase. p40phox is the last NADPH oxidase subunit to be discovered, and although there is evidence of both positive and negative effects on oxidase function, its exact role remains poorly defined. This protein was reported by Wientjes et al.,(1) as a 40 kDa protein which co-purified in a 250 kDa complex with p67phox and p47phox and whose primary association appeared to be with p67phox; furthermore, the amount of this protein was reduced in patients with CGD lacking p67phox. Although the role of p40phox in the NADPH oxidase has been poorly understood (2), recent studies in p40phox-deficient cell lines and in gene targeted mice established that p40phox stimulates. In mice either lacking p40phox or expressing p40phox R58A, a PX domain mutant that prevents binding to PtdIns(3)P, in vitro killing of *Staphylococcus aureus* by neutrophils was reduced to an extent similar to that seen in the complete absence of NADPH oxidase activity, and elimination of *S aureus* after intraperitoneal injection was impaired (3, 4, 5). In contrast, PtdIns(3)P binding to p40phox plays a minimal, if any, role in regulating superoxide release elicited by the chemoattractant

formyl-methionyl-leucyl-phenylalanine (fMLF) or phorbol ester (6).

The p40phox polypeptide is encoded by NCF4 (Neutrophil Cytosolic Factor 4) gene on 22q13.1 chromosome (7). It is predominantly expressed in bone marrow cells: neutrophils, monocytes, basophils, eosinophils, mast cells, megakaryocytes, B and T cells (8, 9). Northern and western blot analyses in bone marrow cells or in HL-60 differentiated to neutrophils and eosinophils revealed that mRNA and protein for p40phox were expressed by the promyelocyte stage together with p22phox and Rac2, whereas mRNA and proteins for gp91phox, p67phox and p47phox were expressed after the myelocyte stage (10). This finding suggests that, although in mature neutrophils p40phox needs p67phox for stable expression, based on studies of CGD patients lacking p67phox, in other cells, p40phox can be stably present alone (11). Northern blot analysis has revealed that two sizes of p40phox mRNAs are present in human promyelocytic HL-60 and bone marrow cells. One is identical to the originally described p40phox cDNA. The other alternatively spliced variant cDNA (1299 bp) contains an additional 245 bp intron 8 sequence in the open reading frame and encodes a protein of 348 residues (39 kDa). The C-terminal 254– 348 residues of the variant protein shares a low homology with p40phox, and, interestingly, this variant protein lacks the PB1 domain (Phagocyte oxidase and Bem 1p). The variant protein was not detected in HL-60 cells and neutrophils (12). Later, it was found that a cytosolic prolyl-endopeptidase is involved in the degradation of p40phox variant protein in myeloid cells (13). NADPH oxidase (NOX) enzymes are a family of heme-containing proteins with primary function being transporting electrons from NADPH to oxygen, forming ROS. Seven members have been

identified in the NOX family including Nox1, Nox2, Nox3, Nox4, Nox5, Dual oxidase1 (Duox1), and Dual oxidase 2 (Duox2), with different NOX family members being expressed in different cell types and tissues/organs. Emerging evidence suggests that Nox/ Duox family members are important ROS producers not only for phagocytic but also for nonphagocytic cells although the biological functions of Nox/Duox in non-phagocytes are still mostly unknown.

Epithelial–mesenchymal transition (EMT) is a cellular mechanism long recognized as a central feature of normal development. Several developmental milestones, including gastrulation, neural crest formation and heart morphogenesis, rely on the plastic transition between epithelium and mesenchyme. More recent studies have revealed that similar but physiopathological transitions occur during the progression of epithelial tumors, endowing cancer cells with increased motility and invasiveness. Multiple oncogenic pathways mediated by peptide growth factors, Src, Ras, integrin, Wnt/b-catenin and Notch signaling, induce EMT. A critical molecular feature of EMT is the down-regulation of E-cadherin, a cell adhesion molecule present in the plasma membrane of most normal epithelial cells. E-cadherin acts de facto as a tumor suppressor inhibiting invasion and metastasis, and it is frequently repressed or degraded during transformation (14).

Recent experimental evidence has shown that the generated reactive oxygen species (ROS) can also induce EMT. Emerging evidence has also implicated the critical role of several microRNAs (miRNAs) in the processes of EMT. Recently, ROS signaling pathway has been reported to be intimately involved with EMT in both physiological conditions and



pathological processes; however the functions of ROS in the processes of EMT remain unclear. Many excellent reviews have documented the cross crosstalk between ROS and signaling pathways in cancer (15, 16, 17); however, the role of ROS in the processes of EMT or in cancer stem cells remains unclear. Therefore, in this study, we studied the effect of ROS in the acquisition of EMT and its biological significance in tumor progression.

3. Materials and methods

3.1. Cell culture and transfection

HeLa (ATCC CCL-2, Manassas, VA, USA) cells were cultured in DMEM with 10% fetal bovine serum (GIBCO Inc., Grand Island, NY, USA). HeLa cells transfected with pEGFP N1-p40phox or pCDNA 3.0-p40phox were selected by G418 (AG Scientific, San Diego, CA, USA) after transfection using Lipofectamin-2000 (Invitrogen, Carlsbad, CA, USA) according to manufacturer's protocols.

3.2. Western blot and antibodies

Plasmid transfected cells were twice washed with PBS and harvested in RIPA buffer (50 mM Tris-HCl pH 8.1, 150 mM NaCl, 1 % NP-40, 0.5 % sodium deoxycholate, 0.1% SDS, and protease inhibitors). Total protein amounts were measured using the biocinchoninic acid (BCA) assay (Pierce, Rockford, IL, USA). Proteins in samples were separated in SDS-polyacrylamide gels, transferred to PVDF membrane (Whatman International, Ltd., Maidstone, UK), probed with specific primary antibodies, washed, and probed with secondary antibody. Signals were detected using an enhanced chemiluminescent substrate (WEST-ZOL, iNtRON Biotechnology Inc, Seoul, Korea). The primary antibodies used include anti-p40phox, p22phox, p67phox (Santa Cruz Biotechnology, Santa Cruz, CA), anti-Slug, anti-Snail, anti-Vimentin, anti-Ecadherin, anti-GAPDH (Cell Signaling Technology, Beverly, MA, USA), NOX 2 (BD Bioscience, San Diego, CA, USA), anti-YB 1 (Millipore, Bedford, MA,

USA).

3.3. RT-PCR analysis

Total RNA was isolated from cells using Trizole reagent (Invitogen, Carlsbad, CA, USA), according to the manufacturer`s instructions. Reverse transcription was carried out using Reverse transcription system (Promega, Madison, WI, USA). Table 1 primers used in this study. After PCR, the samples were analyzed by electrophoresis in 1% agarose gels containing 0.002 % nucleic acid staining solution (RedSafe, iNtRON Biotechnology Inc., Seoul, Korea).

3.4. Plasmid construction

The full-length cDNA encoding the human p40phox was subcloned in-frame with GFP in pEGFP-N1 vector (Clontech, Palo Alto, CA) to produce a p40phox protein fused to the terminus of GFP. A recombinant plasmid was made by inserting the human p40phox gene into the pEGFP - N1 plasmid vector (Clontech, California, USA). The insert was amplified by PCR using a HL-60 cDNA template with addition of Xho I and Hind III restriction sites to primers matching those found in the pEGFP -N1 vector and Hind III and EcoR I restriction sites to primers matching those found in the pcDNA3.0 vector. The following primers (Integrated DNA technologies) were used: p40phox-Xho I Forward 5'- CCCCTCGA-GATGGCTGTGGC-3', p40phox-Hind III I Reverse 5'- CAAGCTTTCATGGCATCGTGT-3` and p40phox-Hind III Forward 5`-AAGCTTATGGCTGTGGCCCAG-3`, p40phox-EcoR I Reverse 5`-GAATTCCTAGACTTCTCTCCG-3`. Restriction digest with Xho I and Hind III

enzymes (New England Bio labs, Ipswich, MA, USA) was performed for both the insert and vector, followed by ligation with T4 DNA ligase (Promega, Madison, WI, USA). . Stably transfected cells were selected with 800ng/ml G418. After transfection with a plasmid containing the neo gene, cells are incubated in their regular growth medium containing G418 to select for stable transfectants. 48 hours post-transfection, pass cells (direct or diluted) in fresh medium containing G418 at the appropriate concentration.

3.5. NADPH Oxidase Assay.

Intracellular ROS were determined by using a DCF-DA assay. DCF-DA enters cells passively and is deacetylated by esterase to nonfluorescent DCF. DCF reacts with ROS to form DCF; the fluorescent product DCF-DA was dissolved in methanol at 10 mM and was diluted 500-fold in HBSS to give DCF-DA at 20 μ M. DCF-DA solutions were always handled under dim lighting. Approximately 1×10^6 cells were incubated in the dark for 30 min at 37°C with 20 μ M DCF-DA, harvested, and resuspended in the medium without DCF-DA. Fluorescence was recorded on the FL-1 channel of flow cytometry (FACSCalibur, BD Biosciences, San Jose, CA), and data were analyzed with the Cell Quest program.

Superoxide generation was assessed in live cells with MitoSOX Red (Invitrogen/Molecular Probes), which is a fluorogenic dye that is taken up, where it is readily oxidized by superoxide, but not by other reactive oxygen species (ROS) or reactive nitrogen species. Cells were loaded with 1 μ M MitoSOX Red in phenol-free DMEM for 10 min at 37 °C. Cells were washed with prewarm buffer. MitoSOX Red fluorescent intensity was de-

terminated by fluorescence microscopy.

3.6. Gelatin Zymography

Samples were applied to nondenaturing 10% polyacrylamide gels containing 1 mg/mL gelatin. After electrophoresis, the gels were washed with 2.5% Triton X-100, incubated overnight at 37°C in zymography buffer, and stained with Coomassie brilliant blue. Gelatinolytic activity was visualized as clear areas of lysis in the gel.

3.7. In vitro wound healing assay

Migration was assessed using a wound healing assay. Cells were plated in 6-well plates and allowed to grow for 3 days to confluences. At time 0, media was removed and cells were wounded with a 10- μ L pipet tip. Cells were washed to remove debris, media was replaced, and plates were returned to a culture incubator. Photographs were taken at time points indicated in Results. Each condition was photographed in three separate fields and the same field at each time point was used, allowing the percent of wound closed by infiltration of migratory cells to be quantitated from the photographs using Image J software (National Institutes of Health).

Table 1. Primers used in the study.

Primer	Forward (5' → 3')	Reverse (5' → 3')
E-cadherin	CCTGGGACTCCACCTACAGA	GGATGACACAGCGTGAGAGA
Vimentin	AATGGCTCGTCACCTTCGTGAAT	CAGATTAGTTTTCCCTCAGGTTTCAG
Snail	CCCAAGCCCAGCCGATGAG	CTTGGCCACGGAGAGCCC
Slug	AGCAGTTGCACTGTGATGCC	ACACAGCAGCCAGATTCCTC
MMP 2	AGGCCAAGTGGTCCGTGTGAA	ACAGTGGACATGGCGGTCTCA
MMP 3	CCT GCT TTG TCC TTT GAT GC	TGA GTC AAT CCC TGG AAA GTC
MMP 7	TACAGTGGGAACAGGCTCAGG	GGCACTCCACATCTGGGCT
MMP 13	CTTCACGATGGCATTGCTGA	AACTCATGCGCAGCAACAAG
p21	AGCAGAGGAAGACCATGTGGA	GCGGATTAGGGCTTCCTCTT
p27	TAACCCGGGACTTGGAGAAG	GCTTCTTGGGCGTCTGCTC
p53	TGCGTGTGGAGTATTTGGATG	TGGTACAGTCAGAGCCAACCAG
NOX 1	GTACAAATTCCAGTGTGCAGAC- CAC	CAGACTGCAATATCGGTGACAGCA
NOX 2	GGAGTTTCAAGATGCGTGGAAC- TA	GCCAGACTCAGAGTTGGAGATGCT
NOX 3	GGATCGGAGTCACTCCCTTCGCTG	ATGAACACCTCTGGGGTCAGCTGA
NOX 4	CTCAGCGGAATCAATCAGCTGTG	AGAGGAACAC- GACAATCAGCCTTAG
NOX 5	ATCAAGCGGCCCTTTTTTTCAC	CTCATTGTCACACTCCTCGACAGC
p22phox	ATGGGGCAGATCGAGTGGGC	TCACAGACCTCGTCGGTCA
p67phox	GTGCTCATGGAGACGCGGCTT	CTAGACTTCTCTGGGAATGCCTTCC
P40phox	ATGGCTGTGGCCAGCAGCT	GCCCTCCAGCCAGTCTTTGT
GPX1	AAGAGAT- TCTGAATCCCTCAAGTAC	ACCAGGAACTTCTCAAAGTTCAGG

XBPI	AAACAGAGTAGCAGCTCAGACTGC	TCCTTCTGGGTAGACCTCTGGGAG
SOD1	GGATGAAGAGAGGCATGTTGGA- GAC	GTCTTTGTACTTTCTTCATTCCACC
Catalase1	TCGAGTGGCCAACTACCAGCGTG	GTACTTGTCCAGAAGAGCCTGGATG
GAPDH	GAAGGTGAAGGTCGGAGTC	GAAGATGGTGATGGGATTTC

4. RESULTS

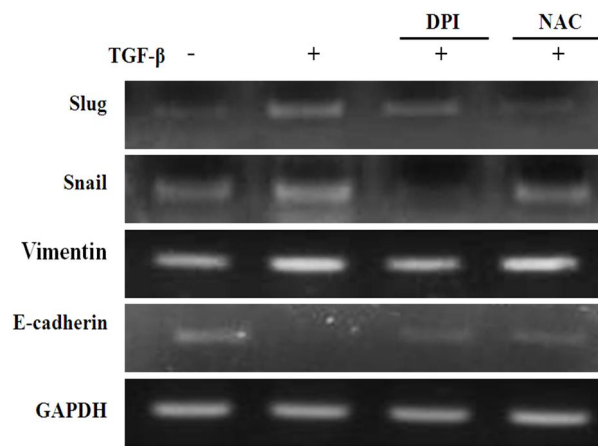
4.1. p40phox Expression and ROS generation during TGF- β 1-induced EMT

Transforming growth factor β 1 (TGF- β 1) is a multifunctional cytokine that controls proliferation, differentiation, migration, and apoptosis of various cell types. In tubular epithelial cells in the kidney, EMT can be induced by TGF- β 1, leading to increased collagen deposition and disruption of the epithelial integrity (18). And a treatment with antioxidants NAC (5mM) and DPI (5 μ M) effectively suppressed TGF- β 1 induced Snail, Slug and vimentin in HeLa cells (Fig. 1A, B). TGF- β 1 induced down regulation of E-cadherin mRNA levels was effectively prevented by pretreatment with antioxidants NAC (5mM) and DPI (5 μ M) but up-regulation of cleaved form of E-cadherin protein levels (Fig. 5 A, B). Both NAC (5mM) and DPI (5 μ M) effectively inhibited TGF- β 1 induced up-regulation of Snail, Slug and vimentin expression in HeLa cells (Fig. 1A, B). Statistically significant changes were observed at 5ng/ml and from day 1 after TGF- β 1. An E-cadherin fragment of approximately 72 kDa was detected in the treated with TGF- β 1. Several studies identified NADPH oxidase as a major source of ROS production in endothelial cells (19).

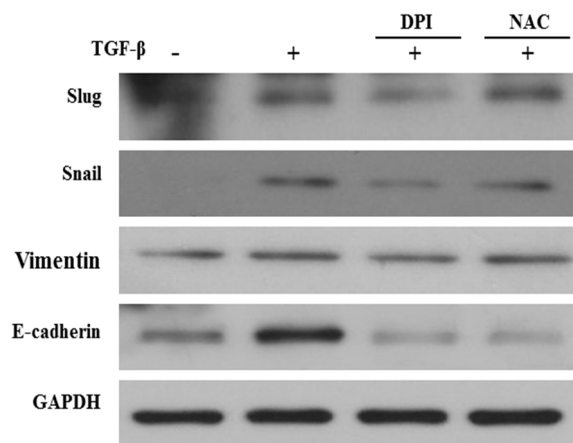
Next, we measured cellular ROS after stimulation with TGF- β 1. Treatment of TGF- β 1 at 5 ng/ml increased DCF-sensitive cellular ROS in HeLa cells for 30 min. Inhibitor NADPH oxidase (5 μ M DPI) and antioxidant (3mM NAC) was significantly reduced TGF- β 1 induced DCF-sensitive cellular ROS (Fig. 5B). Results from the previous-data, we suggested that

EMT gene changes by TGF- β 1 were mediated by ROS in HeLa cells (Fig. 1 A, C). Interestingly, TGF- β 1 has been found to stimulate ROS production in a variety of cell types, including endothelial cells (19, 20). The expressions of different membranes of NOX family were examined. TGF- β 1 treatment was up-regulated NOX 2 and NOX 5. The induction of NOX 2 was confirmed by inducing other subunit of NOX 2 system such as, p67phox, p47phox and p40phox in both mRNA and protein level. These result tests demonstrate the involvement of NOX 2 in EMT in non-phagocytic cells.

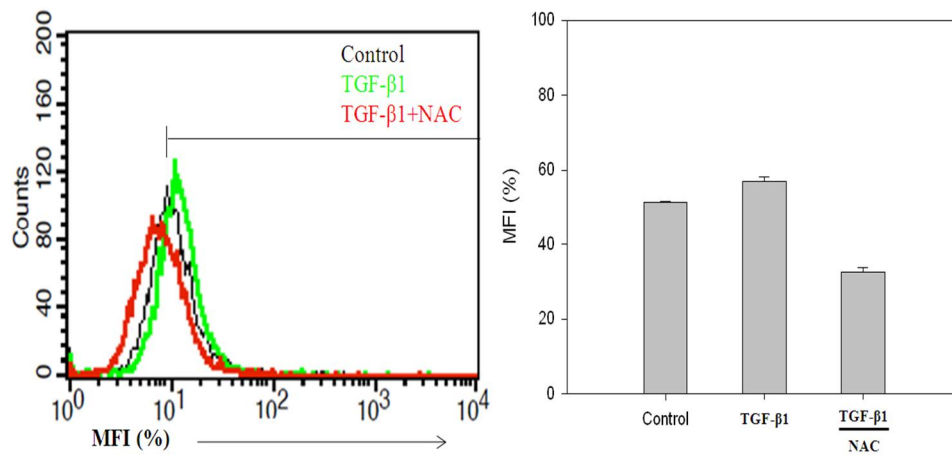
(A)



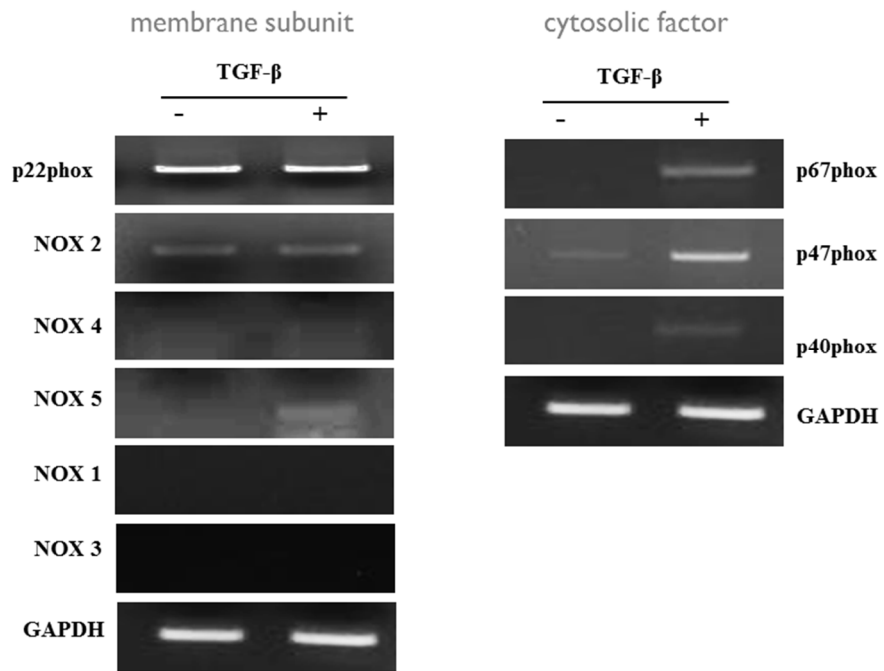
(B)



(C)



(D)



(E)

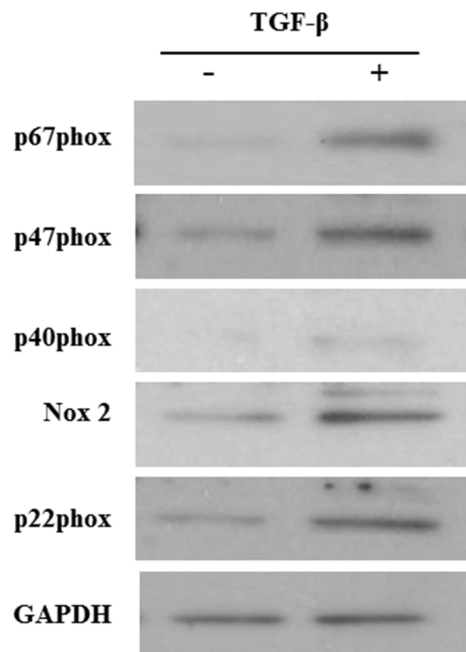


Figure 1. NOX 2 is involved in ROS production in EMT by TGF- β 1.

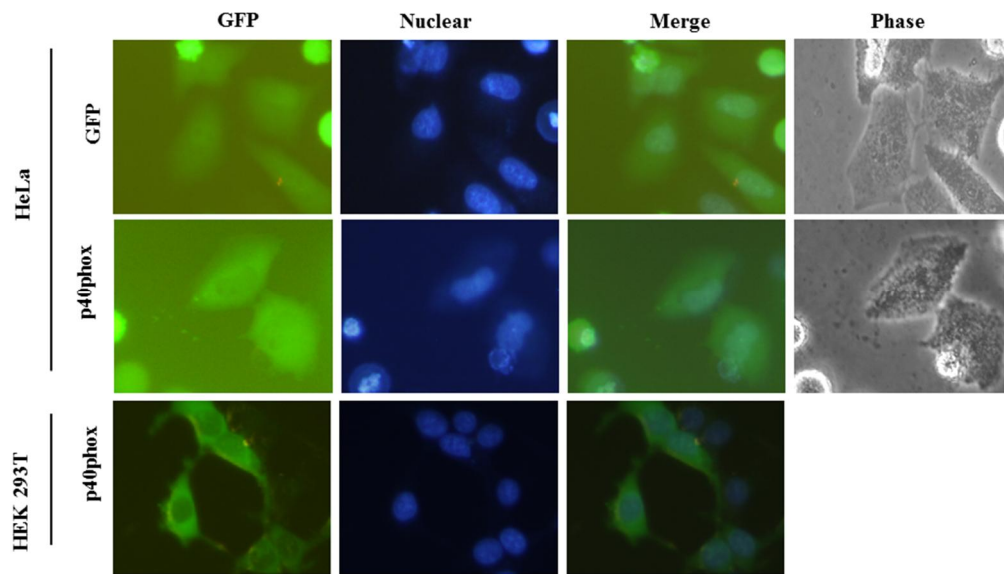
Effects of ROS on EMT were investigated by examining expressions of EMT-related genes by RT-PCR (A) or western blot analysis (B). Cells were treated with TGF- β 1 (5 ng/ml) for 24 hr and antioxidants were administered 1 hr before the addition of TGF- β 1. GAPDH was used for loading control. (C) Cellular ROS changes upon TGF- β 1 treatment were detected by dichlorofluorescein (DCF) with or without antioxidants (NAC, 3mM). HeLa cells were treated with DCF for 30 min and DCF-sensitive cellular ROS were measured as described in materials and methods. Antioxidant was administered 1 hr before the addition of TGF- β 1. Mean fluorescence Intensity (MFI) were expressed as mean \pm SD of least three experiments (left). (D) Expression of NADPH oxidase subunit in HeLa cells. Cells were incubated with TGF- β 1 (5 ng/ml) at 24 hr. Total RNA was extracted, and Expression NOXs was evaluated by RT-PCR analysis using primers (Table 1) specific for each membrane subunit (left) *or* cytosolic factor (right). Results were reproduced three times and representative data are shown. (E) NADPH oxidase NOX 2 subunits were detected by western blot analysis in HeLa cells after incubated with TGF- β 1 for 24 hr. Results were reproduced three times and representative data are shown. The RT-PCR and western blot were GAPDH to control for loading.

4.2. Localization of the full-length p40phox in transfected cells

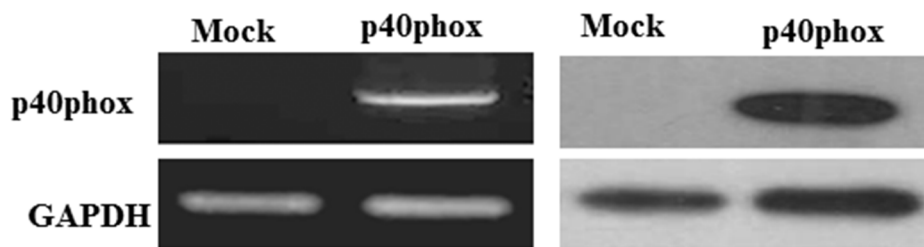
Recently it was reported that ROS stimulate the expression of the transcription factor Snail and EMT (21)(26). Here, we investigate the effect of p40phox induced EMT in the epithelial carcinoma HeLa cell line. This HeLa cell was transiently transfected with the expression plasmid pEGFP-N1 or pEGFP-N1-p40phox, which ensures strong and sustained expression of p40phox (Fig. 2). As was observed in the HeLa cells, p40phox transfected with pEGFP-N1 showed diffuse cytoplasmic fluorescence (Fig 2A). Cellular expression of the fusion proteins was verified by Western blot using an anti-p40phox and p40phox primer by RT-PCR (Fig. 2B). When transduced cells are put under selection with the antibiotic G418, cell lines can be obtained at high frequency that stably maintain the expression and exhibit stable, high-level expression of the reporter gene. To investigate the stability of GFP expression, transfected HeLa cells were placed in selective media until colonies of G418-resistant cells were visible. Resistant colonies were obtained by cell produced GFP. Five randomly chosen clones maintained GFP expression after culture for at least 10 passages in G418-supplemented medium. To analyze the DNA derived from recombinant DNA maintained in HeLa stable derivatives, cellular DNA was isolated from the pooled G418-resistant HeLa cells described above and subjected to RT-PCR analysis. The NADPH oxidase complex is a major source of intracellular ROS generation and ROS has been implicated in multiple physiological and pathological processes as a secondary messenger in cell signaling. To determine whether NADPH oxidase mediated ROS generation is involved induced by p40phox,

we stained live cells with MitoSox Red, a fluorogenic dye that is selective for the detection of superoxide in HeLa-p40phox cells. The MitoSox Red reagent is chemically targeted oxidized by superoxide exhibits red fluorescence in the cells and cells were pre-incubated with the NADPH oxidase inhibitor DPI or antioxidant NAC for 1hr. It is noteworthy that increased in superoxide accumulation was observed in the presence of p40phox and a similar results of DCF fluorescence was assessed (Fig. 2C). As shown in Fig. 2C, p40phox stimulated a sustained increase in MitoSox fluorescence. But, DPI and NAC slightly lowered the MitoSox fluorescence compared with untreated cells (Fig. 2C). These observations are consistent with DCF, indicating ROS generation as the source of p40phox-induced ROS. DPI and NAC of antioxidant positive controls, inhibited the generation of superoxide anions. To measure intracellular ROS concentration, HeLa cells were incubated with the fluorophore DCFDA. The level of DCFDA fluorescence has been previously used as a sensitive, albeit indirect, measure of intracellular ROS (22). We found that the p40phox expression also produced ROS in these cells when analyzed by the DCF-DA fluorescence assay (Fig. 2D). To confirm that the increase in DCFDA fluorescence observed after expression of p40phox was actually due to a rise in ROS, cells were treated for 4 hr with two chemically related cell-permeant antioxidants (N-acetylcysteine (NAC, 3 mM), Diphenyliodonium (DPI, 5 μ M)). As shown in Fig. 1D, generation of ROS was suppressed by treatment with DPI and NAC. These results represented superoxide generation of nonphagocytic HeLa cells by introduced of p40phox gene.

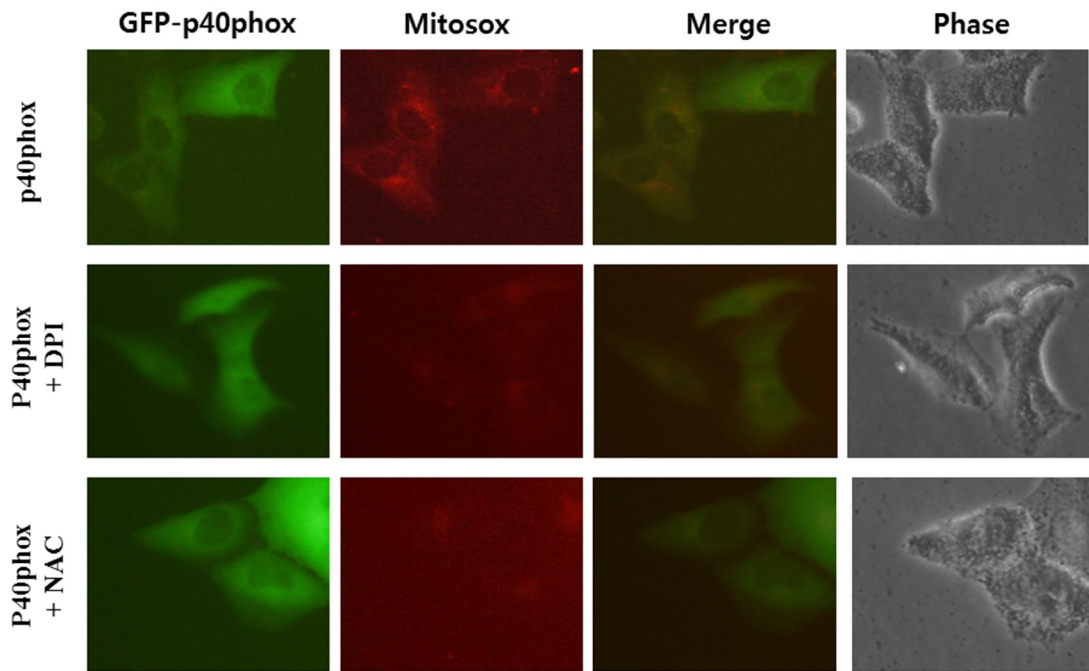
(A)



(B)



(C)



(D)

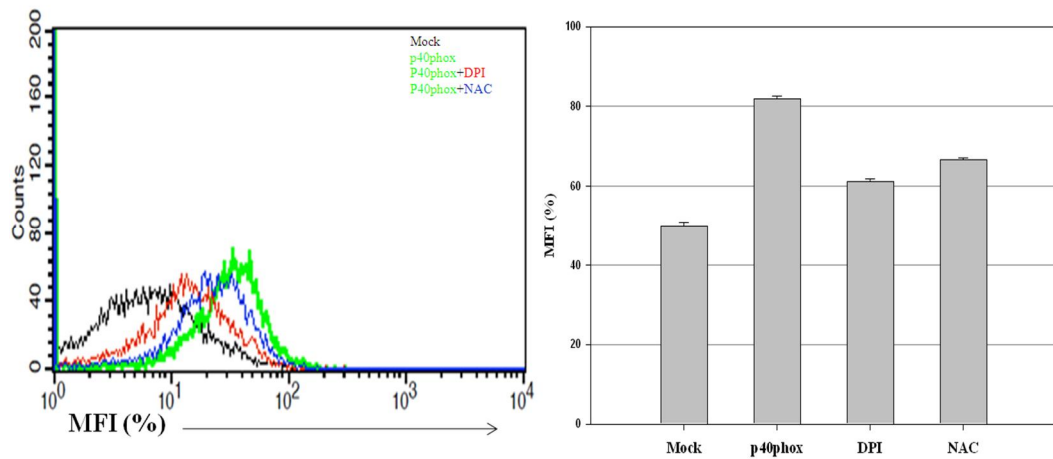


Figure 2. p40phox expression and ROS generation in HeLa and HEK 293T cells.

(A) GFP-p40phox proteins were transiently expressed in HeLa cells for 24 hr. Nucleus stained with Hoechst 33342. Subcellular localization of p40phox proteins (green) and nucle-

us (blue) were examined under a fluorescent microscope. Panel for merge and phase images are also shown. (B) p40phox was transiently expressed in HeLa cells and expression of p40phox was analyzed by RT-PCR and western blot. GAPDH was used as a loading control. (C) Effect of p40phox and selective antioxidants on superoxide production. HeLa-p40phox cells were preincubated with DPI (5u M) and NAC (3mM) for 2hr, and the presence of with mitoSox red (5 uM) the DMEM media (contained 1% FBS). Cells were washed thrice gently with PBS to remove excess unbound dye and replaced with fresh 5% phenol-red free DMEM. Digital images of mitoSox fluorescence were obtained by microscopy and overlaid. This construct was expressed with p40phox or control plasmid pEGFP-N1 in HeLa cells. (D) Detection of superoxide anion by DCF-DA in HeLa-p40phox stable cells. HeLa-p40phox cells were preincubated with DPI (5u M) and NAC (3mM) for 2hr. The index of oxidation was calculated as percentage of mean fluorescence intensity (MFI) compared with vector cells. Typical results were shown from independent experiments performed at least three times.

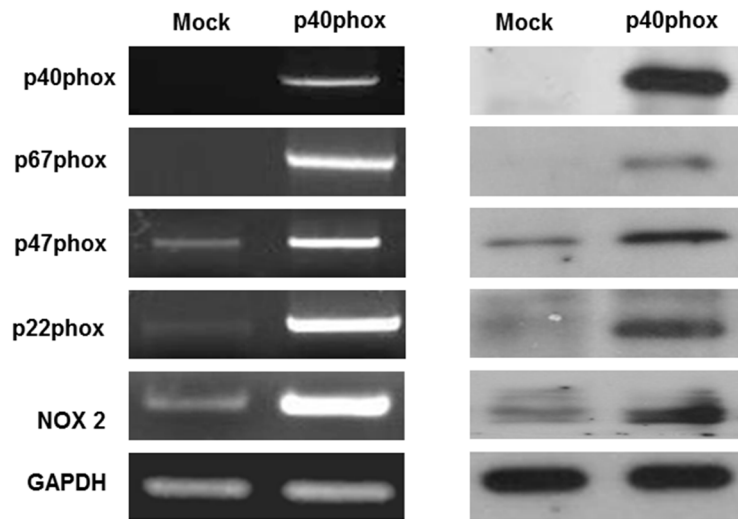
4.3. Introduction of p40phox gene induced NADPH oxidase 2 (NOX 2) subunits and enzymes involved in homeiosis of creative oxygen sepsis (ROS)

The transgenic HeLa-p40phox cells were capable of up-regulation of ROS generation by p40phox expression (Fig. 2D). The flavocytochrome is catalytically inactive in resting cells, but the surface receptors trigger the assembly of the multicomponent NADPH oxidase (19). p40phox is the last NADPH oxidase subunit to be discovered, and although there is evidence of both positive and negative effects on oxidase function, its exact role remains poorly defined. Primary association of p40phox is appeared to be with p67phox; furthermore, the amount of p40phox protein was reduced in patients with CGD lacking p67phox. This finding suggests that, in HeLa cell, p40phox may need p67phox for stable expression. The changed in expression NOX 2 subunits of RT-PCR and western blot in the presence or absence of p40phox (Fig. 3). As expected, HeLa-p40phox cell showed high expression of p67phox, p22phox and Nox2 in mRNA and protein level in HeLa-p40phox cells (Fig. 2A).

We also investigated the gene expression levels of expression antioxidant enzymes by RT-PCR in HeLa-p40phox cells (Fig. 3B). We observed increases in the mRNA levels of Sod 1, Catalase, Gpx 1 (glutathione peroxidase), SOD (superoxide dismutase) and Xbp 1 (X box binding protein 1, antioxidant proteins) (Fig. 3B). The generation of superoxide results from one-electron reduction of oxygen by a variety of oxidases. Superoxide is rapidly dismutated by Sod to the more stable ROS, H₂O₂. Both Cat and Gpx catalyze the dismutation of H₂O₂ to H₂O₂ and molecular O₂. Gpx additionally uses reduced glutathione as a substrate

(23, 24). The following results of observation; the increased level of intracellular ROS induces antioxidant enzyme gene expression via a p40phox overexpression.

(A)



(B)

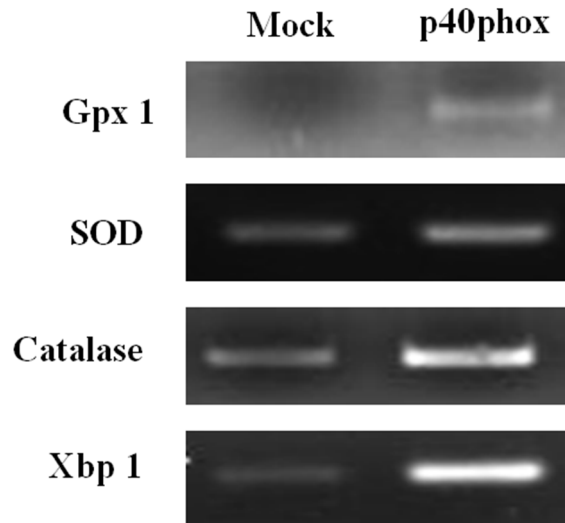


Figure 3. NADPH oxidase 2 subunits and antioxidant enzymes expressed in HeLa-p40phox cells.

(A) Expression of p40phox transfected in HeLa cell line. Expressions of NOX 2, p67phox and p22phox in HeLa-p40phox and in control HeLa cells, analyzed by RT-PCR and western blot. GAPDH was used as a loading control. (B) Effects of p40phox introduction on expression of the antioxidant enzymes. Superoxide dismutase (SOD), glutathione peroxidase (GPx), catalase (CAT), targeting X box-binding protein 1 (Xbp-1).

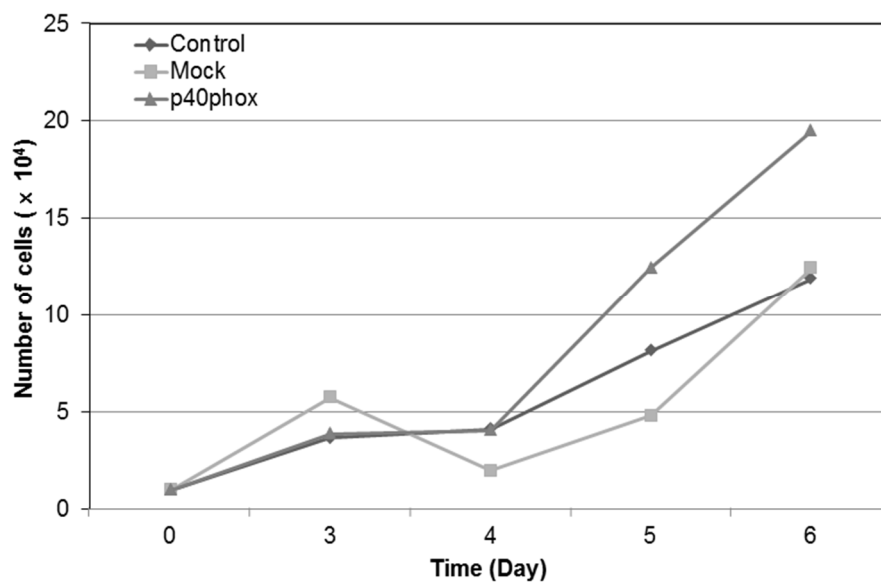
4.4. Overexpression of p40phox induced cell growth rate increase and reduced of p21 and p27

ROS play signaling roles in physiologic or pathophysiologic processes of cell proliferation, adhesion, and atherosclerosis. Moreover, ROS emerge as important intracellular signaling molecules, which act as mediators or second messengers at nontoxic concentrations through receptor-transducing pathways (19). In particular, growth factor-induced ROS generation is considered to be important in the mitogenic process of cell cycle of neoplastic proliferation. An excessive production of ROS beyond the antioxidant capacities of the cell leads to oxidative stresses that result in metabolic disturbances and cell senescence. In the cancer cell system, ROS exert a paradoxical effect. ROS can promote tumor growth by transforming normal cells through activation of transcription factors or inhibition of tumor-suppressor genes, whereas its elevated levels would inhibit tumor cells through the stimulation of proapoptotic signals. The excess ROS generate cell cycle arrest and apoptotic cell death or even necrosis in severe cases (25). Therefore, the maintenance of ROS homeostasis is extremely important to cell signaling and the regulation of cell death. In this study we investigated the differential effect of tumor cell proliferation by p40phox expressed in HeLa cells. ROS might act as modulators of intracellular signaling cascade that use hydrogen peroxide as a principal second messenger molecule, and thus involved in the modulation of cancer cell proliferation (19).

Here we examined the proliferative effect of ROS in the p40phox transfected stable cells.

For growth curves, 1×10^5 cells were plated in 6-mm dishes and were counted in triplicates after 3 days. As shown Fig. 4A, p40phox expressed HeLa cells increased cell growth rate more than mock (only pEGFP-N1 vector) transfected cells. To determine the mechanism by which p40phox regulates HeLa cell proliferation. The roles of p21 and p27 in the proliferation effect HeLa-p40phox stable cells were tested. As seen in Figure 4B, the p40phox expression results in a significant down-regulation of both p21 and p27 mRNA and proteins levels. Increased ROS level may induce cell proliferation via down-regulation of CDKIs.

(A)



(B)

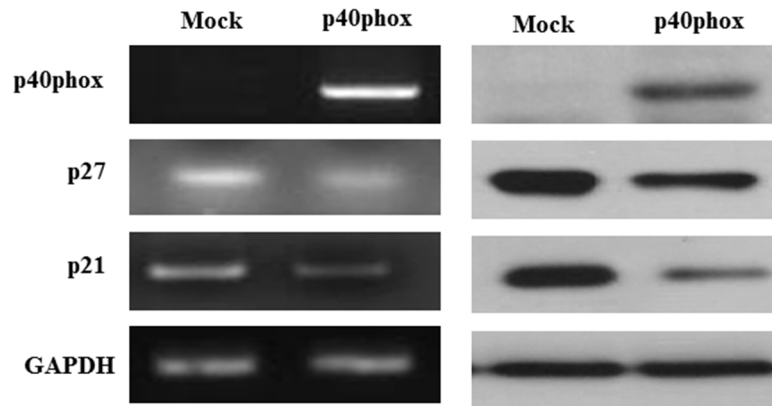


Figure 4. The effects of p40phox on proliferation of HeLa cell

(A) The proliferation rate of HeLa-p40phox cells. HeLa-control and HeLa-p40phox cells were seeded at a density of 1×10^4 cell/ml in 6-well plates. Cells numbers at the count start of 3 days after and cells were measured by counting the cells after 3, 4, 5 and 6 days of plating.

(B) mRNA and protein expression levels of p21 and p27 were estimated by RT-PCR and western blot analysis in HeLa-p40phox cells. Used GAPDH to control for loading. Typical results were shown from independent experiments performed at least three times. Data are represented as mean \pm SEM ($n = 3$). No error bar in (A) (B) do not need \pm SEM.

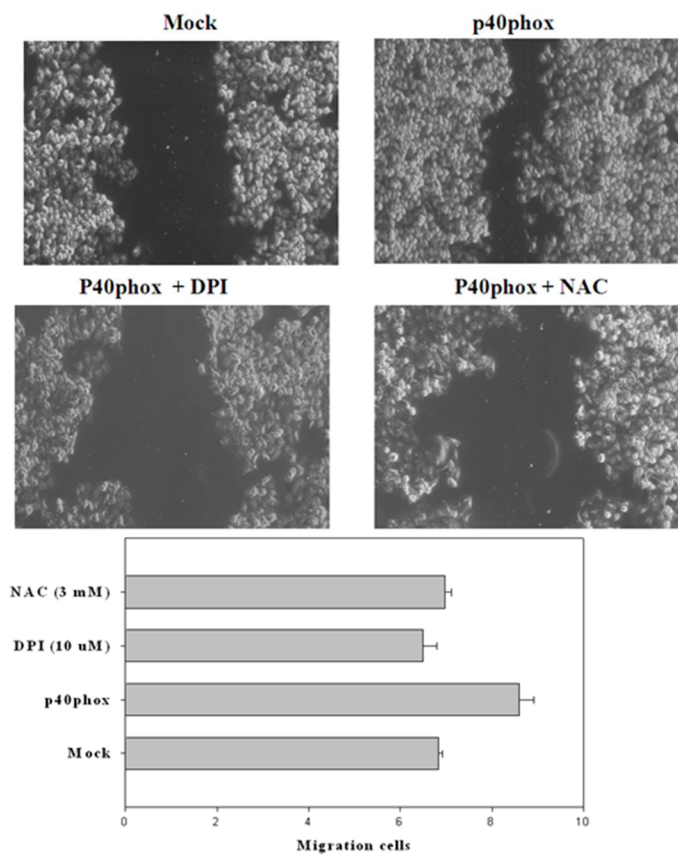
4.5. Activation of matrix metalloproteinase by over-expression of p40phox in HeLa cells involved reactive oxygen species

In a previous study, we showed increased ROS levels were responsible for increased growth rate in HeLa cells. We next studied whether ROS levels correlated with the migration in HeLa-p40phox cells. To examine whether ROS induce migration, cells were incubated with N-acetyl cysteine (NAC, an ROS scavenger) or diphenylene iodium (DPI, and NADPH oxidase inhibitor). Increase of ROS production via p40phox induce the migration which was blocked by treatment with NAC and DPI, suggesting that ROS play a critical role in up-regulation of migration in p40phox expressed HeLa cells (Fig. 5A). Matrix metalloproteinase family is known to play a key role in the tumor invasion of various human cancers (26). It was reported that MMP-1 expression was associated with portal invasion (27). Increased expression of MMP-2, MMP-7, and MT1-MMP had a strong association with dedifferentiation, portal invasion, intrahepatic metastasis, and recurrence (28, 29).

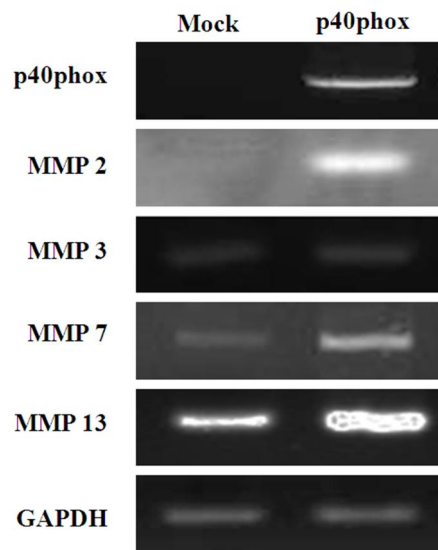
To investigate whether p40phox affect the expression of MMPs, mRNA level of various MMPs in HeLa cells were quantified by PCR. As shown Figure 5B, RT-PCR analysis showed that MMP-2, MMP-7 and MMP-13 mRNA expression was increased in HeLa-p40phox stable cells. And MMP-2, MMP-7 and MMP-13 mRNA level in HeLa-p40phox cell was significantly higher than MMP-3 and MMP-7 (Fig. 5B). To confirm that ROS generated by p40phox is one of the main factors that contributes to increased expression of MMP-2 in HeLa cells (Fig. 5B). In addition, we examined MMP-2 (72 kDa) protein levels in HeLa-

p40phox cells. Zymography analysis showed that with the MMP-2 expression in p40phox transient transfectant and stable HeLa cells (Fig. 5C). Over expression of p40phox cause the significant induction of MMP2 (Fig. 5C), and this result of gelatin zymography was consistent with RT-PCR. We found that gene expression level of MMPs can also be regulated by ROS, and MMPs mRNA is increased in an NADPH oxidase derived, ROS-sensitive manner. Thus ROS modulate matrix remodeling at multiple levels.

(A)



(B)



(C)

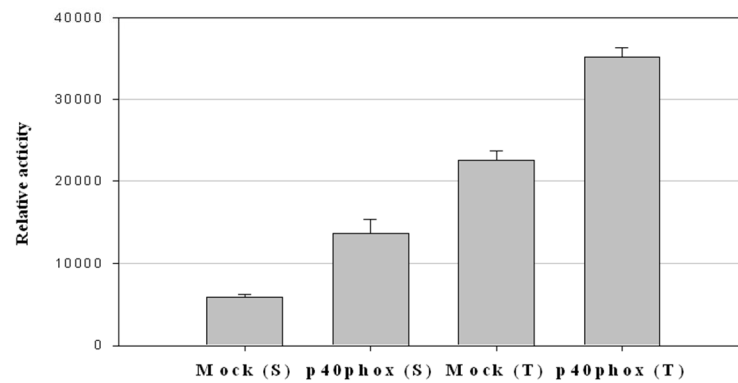
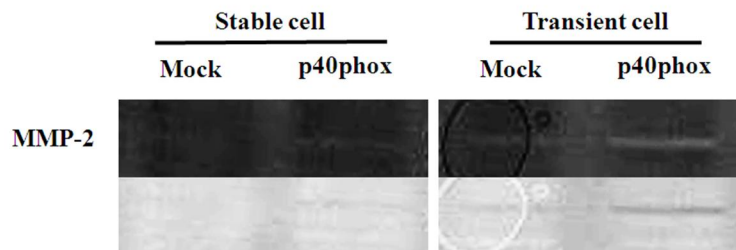


Figure 5. Regulation of matrix metalloproteinase expression in HeLa-p40phox cells.

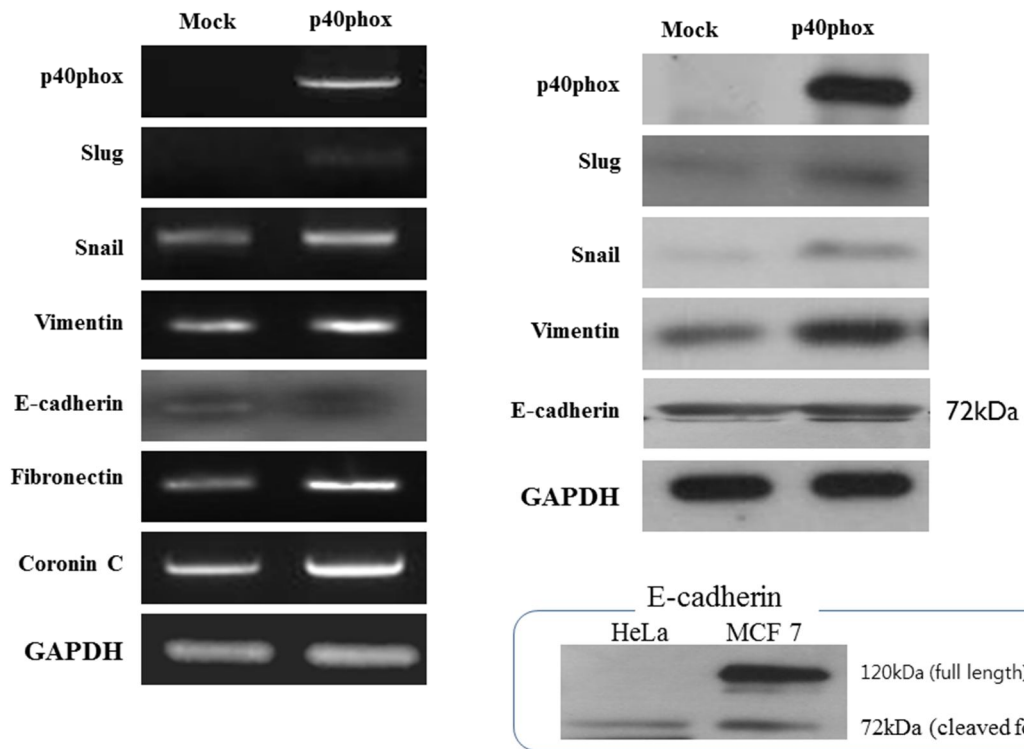
p40phox induced migration in HeLa cells. Vector transfect (Mock) or p40phox stably transfected HeLa cells cultured for 24 hr followed by NAC (5mM) or DPI (10uM) treatment. Cell migration assays was carried out in material and methods. The migrated cells were pictured under phase contrast image. The graph represents the percent of migration. (B) mRNA levels of MMP genes were measured by RT-PCR in HeLa cells with or without p40phox transfection. RT-PCR analysis using the expression loading control GAPDH. (C) MMP-2 activity by gelatin zymography in Mock and p40phox HeLa cell. Typical results were shown from independent experiments performed at least three times. This construct was expressed with p40phox or control plasmid pEGFP-N1 in HeLa cells. The graph represents the quantification of MMP 2.

4.6. ROS mediate p40phox induced EMT

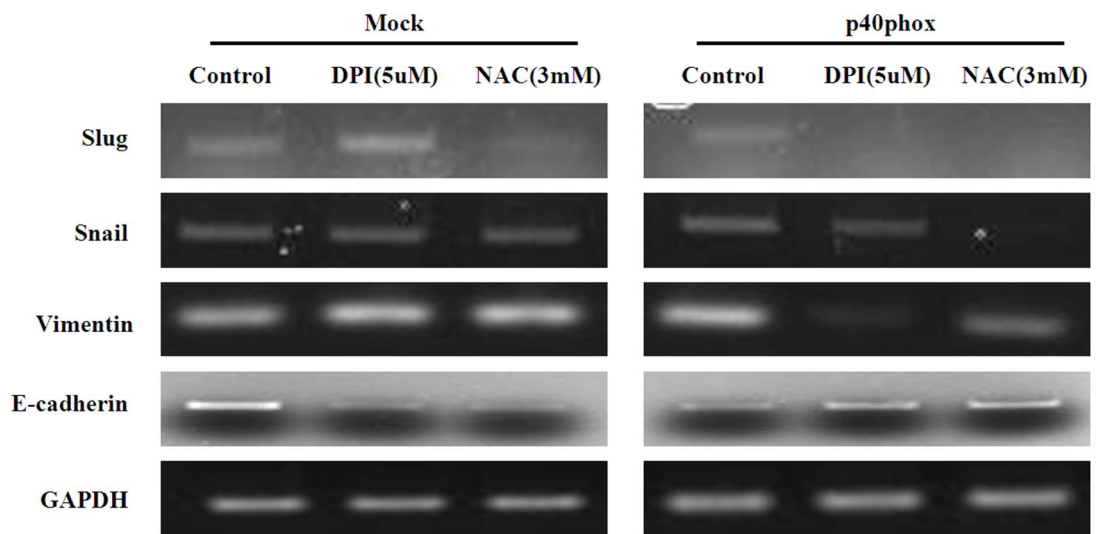
Induction of these signaling (ROS generation by p40phox expression) cascades leads to HeLa cell growth rate increase, migration expression and up regulated MMPs. Previously, elevated oxidative status has been found in many types of cancer cells, which contribute to carcinogenesis (30, 21). Recently, the involvement of ROS signaling in tumor metastasis was highlighted. ROS signaling pathway has been reported to be intimately involved with EMT in both physiological conditions and pathological processes, however the functions of ROS in the processes of EMT remain unclear (31, 32, 33).

Since the p40phox transfected cell showed the characteristic of EMT. Increase of proliferation, cell migration, up-regulation of MMPs, we described to examine the relationship between the ROS increased and EMT. In RT-PCR and western blot analysis, the mRNA and protein levels of epithelial genes like E-cadherin decreased; on the other hand, the mesenchymal gene snail, slug, fibronectin, Coronin 1C and vimentin were up regulated (Fig. 6A). Interestingly, in HeLa cell only the short form (cleaved form) of E-cadherin is detected in reverse manner of full size. This result suggests that Coronin 1C may be a up regulated by ROS generation via p40phox expression. Antioxidants effectively inhibits upregulation of snail, slug and vimentin of mesenchymal gene; on the other hand, the epithelial genes like E-cadherin was up-regulation (Fig. 6B, C). These data show that p40phox mediate ROS induced activation of EMT transcription factors and antioxidants N-acetylcysteine (NAC) and diphenyliodonium (DPI) both block ROS mediated cell EMT.

(A)



(B)



(C)

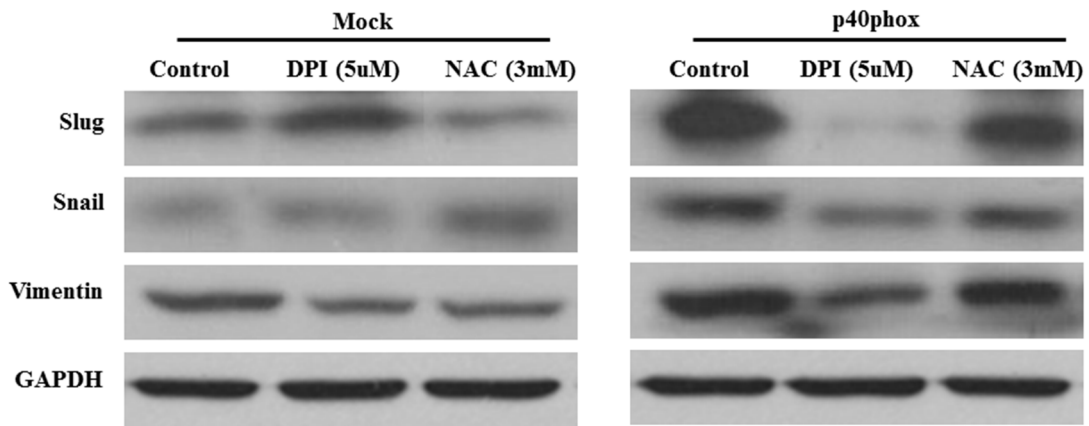


Figure 6. ROS generation by p40phox induced EMT in HeLa-p40phox cells.

(A) The expression levels of EMT-associated factors analysis by RT-PCR and western-blot in HeLa-p40phox cells. RNAs and proteins were prepared from p40phox stable cell. GAPDH was used as a control for equal loading of mRNAs and proteins. (B, C) Effect of antioxidants on ROS induced EMT in HeLa-p40phox stable cell lines. Cells were preincubated with NAC (3mM) and DPI (5uM). mRNA expression of each gene was analyzed using specific primers, as explained in Table 1.

4.7. p40phox mediated YB-1 increase through ROS generation

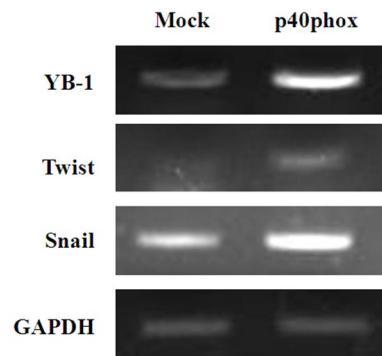
Recently, reactive oxygen species (ROS) has been shown to activate latent TGF- β 1 in rat MCs (rMCS). As a key regulator of gene transcription, YB-1 mediates expression of genes that are involved in ECM turnover matrix metalloproteinase-2 (MMP-2). Transcription regulatory complex including YB-1 controls expression of mouse matrix metalloproteinase-2 Gene in NIH3T3 Cells (34). Microarray gene analysis revealed that YB-1 increases TWIST1 expression on the transcriptional and translational levels and directly activates cap-independent translation of Snail1 mRNA. *In vivo*, YB-1 expression was associated with potentially metastatic breast cancer cells (35). These data suggest that YB-1 might positively involve in NOX 2 mediated EMT.

Next, to confirm whether the function of YB-1 is involved in our p40phox induced ROS overexpression model, we analyzed mRNA levels of YB-1 and Twist by RT-PCR (Fig. 7). Twist, another transcription factor, has also been shown to possibly induce EMT, and is also implicated in the regulation of metastasis. Shown as the figure 6A, YB-1 and Twist were increased HeLa-p40phox cells compare mock transfected HeLa cells and snail mRNA levels were up-regulated (Fig. 7A). The protein expression level of YB-1 also up-regulated by p40phox expression and with antioxidant (NAC) or NADPH oxidase inhibitor (DPI) significantly reduced YB-1 protein expression (Fig. 7B).

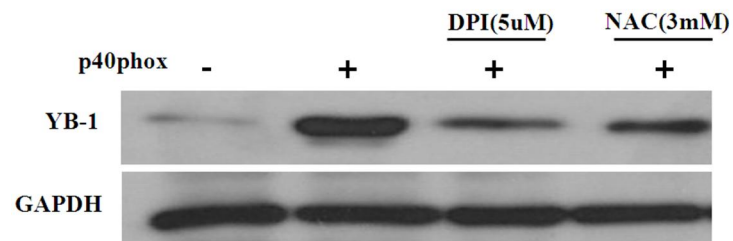
Next, we demonstrate that YB-1 was clearly up regulated by TGF- β treated in HeLa cells (Fig. 7C). Our results shown above suggested that HeLa cells can undergo transition into a

mesenchymal-like phenotype upon TGF- β treatment and NOX 2 mediated intracellular ROS production control YB-1, snail, slug and twist expression.

(A)



(B)



(C)

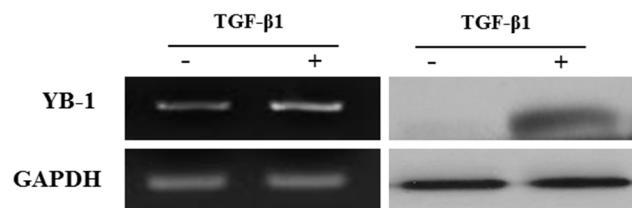


Figure 7. Over-expression of superoxide in HeLa cells increased YB-1 expression.

(A) RT-PCR assays were performed to measure mRNA level of YB-1, Twist and Snail in HeLa-p40phox cells. (B) YB-1 expression was measured by western blotting with antioxidant or NOX inhibitor. (C) Cells were treated with TGF- β 1 for 24. And the RT-PCR and western blot were GAPDH to control for loading.

4.8. ROS generation induced EMT blocked by inhibitors

The above results show that the expression of genes implicated in EMT may be regulated by ROS and up-regulated by TGF- β 1 that trigger ROS-dependent EMT progression in HeLa cells. TGF- β 1 signaling pathway occupies a central position in the signaling networks that control EMT including MEK/ERK, JNK/p38MAP kinases, Rho GTPase and PI3K/Akt signaling pathways (36). On the other hands, there is much evidence that mitogen-activated protein kinases (MAPK) such as p38 MAPK and extracellular response kinase (ERK) also regulate the activation of NADPH oxidase, because SB203580, an inhibitor of p38 MAPK, and PD98059, an inhibitor of ERK, partially attenuate the superoxide (37).

Next, we wanted to elucidate which intracellular signals are implicated in the events induced upon low serum condition (1% FBS). The effects of inhibiting EMT using metabolic inhibitors MEK inhibitor (U0126), p38 MAPK inhibitor (SB203580), PI3K inhibitor (LY94002), ERK inhibitor (PD98050) and JNK inhibitor (SP600125), we found that decreased snail and vimentin expression by JNK/p38 MAP kinases inhibitor or by PI3K/Akt inhibitor (Fig. 8). Both activities JNK/p38 MAP kinases inhibitor and PI3K/Akt inhibitor effectively inhibited ROS induced EMT. ROS induced EMT was effectively inhibited by SB203580 and LY94002 but not by ERK/MEK inhibitor that inhibited the effect of p40phox on snail and vimentin (Fig. 7).

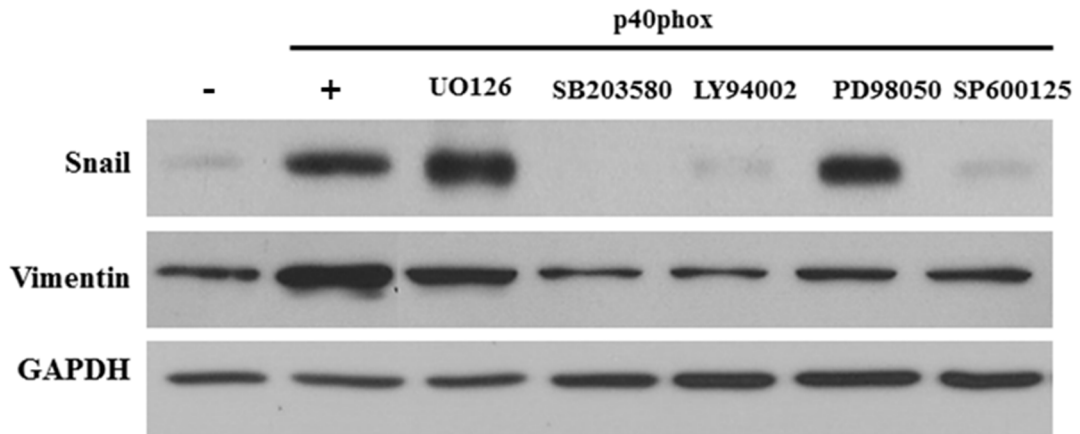


Figure 8. Inhibition of MEK/ERK, JNK/p38 MAP kinases and PI3K/AKT pathways ROS induced EMT. HeLa-p40phox cells were incubated in presence of MEK inhibitor U0126 (5 μ m), PI3K inhibitor (10 μ m) LY 294002 (10 μ m), p38 MAPK inhibitor SB203580 (10 μ m), ERK inhibitor PD98059 (10 μ m) and JNK inhibitor SP600125 (10 μ m) for 2h. The expression of GAPDH was used to control equal protein loading. This construct was expressed with p40phox or control plasmid in HeLa cells.

5. DISCUSSION

The low levels of ROS may modulate protein structure and function in a physiologically relevant manner resulting in activation of signal transduction pathway leading to modulation of gene expression. The recent discovery of the involvement of ROS production in a multitude of normal biological processes defines a new role of ROS in normal cell homeostasis rather than just toxic damage to cellular macromolecules (38, 39). The low amounts of ROS produced by nonphagocytic NADPH oxidase may function as second messengers to influence redox-sensitive signal transduction pathways.

In present study, TGF- β 1-induced EMT in HeLa cells was significantly increased NADPH oxidase systems and induced non-SMAD signaling pathway. And we showed that ROS induced by NOX 2 in non-phagocytic cell, HeLa cells can modulate EMT by regulating Snail, Slug and YB-1. NOX 2 activated model systems conformed EMT like changes.

TGF β 1 has been reported to induce EMT in the epithelial cell line and primary cells (40, 41). We showed that TGF- β 1 treatment increased both EMT markers and ROS generation by up-regulated of two isoforms (NOX 2 and NOX 5) and cytosolic components (p47phox, p67phox and p40phox) of NADPH oxidase 2 (Fig. 1). It has been reported that transforming growth factor- β 1 induces NOX 4 NAD (P) H oxidase and reactive oxygen species-dependent proliferation in human pulmonary artery smooth muscle cells (42) and in lung cancer cells, the TGF may trigger EMT through ROS mediated, the non-smad pathway (37). Also, Hecker *et al.*, (43) reported NADPH oxidase-4 mediated myofibroblast activation and fibrogenic

responses to lung injury. There are many evidences of physiological roles of ROS in non-phagocytic cells and main source of ROS is believed to be a NADPH oxidase (42). However, our results strongly suggested that ROS is involved in the EMT induced by TGF- β 1 and the NADPH oxidase-2 is the main system for generation of ROS (Fig. 1C). Since strong generation of ROS and complex orchestration of subunits for activation, it is believed that NOX2 system is for the phagocytic cells. And subunits of NADPH oxidase-2 were not detected in many of non-phagocytic cells such as Hela cells. However, our results revealed that upon treatment of TGF- β 1, subunits of NADPH oxidase-2 were induced. TGF β 1 treatment in Hela cells up-regulated NOX2 and NOX5 (Fig. 1). In other cells such as MCF-7 (Breast cancer cells) and Huh-7 (hepatocarcinoma cells), we also observed increase of NOX2 and 5 (S 4). NOX 1, 2, 3 and 4 systems commonly requires p22phox subunit for action but not in NOX 5 system. The roles of NOX 5 in TGF induced EMT is under investigation.

There are several components of NADPH oxidase: of these the cytochrome-b558 heterodimer is located in the membrane and consists of the gp91phox and p22phox units (44) and cytosolic regulatory components p47phox, p67phox, p40phox, and the Rac GTPase. p40phox is the last NADPH oxidase subunit to be discovered, and although there is evidence of both positive and negative effects on oxidase function, its exact role remains poorly defined. In HeLa cells the mRNAs of subunits for NADPH oxidase 2 were detected in the absence of TGF β 1 except p40phox mRNA. In order to study the NOX 2 mediated EMT, NOX 2 over-expressed cell line was made by introducing p40phox gene into HeLa cells. NADPH oxidase 2 activated by p40phox overexpression in HeLa cells was associated with increased

production of ROS, decreased epithelial marker and increased of mesenchymal markers (Fig. 6). In transient transfection of p40phox, the amount of gene was critical. In our experimental condition, transfecting above 5ng DNA showed slow cell growth and apoptosis. However, less than 3ng DNA promoted cell growth. In stable cell selection, the cells with proper condition in which favorable level of ROS for cell proliferation may be selected.

In our stable cell model, faster cell proliferation rate seems to be contributed by decreased expressions of p21 and p27. The cell cycle observation also conformed the short G1 phase in those cells. This is first finding that enzymatic overexpression of ROS promotes cell proliferation via p21 and p27 suppression in non-phagocytic cells (Fig. 4).

ROS production by NADPH oxidase 2 systems induced up-regulation of MMP-2 (gelatinase), MMP-7 and MMP-13 (collagenase) (Fig. 5B). Increased expression of MMPs and fast cell migration are general phenomena in EMT. Other previous study showed that Snail-dependent EMT accompanied with increased MMP-2 (45), MMP-7 could also cleave E-cadherin allowing tracheal epithelial cells (46) and MMP-13 was frequently upregulated to drive the invasion of the phenotypically altered cells (47, 48). Radisky *et al.*, (49) reported that MMP-3 treatment to mouse mammary epithelial cells induced EMT. MMP-3 treatment induced highly active Rac1b and ROS production and stimulated production of ROS caused genetic instability. However, our results showed that there was no significant change of MMP 3 expression in NOX 2 activated systems. Even though they did not explain how the MMP-3 induces ROS, we suspect that Rac1b induction may activate NOX 2 system to generate ROS because Rac1 is one of component for NOX 2 activation.

Recently, ROS signaling pathway has been reported to be intimately involved with EMT in both physiological conditions and pathological processes (50, 51) ; however the functions of ROS in the processes of EMT remain unclear. In this study, we have demonstrated that expression of mesenchymal markers (including fibronectin, slug, snail, vimentin and coronin C) were up-regulated by noble NADPH oxidase 2 activated systems. Using our system, we discovered that expression of Coronin C and YB-1 was affected by ROS. Moreno-Bueno *et al.*,(52) suggests that Coronin C may be a strong candidate as both a biomarker for invasive cancer and functionally important for disease progression. We found that the expression of p40phox in epithelial cells induced an YB-1 up-regulation by ROS (Fig. 7). Recent study identified YB-1 as a new player in the regulation of EMT through a novel mechanism in MCF 7 adenocarcinoma cells (33). Interestingly, YB-1 was inhibited by shSLUG in HeLa-p40phox cells (Fig. supplemental data 1) and it suggested that YB-1 is downstream target in ROS induced EMT system. These results support a hypothesis that ROS mediated expression of slug and downstream YB-1, however, inducible YB-1 only is not sufficient to induce EMT; other factors need with ROS to orchestrate this process.

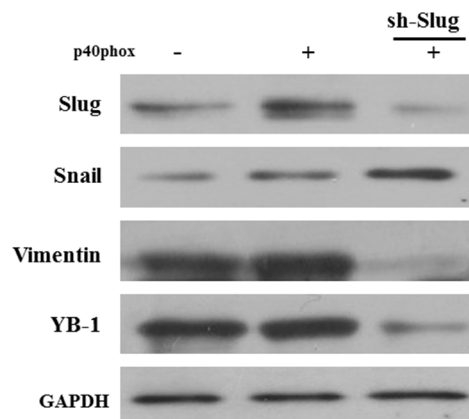
We also tested whether specific inhibitors can block the effect of EMT on the signaling pathway (Fig. 8). It is well established that ROS signals through MAP Kinase cascade. Inhibition of PI3K, p38MAPK and JNK, effectively blocked ROS induced EMT (Fig. 8). But, our results suggested that ROS-PI3K-p38MAPK pathway is the molecular signaling mechanism in ROS induced EMT in HeLa cells. Since Smad-independent pathway is the JNK and

p38MAPK signaling cascades, TGF- β 1-NOX2-ROS-EMT might be more important in Non-Smad pathway.

This study shows for the first time that NADPH oxidase 2 can regulate ROS-mediated EMT regulated in part by PI3K-p38 Map kinase activation in nonphagocytic cell. Therefore, NOX 2 may be an attractive molecule for therapeutic targeting to prevent tumor progression in human EMT

Supplementary data 1. YB-1 expressed blocked by ShSLUG

To determine the molecules downstream of slug, we shSLUG plasmid were transiently transfected in HeLa-p40phox cell. These results show that the knockdown of Slug in HeLa-p40phox cells resulted responsible for repression of YB-1 and mesenchymal protein vimentin and activation of other mesenchymal protein snail. The another study reported that overexpression of YB-1 in H-Ras-transformed MCF-10A cells induces EMT accompanied by enhanced metastatic potential (35). We suggest that the YB-1 gene is a novel upstream regulator of snail, and downstream regulator of slug.

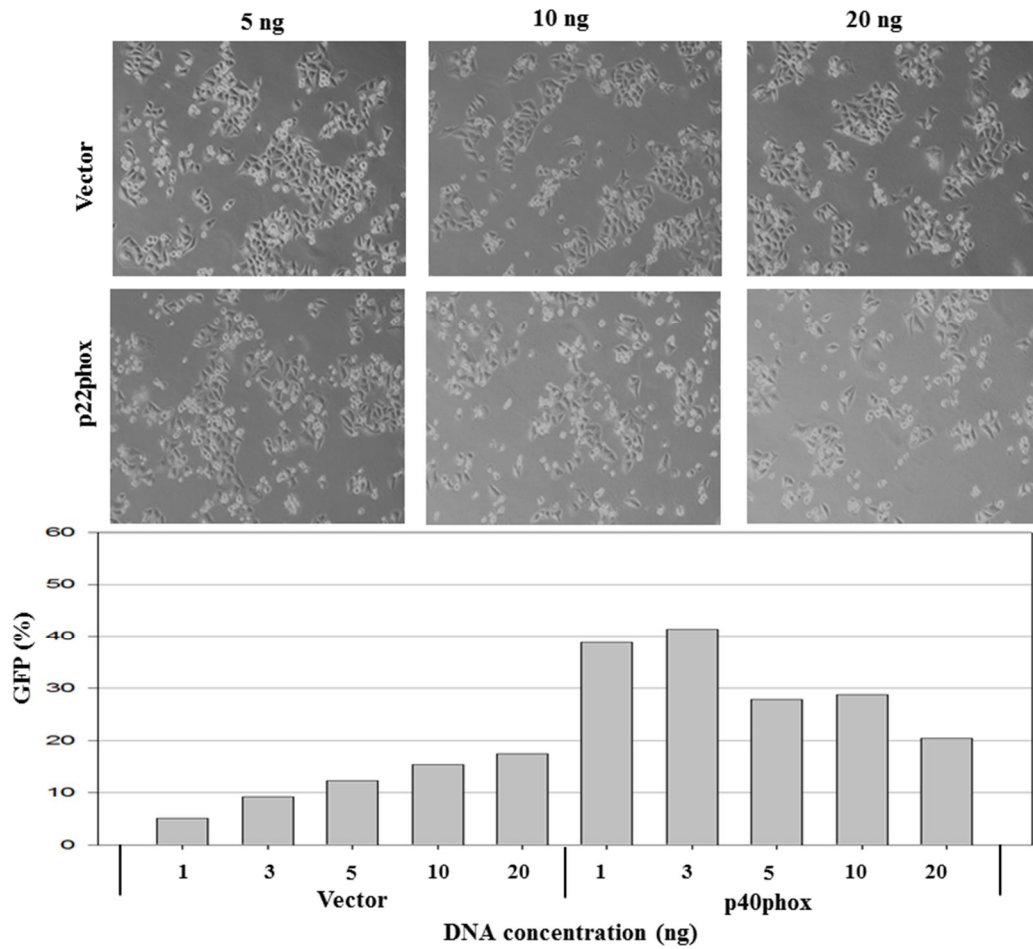


S1. Down-regulation of YB-1 by shSLUG.

The empty/shSLUG transiently transfected (1 μ g, 24 h) in HeLa-p40phox stable cells. YB-1 expression of with shSLUG or without shSLUG in HeLa-p40phox cell were examined by western blot. Western blot were GAPDH to control for loading. This construct was expressed with 40phox or control plasmid pEGFP-N1 in HeLa cells.

S2. In vitro transfection efficiencies

We determined that the effects of p40phox overexpression in HeLa cells. Difference p40phox DNA concentration efficiencies *in vitro* varied depending on the protocol and p40phox plasmid transfection by methods with lipofectamin. We hypothesized that exposure to ROS might lead to cell death through the induction of apoptosis in HeLa cells. Because, previous studied of the low levels is reactive oxygen species (ROS) can function as redox-active signaling messengers, whereas high levels of ROS induce cellular damage (53). The GFP positive cell number were significantly decreased in p40phox plasmid (>3 ng) transfectants when compared to the GFP vector transfectants. In these results suggest that HeLa-p40phox cells death pathways are activated by high level ROS. Indeed, p40phox induces cell death through the generation of oxidant stress in HeLa cells.

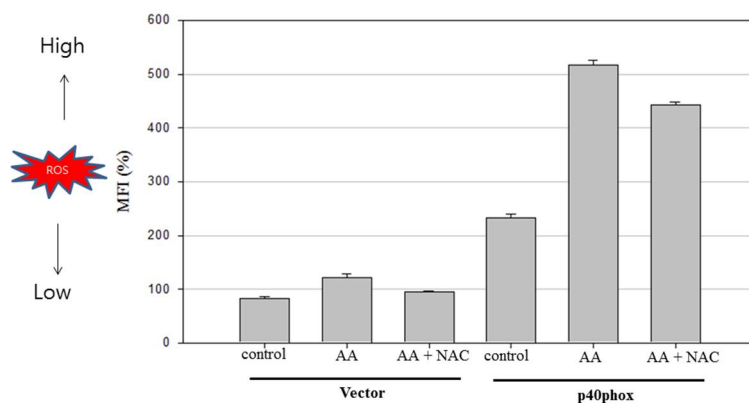


S2. ROS generation at different DNA concentrations in HeLa-p40phox cells.

HeLa cells were transiently transfected with different DNA concentrations between 1 ~ 50 μ g of DNA for 24 hr. Generation of ROS was assessed by DCF-DA fluorescent. And expressed of GFP was visualized by fluorescence microscopy. Flow cytometric analysis of EGFP expression in transfectants. Typical results were shown from independent experiments performed at least three times.

S3. NADPH oxidase activation mediated ROS generation by arachidonic acid (AA)

Arachidonic acid (AA, known activators of NADPH oxidase) has been used frequently as an activator of NOX 2 in cell-free assay systems (54). Recent studies have shown that the orchestration of low concentrations of AA produced by PLA2 together with protein kinase C (PKC)-dependent phosphorylation promotes translocation of p40phox and enhances ROS production by Nox2 (55). Therefore we expected that AA of the regulators of NADPH oxidase activity may be high level ROS production. Results of AA stimulated showed a concentration-dependent ROS generation via NADPH oxidase activation and AA-stimulated ROS was blocked by NAC (antioxidant). We suggest that these results of was significantly higher level ROS generation by AA-stimulated and ROS production was not enhanced by AA non-stimulated.

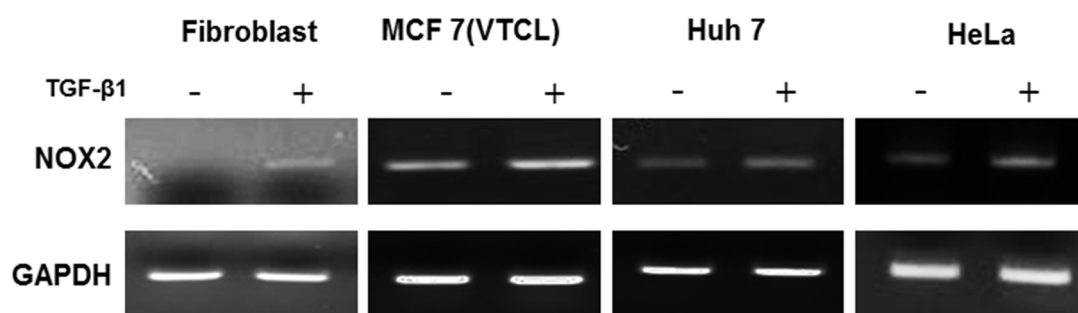


S3. Activation of NADPH oxidase stimulates AA.

Arachidonic acid stimulated ROS generation was examined using DCFDA fluorescence. AA (1 μ M)-stimulated superoxide anion production in HeLa-p40phox cells. And this AA

induced ROS generation was blocked by inhibitors of ROS (NAC, 5 mM). Error bars indicate SD, $n = 3$.

S4. TGF- β 1-induced expression of NOX 2



S 4. TGF- β 1-induced expression of Nox-2 in different nonphagocytic cells.

Cells were treated with TGF- β 1 for 24. And the western blot was GAPDH to control for loading.



PART II

Genetic Analysis of 10 Unrelated Korean Families with p22-phoxdeficient Chronic Granulomatous Disease: An Unusually Identical Mutation of the CYBA Gene on Jeju Island, Korea

Footnote : This chapter was accepted in *J. Korean Med Sci.* and published in internet version in January 2009.

1. ABSTRACT

Chronic granulomatous disease (CGD) is a rare hereditary disorder characterized by recurrent life-threatening bacterial and fungal infections. The underlying defect in CGD is an inability of phagocytes to produce reactive oxygen species as a result of defects in NADPH oxidase. Considering that CGD generally affects about 3-4 in 1,000,000 individuals, it is surprising that the prevalence of CGD on Jeju Island is 20.7 in 1,000,000 individuals. We performed genetic analysis on 12 patients from 10 unrelated families and found that all patients had an identical homozygous single-base substitution of C to T in exon 1 (c.7C>T) of the *CYBA* gene, which was expected to result in a nonsense mutation (p.Q3X). Because Jeju Island has long been a geologically isolated region, the high prevalence of CGD on Jeju Island is presumably associated with an identical mutation inherited from a common ancestor or proband.

Key words : *p22phox*, *CGD*, *Jeju Island*

2. INTRODUCTION

Chronic granulomatous disease (CGD) is a rare hereditary disorder characterized by recurrent life-threatening bacterial and fungal infections (1). The underlying defect in CGD is an inability of phagocytes to produce reactive oxygen species (ROS) as a result of defects in NADPH oxidase (2). NADPH oxidase is composed of several structural and regulatory proteins. Two of these, gp91-phox and p22-phox, are integral membrane proteins that form flavocytochrome_{b558}, the electron-transport center of the oxidase. The cytosolic proteins, p40-phox, p47-phox, and p67-phox, exist as a tight complex in the cytosol of resting phagocytes (3, 4). After ingestion of microbes into phagosomes, the cytosolic proteins translocate to the membrane to complex with the flavocytochrome to form activated NADPH oxidase, which generates ROS (5). CGD is a genetically heterogeneous disease caused by defects in the genes encoding any of the NADPH oxidase components. Approximately 60% of CGD patients showed an X-linked inheritance, which is caused by mutations in the *CYBB* gene encoding gp91-phox. Autosomal recessive forms of CGD are caused by mutations in one of three genes: the *CYBA* (p22-phox) gene, the *NCF1* (p47-phox) gene, and the *NCF2* (p67-phox) gene. Mutations in these three genes collectively account for about 30-40% of CGD patients (6). Mutations in the p67-phox and p22-phox genes are less common, and to date no patients have been reported with defects in p40-phox (6). Although the prevalence of CGD may actually be higher than reported because of the under-diagnosis of milder phe-

notypes, the estimated prevalence of CGD is between 1 in 200,000 and 1 in 250,000 individuals, with variable occurrence in different countries (6-11). According to a collation by the Korean College of Pediatric Clinical Immunology, the prevalence of CGD from 2001 to 2005 in Korea was 0.9 in 1,000,000 individuals. Most regions of Korea had similar prevalence of CGD (from 0.4 to 1.7). The prevalence of CGD on Jeju Island was a surprising 20.7, showing 10-50 times higher than that in other regions of Korea (paper in preparation). The aim of this study was to examine the genotype of CGD patients on Jeju Island.

3. MATERIALS AND METHODS

3.1. Patients

Between January 1993 and December 2007, the available data for CGD patients on Jeju Island were obtained from the medical records of Jeju National University Hospital. The diagnosis of CGD was based on a history of recurrent infections and previously affected family members. The diagnosis was confirmed by an impaired phorbol myristate acetate (PMA)-stimulated nitroblue tetrazolium (NBT) test and/or dihydrorhodamine-1,2,3 (DHR) flow cytometry assay. Twelve patients with CGD (3 males and 9 females) from 10 unrelated families were enrolled for Western blot and mutation analysis. All available family members were analyzed for confirming the heterozygous status. This study was approved by the Institutional Review Board of Jeju National University Hospital (2006-14), and informed consent for genetic analysis was obtained from all patients and/or their parents.

3.2. DHR flow cytometry

DHR flow cytometry was used to evaluate the generation of ROS by phagocytic cells as previously described (12). Red blood cells were lysed by mixing 400 μ L of whole blood with 4 mL of lysis buffer (174 mM ammonium chloride, 20 mM sodium bicarbonate, and 1 mM EDTA). White blood cells (WBCs) suspended in Hank's buffered salt solution containing 0.1% bovine serum albumin were loaded with 1 mM EDTA, followed by 1 unit/ μ L catalase (Roche Diagnostic Cooperation, Indianapolis, IN, U.S.A.) and 100 mM DHR (Molecular

Probes, Eugene, OR, U.S.A.). PMA (Sigma-Aldrich, St. Louis, MO, U.S.A.) was added to the cells at a final concentration of 20 ng/mL, and the cells were incubated for 15 min. After incubation, the cells that had formed rhodamine by oxidizing DHR were counted with an EPICS[®] XL flow cytometer (Coulter, Miami, FL, U.S.A.).

3.3. Western blot analysis of the NADPH oxidase components

WBCs were solubilized in a lysis buffer containing 100 mM KCl, 10 mM NaCl, 10 mM HEPES, 1 mM EDTA (pH 7.4), 0.1 mM DTT, 1 mM PMSF, 10 µg/mL chymostatin, 1 µg/mL protease inhibitor cocktail (Sigma-Aldrich), 1% Triton X-100, 1% deoxycholic acid, 1% NP-40, and 0.05% SDS. The protein content of the cell lysate was resolved by 5-20% SDS-PAGE and electroblotted onto nitrocellulose membranes. Following a blocking step, the membranes were incubated for 2 hr with the following primary antibodies diluted 1:1,000: polyclonal anti-p22-phox (FL-195), anti-p47-phox (H-195), anti-p67-phox (H-300), and anti-p40-phox (D-8) (Santa Cruz Biotechnology, Santa Cruz, CA, U.S.A.); and anti-gp91-phox (Upstate, Lake Placid, NY, U.S.A.). After multiple washing steps, the membranes were incubated with HRP-conjugated anti-rabbit or anti-mouse IgG (1:10,000 dilution; Vector, Burlingame, CA, U.S.A.). Immunoblot signals were visualized with an Enhanced Chemiluminescence Detection System (Pierce Biotechnology, Rockford, IL, U.S.A.).

3.4. Isolation of total RNA and RT-PCR

Total RNA was extracted from WBCs using an RNeasy[®] mini kit (QIAGEN, Valencia,

CA, U.S.A.), following the manufacturer's instructions. First-strand cDNA was synthesized from 2 µg of RNA with 25 ng/mL Oligo dT (Promega, Madison, WI, U.S.A.), 0.5 mM dNTP mix, 0.2 unit/µL Omniscript (QIAGEN), and 0.5 unit/µL RNase inhibitor. The reaction was incubated at 37°C for 60 min. The synthesized cDNA was amplified using primers (Forward, 5'-ATG GGG CAG ATC GAG TGG GC-3' and Reverse, 5'-TCA CAC GAC CTC GTC GGT CA-3'; *CYBA* accession number, NM_000101) in a 50-µL PCR reaction containing 0.2 mM dNTP mix, 0.4 µM primer, and 1.25 units of *Taq* polymerase (Promega). The PCR conditions were 35 cycles of denaturation at 94°C for 15 sec, annealing at 62°C for 30 sec, and extension at 72°C for 1 min. The RT-PCR products were separated in a 2% agarose gel and stained with ethidium bromide for visualization.

3.5. Isolation and amplification of genomic DNA of *CYBA*

Genomic DNA was extracted from peripheral blood using a Wizard® genomic DNA purification kit (Promega) according to the manufacturer's protocol. The six exons of *CYBA* and the exon-intron junctions were amplified by PCR as previously described (13). Primers used for 5' and 3' untranslated region are as follows; 5' untranslated region: forward 5'-AAA CCA CCA AGT GCC TCG GAT G-3' and reverse 5'-TGA GCC AAT GTG GGG TTT GAG G-3', 3' untranslated region: forward 5'-CAG GCC GAC CCA GGT CCT GGC -3' and reverse 5'-CGG CCC CAG GCA GAG GCT CA-3'. PCR was performed in a 50-µL reaction mixture containing 10 pM of each primer, 0.2 mM dNTPs, 100 mM Tris-HCl, pH 8.3, 1.5 mM MgCl₂, and 2.0 units of *Taq* polymerase (Promega). The amplification conditions were 35

cycles of 95°C for 1 min, 59°C for 1 min, and 72°C for 1 min; followed by a final extension time of 5 min at 72°C. The PCR products were separated in a 1.5% agarose gel and stained with ethidium bromide for visualization.

3.6. Sequence analysis

PCR-amplified products were purified using a QIAquick PCR purification kit (QIAGEN, Hilden, Germany) and analyzed by direct sequencing in both directions using an ABIPrism BigDye Terminator Cycle Sequencing Ready Reaction kit and an ABI Prism 3130 XL Genetic Analyzer (Applied Identical Mutation of the *CYBA* Gene in Korean Families 1047 Biosystems, Foster City, CA, U.S.A.). Primers for the sequencing reactions were the same as those used for PCR. The sequences obtained from CGD patients and healthy controls were compared with GenBank data (*GenBank* accession number, NM_000101) and submitted for BLAST analysis.

4. RESULTS

Between 1993 and 2007, 17 patients from 11 unrelated families on Jeju Island were identified as having CGD. There were 7 males and 10 females, and 5 families (45%) had multiple affected siblings. The diagnosis of CGD was made at a mean age of 2.1 yr (median, 0.5 yr; range 0.1-5.4 yr). Four patients (24%) died during the period, at a mean age of 4.7 yr (range, 0.9 to 14.3 yr). Judging from this study, the prevalence of CGD on Jeju Island is 23.1 in 1,000,000 individuals. Among the CGD patients, 12 patients from 10 families were analyzed by DHR flow cytometric assay and Western blot analysis (Table 2). The ages of the patients at the time of genetic analysis ranged from 3.3 to 28.2 yr. With the DHR flow cytometric assay, all of the patients showed an absence of ROS production, but all other family members with normal phenotype did not show any impairment compared with healthy controls (Fig. 9). Western blot analysis demonstrated the absence of p22-phox expression in all patients, while the expression of gp91-phox, p47-phox, p67phox, and p40-phox was normal in all patients (Fig. 10). Thus, all the patients exhibited the A22° biochemical phenotype of the disease.

The mRNA of *CYBA* gene was reverse transcribed as described above. The cDNA for p22-phox in all patients and family members did not differ in size from that in healthy controls (Fig. 11). Sequence analysis of genomic DNA for *CYBA* gene revealed that all patients

had an identical, homozygous, single-base substitution of C to T in exon 1 (c.7C>T), which was expected to result in a nonsense mutation (p.Q3X). The genomic DNA sequencing results for both parents of all the patients showed a double signal at the same position, which indicated they were heterozygous for the mutation in the *CYBA* gene (Fig. 12). This mutation has been previously reported at the same position in Japanese patients (14, 15). In addition to the mutation described above, six different single nucleotide substitutions (SNP) within the *CYBA* gene were detected in all patients in the same manner during the course of genetic analysis (Table 3).

Table 2. Characteristics of CGD patients in Jeju, Korea.

Family	Patient	Age (yr)	Age at diagnosis	Gender	NBT/DHR test (%)	Phox protein expression				
						gp91	p22	p47	p67	p40
I	1	28 ²	5 ³	F	0	Normal	Null	Normal	Normal	Normal
II	2	14 ^{3*}	5 ⁵	M	0 ¹	ND	ND	ND	ND	ND
	3	20 ⁸	3 ¹¹	F	0	Normal	Null	Normal	Normal	Normal
III	4	19 ⁹	1 ³	F	0	Normal	Null	Normal	Normal	Normal
	5	14 ⁵	2 ³	F	0	Normal	Null	Normal	Normal	Normal
IV	6	1 ^{1*}	ND	F	ND	ND	ND	ND	ND	ND
	7	0 ^{11*}	0 ⁹	M	0 ¹	ND	ND	ND	ND	ND
	8	12 ⁹	0 ¹⁰	F	0	Normal	Null	Normal	Normal	Normal
V	9	12 ⁶	0 ²	F	0	Normal	Null	Normal	Normal	Normal
	10	2 ^{7*}	0 ⁵	M	0 ¹	ND	ND	ND	ND	ND
VI	11	10 ⁶	0 ⁶	M	0	Normal	Null	Normal	Normal	Normal
VII	12	9 ¹⁰	0 ⁵	F	0	Normal	Null	Normal	Normal	Normal
	13	4 ¹	0 ¹	M	0	Normal	Null	Normal	Normal	Normal
VIII	14	9 ⁴	4 ¹	M	0	Normal	Null	Normal	Normal	Normal
IX	15	8 ⁵	4 ⁶	F	0	Normal	Null	Normal	Normal	Normal
X	16	3 ⁴	2 ¹⁰	F	0	Normal	Null	Normal	Normal	Normal

*age at death; confirmed by NBT test.

CGD, Chronic granulomatous disease; NBT, Nitroblue tetrazolium; DHR, Dihydrohodamine-1,2,3; Phox, Phagocyte oxidase; ND, Not determines.

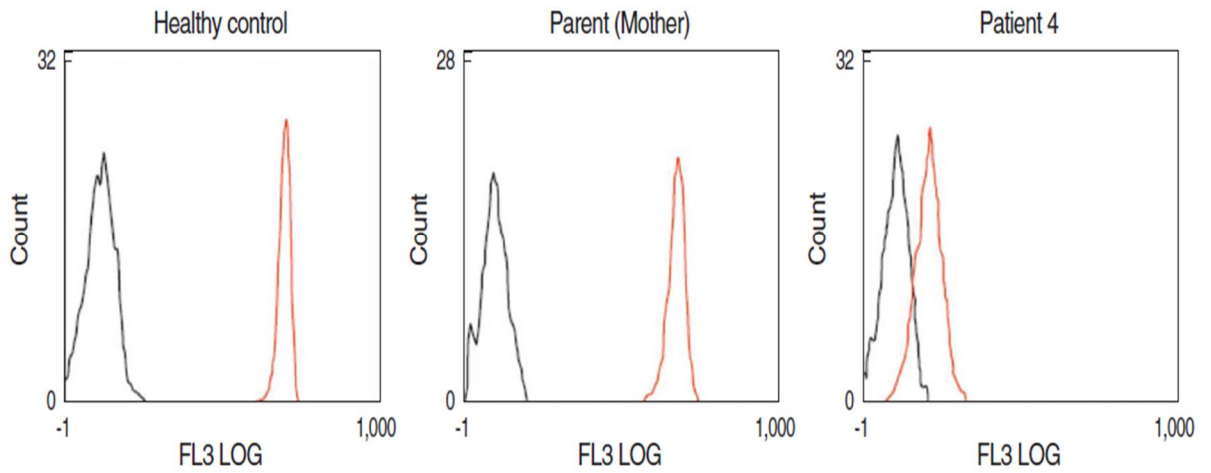


Figure. 9. Dihydrorhodamine-1,2,3 (DHR) flow cytometric analysis of granulocyte oxidative activity in family III. There was no difference in phagocyte oxidative activity between the parents of patient 4 and healthy controls after no stimulation (black) or stimulation with PMA (red). A lack of phagocyte oxidative activity after stimulation with PMA was observed in patient 4.

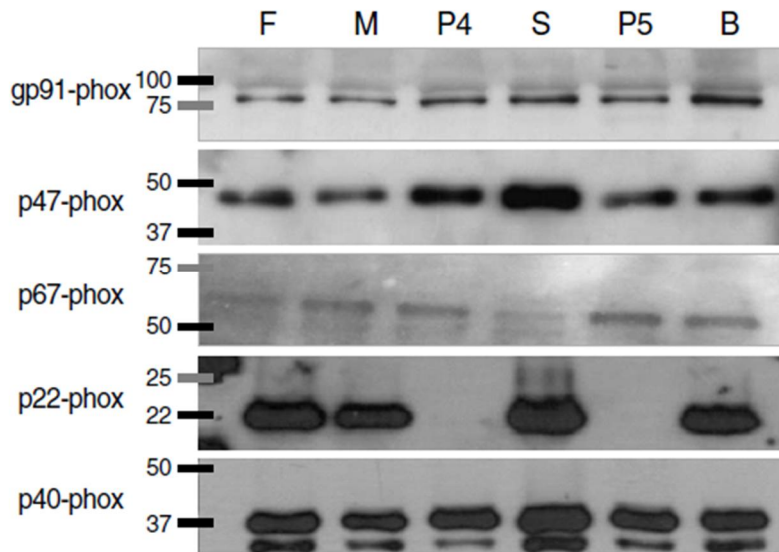


Figure. 10. Western blot analysis of NADPH oxidase components in family III. Western blot analysis demonstrated the absence of p22-phox expression in patients 4 and 5, but the expression of gp91phox, p47phox, p67phox, and p40-phox were normal. There was no abnormal expression of any NADPH oxidase components in other family members. F, Father of patients 4 and 5; M, Mother of patients 4 and 5; P4, Patient 4; S, Elder sister of patient 5; P5, Patient 5; B, Younger brother of patient 5.

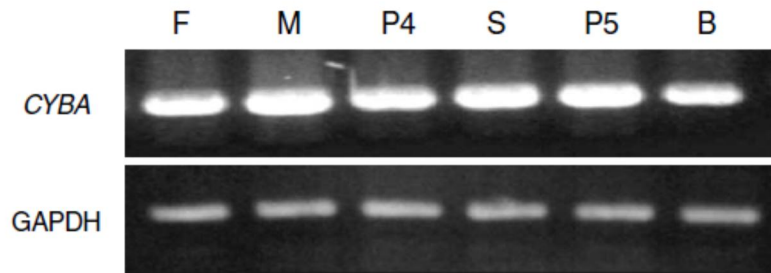


Figure 11. RT-PCR of *CYBA* cDNA from family III. The mRNA of p22-phox was reverse transcribed as described above. There was no difference in size between the p22-phox cDNAs in family III and those in healthy controls. F, Father of patients 4 and 5; M, Mother of patients 4 and 5; P4, Patient 4; S, Elder sister of patient 5; P5, Patient 5; B, Younger brother of patient 5.

Table 3. Single nucleotide substitution within the *CYBA* gene in CGD patients.

Nucleotide changes	Amino acid changes	References
-930 A>G (5' UT region)	NA	16
36 G>A	13 Q > Q (silent)	NR
214 C>T	72 H > Y	16
521 C>T	174 A > V	16
612 A>G (+24 of 3' UT region)	NA	16, 21
646 C>T (+49 of 3' UT region)	NA	NR

CGD, Chronic granulomatous disease; UT region, Untranslated region; NA, Not applicable; NR, Not registered.

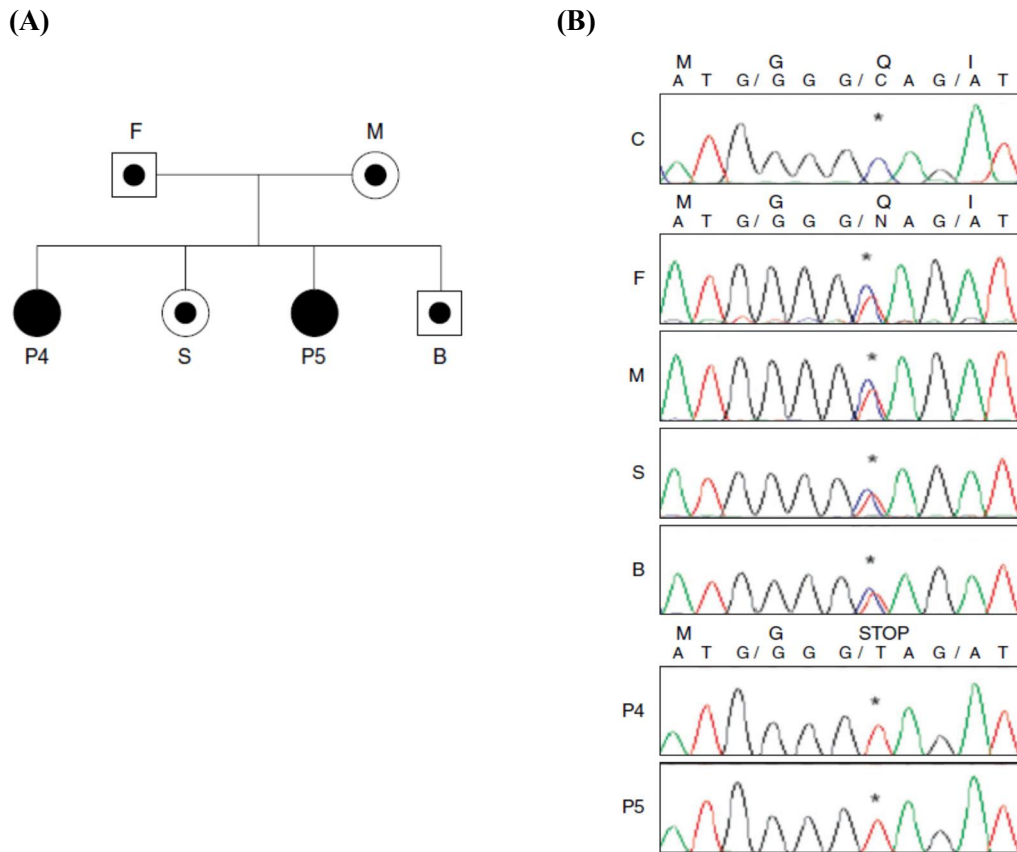


Figure 12. Sequence analysis of the *CYBA* gene from family III. (A) Pedigree of family III. (B) Sequence analysis of the *CYBA* gene from family III. Patients 4 and 5 had an identical, homozygous, singlebase substitution of C- to T in exon 1 (c.7C>T), which was expected to result in a nonsense mutation (p.Q3X). The sequencing results for other family members showed a double signal at the same position, indicating that they were heterozygous for the mutation. *site of mutation. F, Father of patients 4 and 5; M, Mother of patients 4 and 5; P4, Patient 4; S, Elder sister of patient 5; P5, Patient 5; B, Younger brother of patient 5.

5. DISCUSSION

Jeju is a large island off southwest of Korean peninsula. The total population of Jeju Island is 563,388 (Statistics of Jeju Special Self-Governing Province, 2007). Mt. Halla rises in the center of Jeju Island, dividing it into two geographically separated regions, Jeju City and Seogwipo City. In this study, 17 patients from 11 unrelated families on Jeju Island were identified as having CGD; 14 patients were from Seogwipo City and three from Jeju City. The overall prevalence of CGD on Jeju Island is 23.1 in 1,000,000 individuals. Although we tried to identify as many patients as possible, this may be an underestimation of the actual prevalence of CGD on Jeju Island. We hypothesized that the high prevalence of CGD on Jeju Island is associated with an identical mutation inherited from a common ancestor or proband. According to the studies carried out to date, the most common form of CGD is the Xlinked form. The approximately 30-40% of CGD are inherited in an autosomal recessive traits. One of the rarest forms of CGD is caused by mutations in *CYBA* gene, accounting for only 5% of CGD patients (6). Up to the date, 27 mutations in *CYBA* gene are listed in the Human Gene Mutation Database (HGMD; <http://www.hgmd.cf.ac.uk/ac/all.php>) and all 27 mutations reported for *CYBA* gene showed the allelic heterogeneity with no preponderance of common affected alleles or hot spots (16). However, all CGD patients on Jeju Island had an identical, homozygous mutation in the *CYBA* gene and six different SNPs within the *CYBA* gene in the same manner. Moreover, one of the reported Japanese patients with p22-

phox-deficient CGD, sharing the same mutation with CGD patients on Jeju Island, has consanguineous parents (14). In regions with a higher incidence of consanguinity in the population, there is an increase in the prevalence of autosomal recessive genetic disorders, including CGD, as a direct result of a higher rate of inbreeding (10, 11). Altogether, these results strongly suggest that there might have been unique marriage patterns similar to endogamy or consanguineous marriage on Jeju Island. In contrast to previous reports (13-16), a normal level of gp91-phox protein expression was detected in all CGD patients on Jeju Island. By using transgenic expression of gp91-phox and p22-phox in monkey kidney COS7 cells, which lack endogenous p22-phox and gp91-phox expression, gp91-phox was expressed on the cell surface in the absence of p22-phox expression. However, co-expression of gp91-phox and p22-phox were required to support the generation of oxygen radicals in a cell-free NADPH oxidase assay (17). This implies that the association of p22-phox with gp91-phox may be essential for regulation of electron transfer in the redox cycle, but p22-phox may not be necessary for the expression of gp91-phox protein. Further studies are required to understand the expression of gp91-phox in p22-phox-deficient CGD. Based on different clinical parameters, X-linked CGD has a different, more severe, clinical phenotype than the autosomal recessive CGD (6). The prognosis of X-linked CGD and p22-phox-deficient CGD was not better than that of p47-phox-deficient CGD (10), and p22-phox-deficient CGD with the young age at diagnosis appears to be as severe as X-linked CGD (16). Although genetic study has not been performed, X-linked CGD had a significantly earlier age of symptom onset and age at diagnosis than autosomal recessive CGD in Korea (18). To our knowledge,

there were only 2 reports about the genetic analysis of X-linked CGD in Korea (19, 20). It is hard to evaluate the clinical course of CGD patients on Jeju Island in comparison with the different genotype. However, the clinical course of CGD patients on Jeju Island seems to be considered mild in that 30% of the living patients are 20 yr of age or older. There is an increase in the prevalence of autosomal recessive genetic disorders in regions with a higher incidence of consanguinity in the population, as a result of a higher rate of inbreeding. All the CGD patients tested on Jeju Island had an identical and homozygous mutation in the *CYBA* gene. This result is specific to our cohort, as the most common form of CGD in other reports is the X-linked form of CGD. Even though this study is not a nationwide survey of CGD in Korea, the finding of an identical mutation in a single region with a highly prevalent rate is quite unique. This is not consistent with the generally accepted principle of recessively inherited rare diseases. In Korea, there is a law prohibiting marriage between people with the same surname and the same family origin. However, since Jeju Island has been a geologically isolated region for a long time, there might have been unique marriage patterns similar to endogamy or consanguineous marriage. This may explain the unusual identical mutation of the *CYBA* gene and the high prevalence of autosomal recessive forms of CGD on Jeju Island. We are preparing to investigate the genotyping further by using microsatellite markers. This approach may help to elucidate the genetic characteristics of the population by revealing a particular familial structure on Jeju Island. In this study, six SNPs within the *CYBA* gene were detected in the course of genetic analysis. Although we did not check for these SNP sites in a larger scale population, two SNPs in the *CYBA* gene have not yet been regis-

tered as a polymorphism in the database of SNPs (<http://www.ncbi.nih.gov/> SNP/): one located at nucleotide position G-36>A, which changes 13 Q codon GGG into the alternative Q codon GGA; and the other at nucleotide position 646 C>T in the 3'untranslated region of the *CYBA* gene. In conclusion, we demonstrate all patients of CGD in Jeju Island have an identical, homozygous mutation in the *CYB* gene.



PART III

**Survey on the present condition of heterozygote carriers
with p22-phox-deficient CGD on *Jeju Island*, Korea**

1. ABSTRACT

Chronic granulomatous disease (CGD) is a genetically heterogeneous disease caused by defects in the genes encoding any of the NADPH oxidase components. The estimated prevalence of CGD is between 1 in 200,000 and 1 in 250,000 individuals, with variable occurrence in different countries. According to a collation by the Korean College of Pediatric Clinical Immunology, the prevalence of CGD in Korea was 0.9 in 1,000,000 individuals. However, it is surprising the prevalence of CGD on *Jeju Island* is 20.7 in 1,000,000 individuals. We found that 12 patients from 10 unrelated families on *Jeju Island* had an identical homozygous single-base substitution of C to T in exon 1 (c.7C>T) of the *CYBA* gene. We hypothesized that the high prevalence of CGD on *Jeju Island* is associated with an identical mutation inherited from a common ancestor or proband. The aim of this study was to investigate the present condition of heterozygote carriers with p22-phox-deficient CGD on *Jeju Island*. Seven hundred four subjects were enrolled from residents on *Jeju Island*. To detecting a heterozygote carrier with specific genotype on *Jeju Island*, nested PCR was employed with using specific primers, using whole blood samples as a source of genomic DNA. The number of detected carrier was nine and the expectable number of carrier is 1.3 in 100 individuals. The heterozygote frequencies for p22phox in higher of the p22phox heterozygote carrier were observed among differently regions. The heterozygote carriers were found in whole regions on *Jeju Island* and there was unrelated between the detected carriers. Alto-



gether, these results strongly suggest that there might have been unique marriage patterns similar to endogamy or consanguineous marriage on *Jeju Island*.

Keywords; Chronic granulomatous disease, p22phox, Carrier, Survey

2. INTRODUCTION

Chronic granulomatous disease (CGD) is a genetically heterogeneous disease caused by defects in the genes encoding any of the NADPH oxidase components (1-3). The estimated prevalence of CGD is between 1 in 200,000 and 1 in 250,000 individuals, with variable occurrence in different countries (1, 4-7). According to a collation by the Korean College of Pediatric Clinical Immunology, the prevalence of CGD in Korea was 0.9 in 1,000,000 individuals. Most regions of Korea had similar prevalence of CGD (from 0.4 to 1.7), but the prevalence of CGD on *Jeju Island* was a surprising 20.7, showing 10-50 times higher than that in other regions of Korea .

Jeju is a large isolated island located to the southeast of Korea. Mt. Halla rises in the center of *Jeju Island*, dividing it into two geographically separated regions, *Jeju City* and *Seogwipo City*. We demonstrated that the overall prevalence of CGD on *Jeju Island* is 23.1 in 1,000,000 individuals, with a prevalence of 7.4 in 1,000,000 individuals in *Jeju City*, and a surprising 64.6 in 1,000,000 individuals in *Seogwipo City* (8). Moreover, all CGD patients on *Jeju Island* had an identical mutation in the *CYBA* gene.

The polymerase chain reaction (PCR) is ideally suited to providing numerous DNA templates for mutation screening, because of its rapid and versatile method for amplifying defined target DNA become an individually technique for the detection (4, 9-11). We hypothesized that the high prevalence of CGD in *Seogwipo City* is associated with an identical muta-

tion inherited from a common ancestor or proband. The application describes a novel method for detection of a heterozygote carrier, e.g., the 7 C/T nonsense mutation, in the p22phox gene using nested PCR. Thus, we expected that based on the results carrier detected in p22phox heterozygote analysis, the present invention provides specific, efficient, reproducible, and accurate detection of such heterozygote carrier in genomic DNA.

3. MATERIALS AND METHODS

3.1. Study population

Seven hundred four unrelated subjects (0.5% of the population of *Seogwipo City*) were enrolled from *Seogwipo City* (Table 1). Age and district distribution of subjects were similar to the population of *Seogwipo City*. Blood samples were taken from between January 2008 and December 2008. This study was approved by the Institutional Review Board of Jeju National University Hospital, and informed consent was obtained from all enrolled subjects and/or their parents.

3.2. Nested PCR amplification of a specific region on *p22phox* exon 1

Isolation and amplification of genomic DNA of *p22phox* Genomic DNA was extracted from peripheral blood using QIAamp Blood kit (Qiagen, Hilden, Germany) according to the manufacturer's instructions. To detect a specific region on *p22phox* exon 1, we used a nested PCR amplification method. The first PCR for a specific region on *p22phox* exon 1 was carried out with the primers (Forward, 5'- TAT GCC TCG GCG TGG CTA GAG A -3' and Reverse, 5'- TCA GAA CTC CTC CTT CCA GCC -3') in a 50- μ L reaction mixture containing 10 pM of each primer, 0.2 mM dNTPs, 100 mM Tris-HCl, pH 8.3, 1.5 mM MgCl₂, and 0.25 units of Taq polymerase (EF Taq, Solgent, Korea). The amplification conditions were 25 cycles of 95°C for 1 minute, 64°C for 30 seconds, and 72°C for 1 minute; followed

by a final extension time of 5 minute at 72°C. The second PCR was performed with primers (Forward, 5'- GGT TCG TGT CGC CAT GCT GT - 3' and Reverse, 5'- GGT TCG TGT CGC CAT GGT GT - 3'). The second PCR condition was initial denaturation for 5 minute at 95°C, 30 cycles of amplification with denaturation at 94°C for 50 seconds, primer annealing at 68°C for 59 seconds, extension of primer at 72°C for 2 minute.

3.3. Sequence analysis for precision test of heterozygote-specific primers

In order to test the specificity of mutation-specific primers, *one hundred* PCR products randomly selected from subjects presumptively without carrying the mutation in the *CYBA* gene. PCR products were purified using a QIAquick PCR purification kit (QAIGEN, Hilden, Germany) and analyzed by direct sequencing in both directions using an ABI-Prism BigDye Terminator Cycle Sequencing Ready Reaction kit and an ABI Prism 3130 XL Genetic Analyzer (Applied Biosystems, Applied Biosystems/Life Technologies Corporation, USA). Primers for the sequencing reactions were the same as those used for PCR, but at 2 pM concentration. The sequencing reaction was performed under conditions of 25 cycles of denaturation at 96°C for 10 seconds, annealing at 50°C for 5 seconds and extension at 60°C for 240 seconds. The sequences were compared with GenBank data (GenBank accession number, NM_000101) and submitted for BLAST analysis.

3.4. Data analysis

Data are expressed as the mean \pm SD. Statistical analyses were performed using SPSS ver.13.0 (SPSS Inc., Chicago, IL, USA). All statistical comparisons were made with t-test and χ^2 test. A *P* value of less than 0.05 ($P < 0.05$) was considered to be statistically significant.

4. RESULTS

In a previous study we found that 12 patients from 10 unrelated families on *Jeju Island* had an identical homozygous single-base substitution of C to T in exon 1 (c.7C>T) of the *CYBA* gene (8). We hypothesized that the high prevalence of CGD on *Jeju Island* is associated with an identical mutation inherited from a common ancestor or proband. We used the nested PCR assay to detect heterozygote carrier for 704 populations (Table 4). However, heterozygote specific primers were designed to the desired region of p22phox gene. The sensitivity of the nested PCR assay was detection using gDNA templates prepared from subjects. In this study, total 704 subjects comprised of the between age range >20 and 65< years (347 males and 357 females) by detection of the specific genotype on *Jeju Island* (Table 4).

Table 4. Characteristics of study population

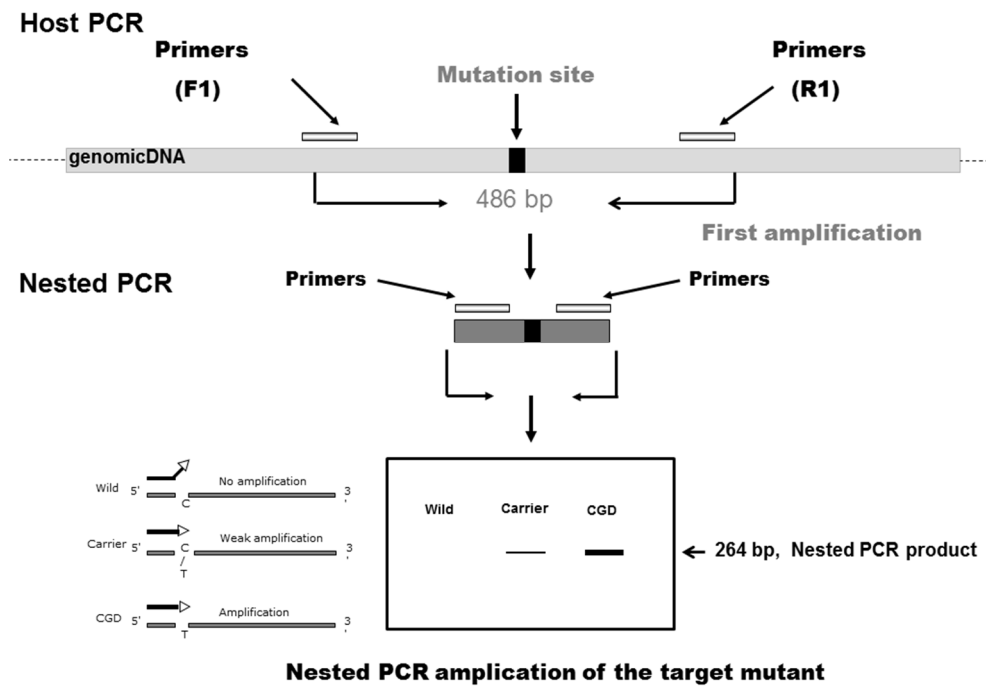
	No. of subjects (%)			P value
	Total	male	female	
	704(100.0)	347(49.3)	357(50.7)	
Age(mean±S.D, years)	50.20±24.39	50.20±24.99	50.19±23.84	0.996*
≤ 20	138(19.6)	70(20.2)	68(19.0)	0.772**
21-30	35(5.0)	17(4.9)	18(5.0)	
31-40	46(6.5)	22(6.3)	24(6.7)	
41-50	73(10.4)	34(9.8)	39(10.9)	
51-60	90(12.8)	41(11.8)	49(13.7)	
61-70	155(22.0)	74(21.3)	81(22.7)	
≥ 71	167(23.7)	89(25.6)	78(21.8)	
area				
Namwon	186(26.4)	86(24.8)	100(28.0)	0.441**
Daejeong	67(9.5)	37(10.7)	30(8.4)	
Seogwiposi	249(35.4)	121(34.9)	128(35.9)	
Seongsan	106(15.1)	50(14.4)	56(15.7)	
Andeok	39(5.5)	24(6.9)	15(4.2)	
Pyoseon	57(8.1)	29(8.4)	28(7.8)	

*, using t-test.; **, using χ^2 test

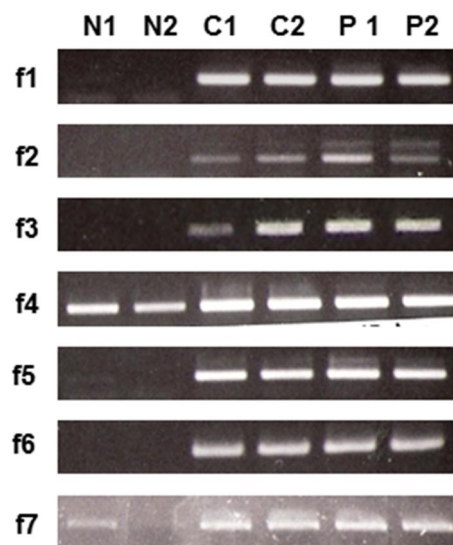
When specific primers for nested PCR amplifications were used, the nested PCR assay amplified a specific 264 bp product with DNA template prepared from blood of subjects. Figure 13A, illustrates nested PCR reactions for the p22pox gene. For this technique, an oligonucleotide primer is designed for the detected of heterozygous site. Various combinations of the primers listed in Table 5 were used to identify the optimal set of host and nested PCR. We also observed a reduction in sensitivity compared with nested PCR amplifications when the two primer pairs (f 4 and f 7) were sets used. Also, we found that five primers (f1, f2, f3, f5 and f6) were increased of detection sensitivity in a nested PCR amplification. Because of the f2 and f3 primers were much more efficient at higher than the other primers (Fig. 13B). In this study, we used f2 and f3 primer for the detected of heterozygote carrier.

In this study, the heterozygote samples compared with the wild-type control samples. The interactions among the primers in nested PCR, reactions were performed with different sets of the seven primers on genomic DNA template. Nested PCR in experiments to optimize the sensitivity of detection, and amplified products was observed on agarose gels (Fig 13C). When the oligonucleotide primers were used in PCR amplification, as opposed to nested reactions, the sensitivity of detection was drastically increased. And then, the heterozygote samples showed positive results by the nested PCR. And, the positive samples were analyzed by sequencing.

(A)



(B)



(C)

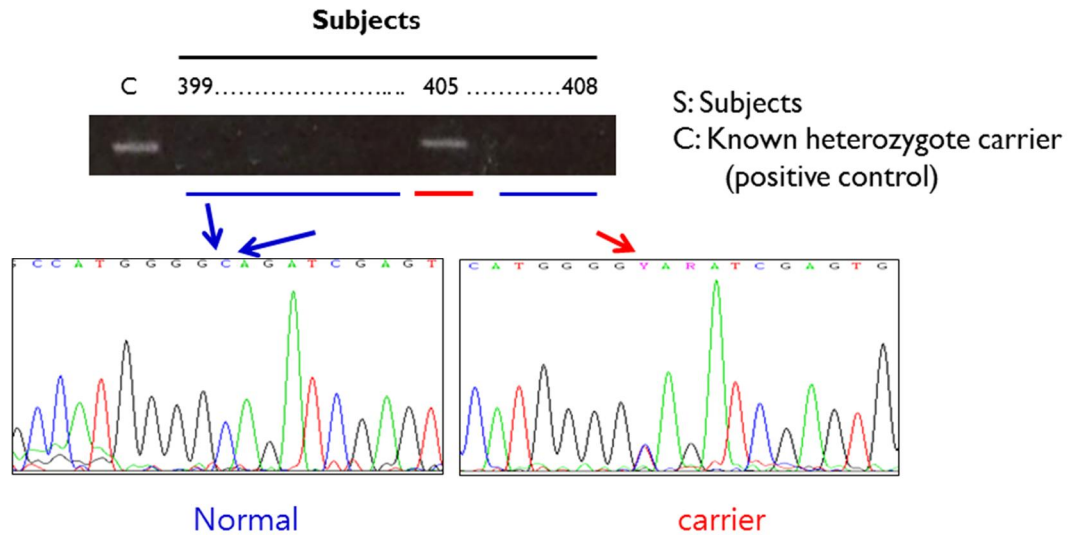


Figure 13. Identification of the mutant site by nested PCR for the determination of the

p22phox heterozygous carrier. (A) Mutant site gDNA from human blood was subjected to nested PCR. The first-host PCR was performed using the primer F1 and R1 p22phox gene-specific primer, whose positions are illustrated in (A). The nested PCR was performed using the heterozygote-specific primer, whose positions are also illustrated in (A). The resulting nested PCR product was analyzed by 1.2% agarose gel electrophoresis and visualized by ethidium bromide staining. (B) Analysis of specificity for representative heterozygote specific primer pairs. Identification of normal and p22phox heterozygote by PCR amplification: gDNA isolated from normal, heterozygous and homozygous individuals for the p22phox. Lanes 1 and 2, normal control (N1 and N2); lanes 3 and 4, heterozygote carrier (C1 and C2); lane 5 and 6, CGD p22phox defective patients (P1 and p2)

(C) Detection of normal and heterozygote by nested PCR assay. And positive samples ana-

lyzed by sequencing analysis. gDNA isolated from 704 subjects.

Table 5. List of primers used in this study.

Primers	sequence
Host PCR primers	
p22phox F1	5' – TATGCCTCGGCGTGGCTAGAGA
p22phox R1	5'- TCAGAACTCCTCCTTCCAGCC
Nested PCR primers (sensitivity primer)	
f 1	5' – GGTTTCGTGTCGCCATGCTGT
f 2	5'- GGTTTCGTGTCGCCATGGTCT
f 3	5'-GGTTTCGTGTCGCCATGGTGT
f 5	5' – GGTTTCGTGTCGCCATGGTCTA
f 6	5' - GGTTTCGTGTCGCCATGCTGTA
Nested PCR primers set (nonsensitivity primer)	
f 4	5' – GGTTTCGTGTCGCCATGGTGTA
f 7	5' - GGTTTCGTGTCGCCATGGGTTA
R	5' - TCAGAACTCCTCCTTCCAGCC CG

A total of 704 samples were screened using by nested PCR. And, the heterozygous gene determined by the nested PCR using the specific primers. The finding from our study, we found that 9 samples were positive by nested PCR (Table 3), and the samples were reanalyzed by sequencing analysis.

Table 6. District distribution of heterozygote carriers and CGD patients

Area	subjects	Heterozygote carriers	CGD patients	P-value
Namwon	186(26.4)	1(11.1)	1(7.1)	0.441*
Daejeong	67(9.5)	2(22.2)	1(7.1)	
Seogwiposi	249(35.4)	2(22.2)	5(35.7)	
Seongsan	106(15.1)	1(11.1)	3(21.4)	
Andeok	39(5.5)	0(0)	0(0)	
Pyoseon	57(8.1)	3(33.3)	4(28.6)	
	704	9	14	

*; using χ^2 test

We were reported the geographic and age distribution of carrier detected by nested PCR. Geographic distribution of the p22phox heterozygous carrier using by nested PCR. In our study obtained results for the *Seogipo* (4 people), *Pyoseon* (3 people), *Namwon* (1 people), and *Daejeong* (1 people) as compared to the overall subjects. In contrast, the heterozygous carrier could not be found in *Seongsan* and *Andeok* (Table 6).

In case of age distribution of carriers is shown in Table 7. The heterozygote carrier of p22phox in the different age subjects were estimated to be 1.2% (> 60 age, 4/329), 0.7% (<20 age, 1/144), 1.3% (40-59 age, 2/152) and 1.3% (20-39 age, 2/79).

Table 7. Age distribution of heterozygote carriers.

Age	Heterozygote carriers	Carrier (%)
>60	4/329	1.2%(1:83)
40 - 59	2/152	1.3%(1:76)
20 - 39	2/79	1.3%(2:79)
<20	1/144	0.7%(1:144)
	9/704	

5. DISCUSSION

In this study, we have described a nested PCR assay that has a sensitivity of detection of heterozygote carrier in p22pox gene. *Jeju* is a large isolated island located to the southeast of South Korea. Mt. Halla rises in the center of *Jeju Island*, dividing it into two geographically separated regions, *Jeju City* and *Seogwipo City*. The overall prevalence of CGD on *Jeju Island* is 23.1 in 1,000,000 individuals, with a prevalence of 7.4 in 1,000,000 individuals in *Jeju City*, and a surprising 64.6 in 1,000,000 individuals in *Seogwipo City*, almost nine times that in *Jeju City* (11). We hypothesized that the high prevalence of CGD on *Jeju Island* is associated with an identical mutation inherited from a common ancestor or proband. However, the finding from our study suggest that out of the 704 subjects, 9 (1.3%) were found to be heterozygous carrier for p22pox gene. Indeed, out of 704 subjects 9 had heterozygous gene (7 C/T) and the expectable number of heterozygote carriers in the population of *Seogwipo City* by extrapolation is 2,013.6 (154,895, Statistics of *Jeju* Special Self-Governing Province, 2007).

To test the sensitivity of nested PCR amplification using seven designed primers. Resulted in five primers successive and two primers failed to amplify a specific products in all 704 individuals tested. To test the sensitivity as specific of nested PCR, under actual screening conditions a randomly analysis of the p22pox gene in 704 subjects. The sensitivity and specificity were 98 %, respectively; the two failed positive subjects not detection by nested

PCR. The data also suggest that the failure to detection of heterozygous carrier in the nested PCR assay might be due to experiment error. Results indicate that when both primer sets (f2 and R, f3 and R) were used in nested PCR to amplify the 704 subjects, showed 98 % agreement between the heterozygous amplified by the two primer sets f2 and R or f3 and R. These results suggesting that these primer sets had amplified the target loci correctly and thus are reliable. However, reactions were designed successfully to detect sequence changes in the p22phox genes. Furthermore, we suggest that for future studies prenatal diagnosis, it is recommended that the new techniques be used to improve the sensitivity of detection of p22phox heterozygous carrier by the nested PCR.

In conclusion, nested PCR is an efficient method for detecting known mutant gene. This technique could also be used to detect small deletions and insertions. It is particularly useful for determining the zygosity of common sequence changes in which heterozygotes are likely to be common. Nested PCR can be used to perform population screening, patient screening and carrier testing. This is rapid and inexpensive to automation.



PART IV

**Development of Lentiviral vector and efficient infection
method for the gene therapy of p22phox defective CGD**

1. ABSTRACT

Chronic granulomatous diseases (CGD) are caused by impaired antimicrobial activity in phagocytes, due to the absence or malfunction of the respiratory burst NADPH oxidase. In a previous study we found that 12 patients from 10 unrelated families on *Jeju Island* had an identical homozygous single-base substitution of C to T in exon 1 (c.7C>T) of the *CYBA* gene. Lentivirus vectors expressing gp91phox can't be used in the patients with p22-phox gene defects. Indeed, twelve of the patients have mutations in their autosomal recessive CGD gene encoding p22phox, the largest subunit of the NADPH oxidase. The autosomal recessive p22phox defective CGD carrier derived WBCs were efficiently transduced by the EF1a lentivirus constructs up to 90 % eGFP positive cells at least 3 days post transduction). pLL3.7 driven eGFP expression was stable at least 4 weeks after transduction and persisted after CGD carrier derived cells immortalized by hTERT and Bmi-1. Upon macrophagy (like) differentiation of the transduced HL 60 cells with Dimethyl sulfoxide (DMSO), up to 28 % of the cells were found to be functionally with mean levels of superoxide production of 30 % compared to non-differentiated cells. This study reported the lentivirus efficiently transduced and express genes for extended periods of time.

Key words : p22phox, lentiviral

2. INTRODUCTION

Chronic granulomatous disease is a rare inherited disorder in which superoxide generation by the leukocyte NADPH oxidase is absent or markedly deficient. Because the superoxide generating enzyme is essential for microbicidal activity in phagocytes, patients with CGD who lack the functional oxidase suffer from recurrent and often life-threatening bacterial and fungal infections. The disorder, which has an incidence of approximately 1 in 500,000 individuals, results from mutations in any one of four essential subunits of the NADPH oxidase complexes (1, 2).

Approximately two thirds of cases are caused by defects in the X-linked gene encoding the larger subunit (gp91phox) of flavocytochrome b558, a plasma membrane heterodimer that is the redox center of the oxidase. A rare autosomal recessive form of CGD is caused by mutations in the gene encoding p22phox, the smaller subunit of flavocytochrome b558 (3, 4).

In myeloid cells, the absence of p22phox protein because of genetic defects also results in the loss of gp91phox expression and vice versa, indicating that each of these proteins requires the other for mutual stability. However, this is apparently not true of all cell types, as gp91phox and p22phox are stably expressed in the absence of their partners in COS7 cells (5). The primary structure of p22phox suggests it contains 4 membrane-spanning domains in the N-terminal two-thirds of the molecule, and a proline-rich domain in the C-terminal cytoplasmic tail. Such proline-rich regions can mediate protein-protein association by binding to

SH3 domains that are found in a variety of proteins involved in signal transduction, including the cytosolic phox proteins. The proline-rich domain of p22phox binds the N-terminal SH3 domain of p47phox, and this interaction is believed to play a dominant role in promoting the association of the cytosolic complex, containing p40phox, p47phox, and p67phox, with flavocytochrome b558 (6). Autosomal recessive CGD, seen in the remaining 35% cases, arise due to mutations of the other components of the NADPH oxidase (except p40phox and Rac which are yet to be associated with any CGD phenotype); these include-p22phox, p67phox and p47phox. Of these, the dominant mutations observed is of the p22phox gene which accounts for almost 25 % cases (7-10). But, recently reported the first CGD case with mutations in the *NCF-4* (p40phox subunit) gene (11).

Although almost all patients with CGD died in childhood at the time the disorder was first described in the 1950s the outlook has improved in the past two decades. Currently, in order to prevent microbial infections, conventional management of CGD patients consists of lifelong prophylaxis with antibiotics such as cotrimoxazole, antimycotis such as itraconazole, and interferon- γ (12, 13). However, morbidity caused by infection or granulomatous complications remains significant for many patients, particularly patients with X-CGD, and the overall mortality rate has recently been estimated to be about 2% per year (14). According to a collection by the Korean College of Pediatric Clinical Immunology, the prevalence of CGD from 2001 to 2005 in Korea was 0.9 in 1,000,000 individuals. Most regions of Korea had similar prevalence if CGD (from 0.4 to 1.7). The prevalence of CGD on Jeju Island was a surprising 20.7, showing 10-50 times higher than that in other regions of Korea (15). In the

Prevalence, We performed genetic analysis on 14 patients from 12 unrelated families and found that all patients had identical homozygous single base substitution of C to T in exon 1(c. 7C>T) of the CYBA gene, which was result of nonsense mutation (p. Q3X) (Fig. 14.).

Recombinant retroviral vectors were first shown in the early 1980s to be capable of transferring a functional gene into murine BM cells (16). However, the application of this technology to the treatment of CGD and other hematologic disease in patients has been more difficult than origin all anticipated. Notably, recent work has shown that RV-based HSC gene therapy can provide significant clinical benefits in patients with severe combined immune deficiency (SCID) (17, 18). Unfortunately, RV therapy in both X-linked SCID and chronic granulomatous disease has led to unanticipated adverse events due to LTR-mediated, protooncogene transcriptional activation (19, 20). Thus, activating RV insertions can lead to emergence of clonal dominance, as well as clonal fluctuation that may also eliminate or reduce ongoing clinical benefit. These events have focused attention on self-inactivation (SIN) lentiviral vectors as potential alternative delivery platforms for hematopoietic disorder. LV offer the advantage of targeting non-dividing cells and can efficiency target multipotent, nonhuman primate or human HSC at low viral copy number (21, 22). The self-inactivation design abolishes the transcriptional activity of the viral long terminal repeat (LTR) in target cells and minimizes the risk of emergence of replication-competent recombinants (RCRs) in the vector producer and target cells. In more recent third generations of HIV-1-based vectors HIV 5' LTR sequences were replaced by functionally homologous regions from either Rous sarcoma virus (RSV) or CMV. Further, there is less evidence for

transcriptional silencing of internal promoters within integrated LV, and no bias for integration within transcription start sites (23). Most work with lentivectors has been performed with nontherapeutic marker genes such as eGFP (24-28). It is important to demonstrate that EF1a lentivector efficiently transduced primitive cells with each therapeutic gene of interest, such as the p22phox required for correction AS-CGD.

The previous study, sought to analyze the clinical features and to investigate the molecular genetic defects leading to CGD in Jeju Island (Fig. 14) (15). Also, all CGD patients on *Jeju Island* had an identical mutation in the *CYBA* gene. Here we develop new lentiviral vector for *CYBA* gene defected CGD. The transduction efficiency of new vector in various myeloid cells of CGD carrier derived WBC^{hTERT+Bmi-1} and differentiated HL-60 (macrophagy like) cells were determined. The expression of p22phox via HLV-1 based lentiviral delivery systems efficiently increase the production of superoxide upon stimuli.

3. MATERIALS AND METHODS

3.1. Construction of vectors encoding p22phox

Lentiviral vector pLL3.7-EF1a-p22phox was constructed by replacing the U6 promoter in pLL37 with elongation-factor-1-alpha (EF1a) promoter by using the Xba I and Xho I, and then human 22phox was inserted in the *Hpa I* and *Xho I* to down-stream of the EF1a promoter (Fig . 2).

3.2. Maintenance of cell culture and transfection

The human embrionic kidney HEK 293T and human cervical adenocarcinoma cell line HeLa cell lines were maintained in DMEM (Gibco, life Technologies GmbH, Karlsruhe, Germany) supplemented with 10% heat-inactivated FBS (Gibco), penicillin (100units/ml, Gibco), and streptomycin (100ug/ml, Gibco). The human premyeloid leukemia cell line HL60 was culture RPMI 1640 (containing 10% FBS, Gibco), penicillin (100units/ml, Gibco), and streptomycin (100ug/ml, Gibco).

3.3. Vector production

Lentiviral generation procedure; 1.2×10^7 293 T cells grown in complete DMEM were seeded in 175 cm² tissue culture flasks on the day before transfection. Lentiviral vector DNA (45μg) and packaging plasmids pMDG.2, carrying the envelope transgene (VSV-G)

(11 μ g) and pCMV Δ 8.74, carrying the lentiviral transgene (gag-pol) (32 μ g) were added to 5 mls OPTI-MEM, filtered through a 0.22 μ m filter, and combined with 5 ml filtered OPTI-MEM supplemented with 1 μ l 10mM polyethylenimine (PEI; Sigma, St. Louis, MO) transfection reagent. The transfection reaction was carried at room temperature for 20 minutes during which time the 293T cells were washed once with OPTI-MEM media. The 10 mls of DNA/PEI complexes were subsequently added to the cells and they were then incubated at 37°C/5%CO₂ for 4 hours, then which the media was replaced with 14 mls of complete DMEM. Viral supernatant was harvested at 48 and 72 hours post transfection, filtered through a 0.22 μ m filter and concentrated by ultracentrifugation at 23,000 rpm for 2 hours. Lentiviral pellets were resuspended in 100 μ l serum free media (OPTI-MEM), stored on ice for 20 minutes and then snap frozen in aliquots at -70°C.

3.4. Virus titration

HeLa cells and HEK 293T cells were plated at 8x10⁴ per well in 6-well plates in DMEM medium. The following day, 2 μ l of 8mg/ml polybrene (Sigma, St. Louis, MO, USA) was added per well (1:1000 final dilution) and supernatant virus containing added at 1:10 to 1:10000 dilutions in a final volume of 2 ml. After 48h incubation, virus titer was quantified by flow cytometric (FACS, BD bioscience) analysis of the eGFP reporter gene.

3.5. Transduction and calculation of the titer in transducing units

For transduction assays, HeLa or HEK 293T cells were seeded at 1×10^5 to 3×10^5 per well in 12-well plates the day before transduction. At day 1, the medium was removed and replaced with transduction medium made of 100 μ l of vector, 300 μ l of serum-free medium, and polybrene at 4 μ g/ml. After 3 h of incubation, 1 ml of complete medium was added. At day 1, cells from three nontransduced wells were trypsinized and fixed to allow calculation of the rate of cell division. At day 3, cells were trypsinized and GFP expression was analyzed by flow cytometry (FACScalibur; Becton-Dickinson). Transduction titers (in transducing units per milliliter) were calculated using the percentage of GFP-positive cells, the rate of cell division between the day of transduction and the day of analysis, and the flow of the FACScalibur (21). Multiple serial dilutions of vector-containing medium (1/10, 1/100, and 1/1,000) were used for the transduction assays, and titers were calculated for linearly correlated values.

3.6. Infection of hTERT and Bmi-1 constructs

The full-length human hTERT cDNA was cloned by RT-PCR using RNA extracted from HeLa cells by RT-PCR using RNA extracted from K562 cells. Thermoscript RT-PCR (Invitrogen) and KOD polymerase (TOYOBO) were used for the RT and PCR reactions, respectively. The forward primer, 5'-GGAATTCGCCGCGCGCTCCCCGCTGCCGAGCC-3', and reverse primer, 5'-GCTCTAGATTAGTCCAGGATGGTCTTGAAGTCT-3', were designed to obtain the coding sequence of human hTERT flanked. PCR product was cloned between the multicloning sites of pCLXSN to generate pCLXSN-ACC- hTERT.

Also, the full-length human *bmi-1* cDNA was cloned by RT-PCR using RNA extracted from K562 cells. Thermoscript RT-PCR (Invitrogen) and KOD polymerase (TOYOBO) were used for the RT and PCR reactions, respectively. The forward primer, 5'-ACGCGTCGACCGCCATGCATCGAACAACGAGAAT-3', and reverse primer, 5'-CGGATCCTCAACCAGAAGAAGTTGCTG-3', were designed to obtain the coding sequence of human *bmi-1* flanked by a *SalI* site (underlined), a Kozak consensus sequence at the 5'-end, and a *BamHI* site (underlined) at the 3'-end. The *SalI* - *BamHI* segment of the PCR product was cloned between the *XhoI* and *BglIII* sites of pMVSCV-puro to generate pCMV-puro-hBmi-1. Production of pCLXSN-ACC-hTERT and pCMV-puro-hBmi-1 retroviruses were obtained from **Kyu-Kye Hwang** Laboratories (*College of Veterinary Medicine, Jeju National University*). One milliliter of producer cell culture fluid was added isolated monocyte in the presence of polybrene (8 ug/ml). For combination retroviral infection, cells were sequentially transduced with LXSN-Bmi-1 and then with LXSH-hTERT (29, 30). Stably transduced cells were maintained in the RPMI (10 % FBS contained).

3.7. Induction of differentiation

HL-60 cells were suspended in growth media containing 1.3% DMSO (Sigma., St. Louis, MO, USA), for periods of up to 6 days, whereupon >96% of cells are viable, and >90% of the cells have the appearance of mature granulocytes (31, 32).

3.8. Dihydrorhodamine 123 FACS quantitation of superoxide production

The NADPH oxidase activity was quantified by dihydrorhodamine 123 (DHR 123, Sigma) flow cytometry (FACS) (33, 34). Differentiated granulocytic cells were washed twice and resuspended in 500 μ l HBSS (without Ca²⁺ and Mg²⁺, Sigma) in duplicate: one sample was stimulated with PMA and second sample was unstimulated. All samples were pre-incubated for 5 min in a 37 $^{\circ}$ C culture incubator in the presence or absence of 20 μ M PMA. Afterwards, 7.5 μ l DHR 123(Sigma) was added to each sample and incubated for a further 15 min at 37 $^{\circ}$ C. Samples were then immediately put on ice and analyzed by flow cytometry. Unstimulated cells incubated with DHR 123 served as negative controls. Superoxide production in positive cells was determined by measuring the shift in FL-1 (green light) relative to the corresponding negative control, and the percentage of superoxide-producing cells could be assessed by analyzing single histograms. The relative percentage of functionally corrected cells compared to cells was calculated as the ratio (PMA-stimulated transduced cells)/(PMA-stimulated cells) of the respective geometric mean fluorescence intensities.

3.9. Isolated WBC (white blood cell)

Human WBC were isolated from buffy coats (from healthy donor blood). Buffy coats were diluted 1:1 with sterile PBS, layered onto a Ficoll Plaque PaqueTMPlus (GE Healthcare Bio-Sciences AB, Uppsala, S) cushion at a ratio of 2:3 and centrifuged at 2000 \times g for 30

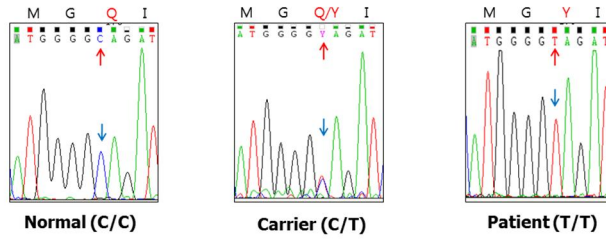
minutes with no braking. White blood cells were harvested from the Ficoll interface, diluted 1:1 with sterile PBS and centrifuged at $1,500 \times g$ for 5 minutes to pellet cells. The pellet was resuspended in PBS and centrifuged at $1,000 \times g$ for 5 minutes. This step was repeated until the supernatant was clear, indicating removal of platelets. After the final wash, the cell pellet was resuspended in RPMI 1640 with 20 % FBS and counted. 1×10^6 cells per ml were added to tissue culture flasks and incubated at 37°C in a humidified atmosphere of 5 % CO_2 . After 1 hour, adherent cells were removed by washing with warm PBS and RPMI 1640 with 20 % FBS.

4. RESULTS

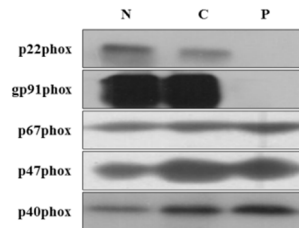
(A)

```

ccctacagat gcgggtctcc gccacgccgc ggtaacctgg ggggctgggg gcggggcctg ggcggggcgg
ggttcgccgc ggagcgcagg ggcggcagtg CGCGCCTAGC AGTGTCCAGCCGG GTTC
GTGTCGCC ATGG GGCAGATCGA GTGGGCCATG TGGGCCAACG AACAGGCG
CT GGCGTCCGGC CTGAgtgagt gcactcagg gacggtggag gctgcagcct ggaggggtgtccc
aagaccc cagccggggac ctggggctac ttacagggtg gggaaagttgg gcgccaggcg
  
```



(B)



(C)

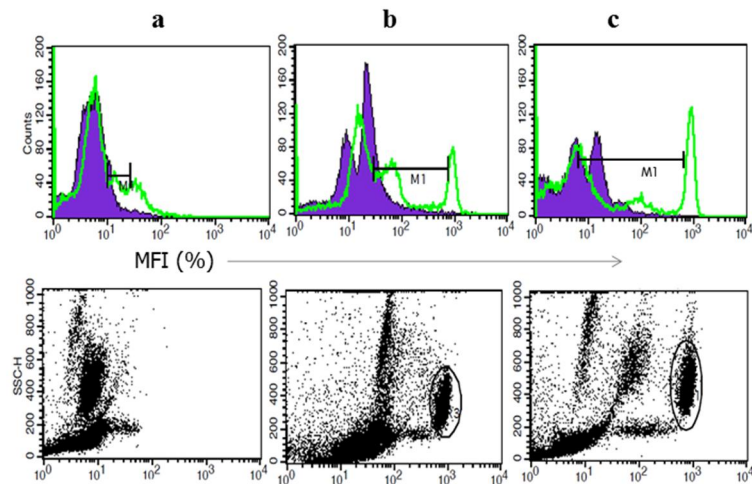


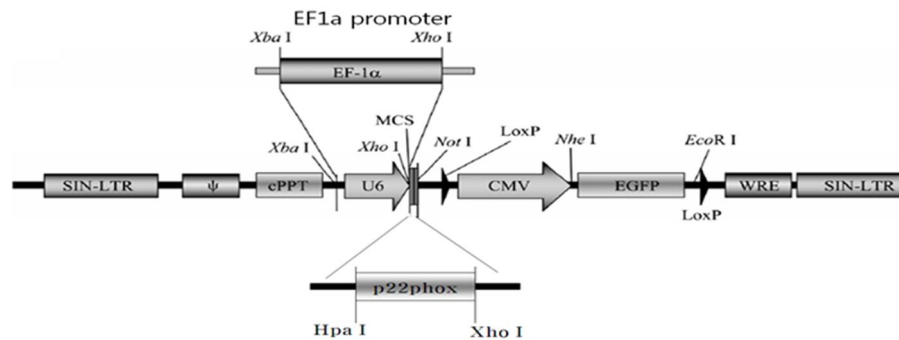
Figure 14. We found that the CGD patients the results of sequence analysis of two patients with p22-phox-deficient CGD.

(A) Uppercase letters Coding sequences (exons 1), lower-case letters intron 1 sequence, hatched boxes exon1 sequence in the p22phox mRNA of the patient, underlined ATG sequence for transcription site responsible for the p22phox mRNA of the patient. The sequence and position of primers used are as described in the methods. (B) The WBC soluble extract from neutrophils of the patient (lane 1), his mother (lane 2) and control neutrophils (lane 3) were subjected to SDS-PAGE and blotted onto a PVDF sheet. Western blot showing p22phoxphox protein, gp91phox and p40phox in the granulocyte fraction of patient (P) compared with a normal control (N) subject. (C) Dihydrorhodamine (DHR) analysis of oxidation in peripheral blood neutrophils. In brief, after red blood cell lysis, neutrophils are loaded with DHR. After DHR loading, cells were stimulated for 15 mins with phorbol myristate acetate (PMA) and immediately analyzed by flow cytometry. DHR is a fluorescent dye taken up by neutrophils. When the neutrophils are stimulated and undergo respiratory burst the dye is oxidised with a shift of fluorescence to the right. Shown are (c) normal with right shift of fluorescence after PMA stimulation; (a) the patient who has virtually absent shift in stimulated neutrophils consistent with AR-linked (autosomal recessive) CGD; (b) the mother of the patient demonstrating dual population of neutrophils in peripheral blood of AR-linked CGD carriers (C).

4.1. Generation of a EF1a lentiviral vector carrying the therapeutic p22phox gene

HIV-1 based p22phox vectors generated in this study was illustrated in Fig. 2. For the generation of lentivirus particles we used the PEI-transfection procedure described in the method. The packaging cell line was derived from 293T cells. The advantages of the 293T host cell are the human origin, good transfectability and good adaptation to growth in suspension and a safe track record in the production of lentiviral vectors. 293T cells were plated at 6×10^6 cells per. The transfer plasmid (pLL3.7 EF1a) represents a further development of the formerly described parental HIV-1-based vector pLL3.7. pLL3.7 EF1a plasmid was replaced by a HpaI - XhoI 590bp p22phox cDNA fragment there by generating the pLL3.7 EF1a-p22phox plasmid (Fig. 15A). In this vector, the therapeutic p22phox gene is exclusively expressed from an internal EF1a promoter. Transcription of the p22phox coding sequence is regulated by the human elongation factor 1 α (EF1 α) gene promoter (29), except that the immediate early promoter of the cytomegalovirus (CMV) regulates expression of which is GFP in here. In target cells, transcription of the p22phox-coding sequence is regulated by the LTR. Lentiviral particles were generated by transient co-transfection of the three plasmids into human embryonic kidney 293T cells. The figure 15B following procedure steps for lentivirus production in 293T packaging cells. pLL3.7EF1a-p22phox lentiviral particles were generated by transient cotransfection of the specific transfer vector plasmid with the 3 packaging plasmids(pMDG2 and pCMV- Δ 8. into HEK 293T cells with PEI (Fig. 15B).

(A)



(B)

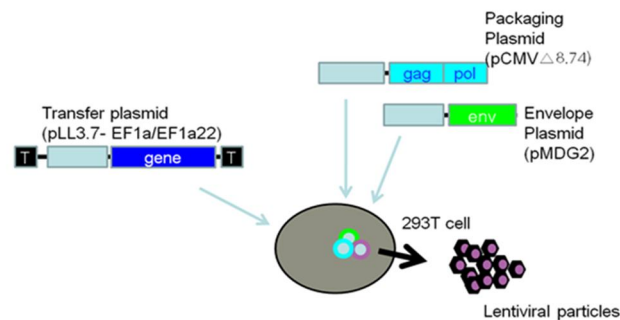


Figure 15. Schematic diagram of lentiviral vector construction and transduction.

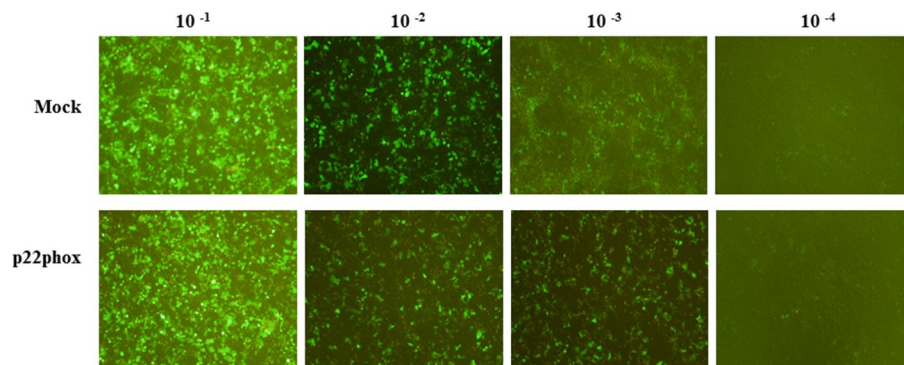
(A) Linear map of the vectors used in this study. The recombinant lentiviral vector was replacing the U6 promoter in pLL37 with elongation-factor-1-alpha (EF1a) promoter, and then human p22phox was inserted in the Hpa I and Xho I to down-stream of the EF1a promoter.

(B) Lentiviral vectors produced by transient cotransfection. Lentiviral vectors were produced by transient cotransfection of HEK293T cells with 3 plasmids (the lentiviral vector, pMD.G2 [envelop plasmid], and pCMV8.91 [packaging plasmid, both produced by Plasmid Factory, Bielefeld, Germany]), employing polyethylenimine (PEI; Sigma-Aldrich) as previously described.

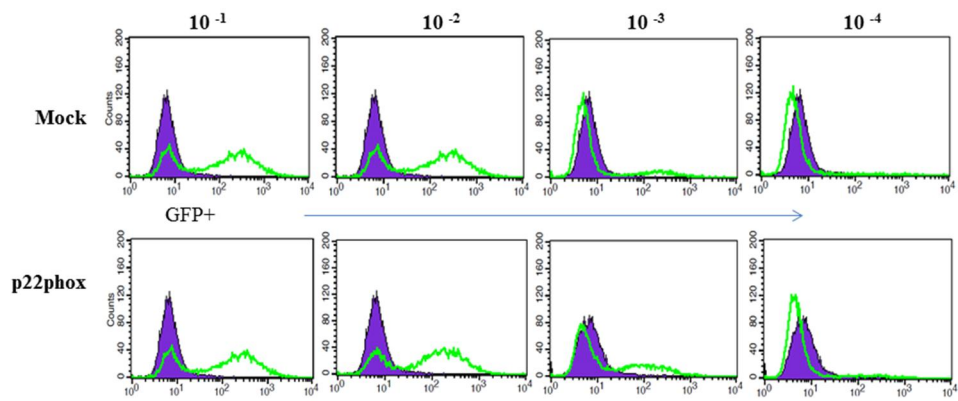
4.2. Transduction of p22phox to cells by pLL3.7 EF1a

The pLL3.7 EF1a can drive reproducible, stable, and long-term eGFP transgene expression in cell lines in the absence of drug-selective pressure. We therefore assessed the efficiency and efficacy of the expression in HeLa and HEK 293T cells. Efficiency of viral vector were determined by transducing HeLa and HEK293T cells. The initial transduction efficiency was assessed by then serial 10 fold dilutions of virus and monitoring eGFP gene expression after 3 days by FACS analysis (Fig. 16). As a control for transduction efficiency we used a lentiviral vector expressing green fluorescent protein (eGFP). On day 3, all the transduction with different dilution lentiviral vector showed eGFP-positive cells by microscopic examination (Fig. 16A). In addition flow cytometric analysis carried out on day 3 showed a peak shift in histograms corresponding to the presence of eGFP-positive cells for all transduced cultures compared with non-transduced control cells (Fig. 16B). These findings correlated with the qualitative results found by direct visualization of the cells with the fluorescence microscope. These results show that 10^{-1} dilution transductions in HeLa cells were highly efficient with values between 70 % and 96 % of cells showing eGFP fluorescence (Fig. 16C).

(A)



(B)



(C)

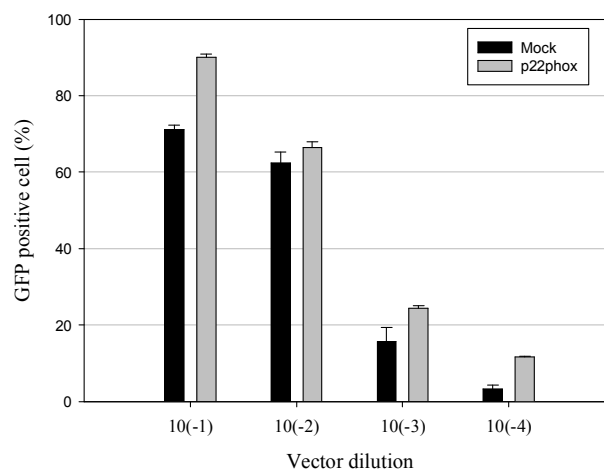


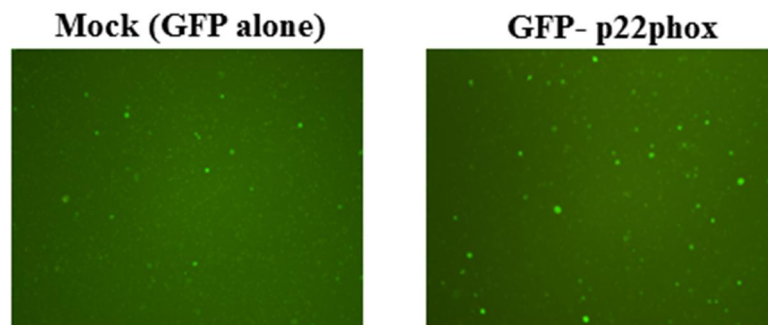
Figure 16. Transducing efficiency in HeLa cells.

(A) An expression plasmid for eGFP was added to verify transduction efficiency and expression was visualized by fluorescence microscopy. 10^{-1} (MOI=10). (B) Relative cell infection by lentiviral vectors preparations transducing eGFP were used to infected cells by flowcytometry. Percentages of eGFP positive cells. (C) The graph indicate percentage of infections assayed by flow cytometry.. The results are means \pm SD of three independent experiments.

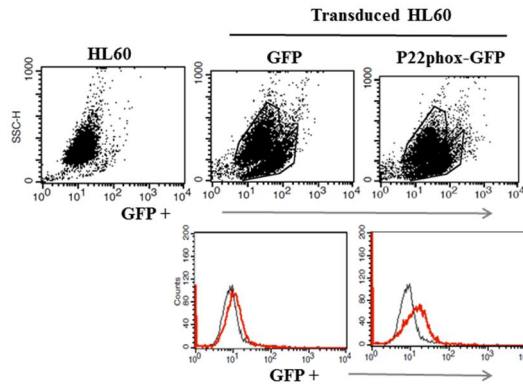
4.3. Transduction of promyelocytic HL-60 by spin and polybrene infection

To increase efficiency of infection in suspension cells. We modified simultaneous seeding and infection followed by spin method. The spin infection method and conditions used were modified in the present study (35). Six days post-transduction, cells were analyzed by flow cytometry (Fig. 17A). In all transduced cultures a peak shift corresponding to the presence of eGFP-positive cells was found (Fig. 17B). Taken together, these results in levels of gene transfer of 20~30% eGFP-positive cells detected 6 days post-transduction and indicate that the pLL3.7 EF1a vector allows for efficient gene transduction into HL 60 cells using spin infection method presence of polybrene (Fig. 17B).

(A)



(B)



(C)

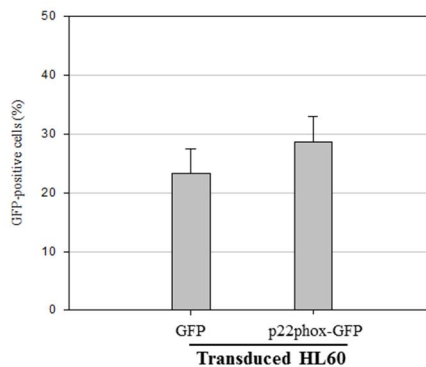


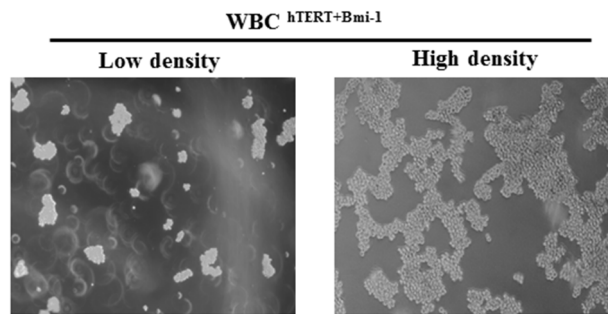
Figure 17. Transduction efficiency of pLL3.7 EF1a and pLL3.7 EF1a p22phox lentiviral vector in promyelocytic HL60 cells. HL 60 cells were transduced by spin-infection in the presence of 8 ug/ml polybrene with eGFP lentiviral vectors. (A) Cells were analyzed for eGFP (green fluorescence) using a fluorescence microscope. (B) Representative flow cytometric analysis of lentiviral vector-mediated transduction of HL 60. (C) represent relative transduction efficiencies using HL 60 transduced 6 days after plating. Quantitative analysis of HL 60 transduction using eGFP-positive cells. The graphs shown The results represent a mean \pm SD of three experiments.

4.4. hTERT/Bmi-1 infected CGD carrier derived WBC cells

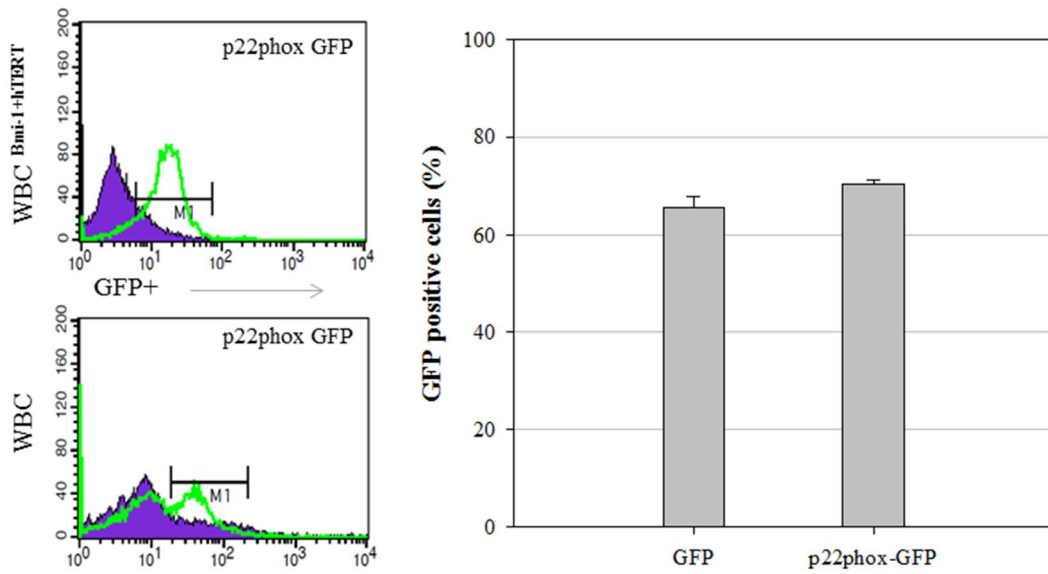
Human primary cells are easy to isolate but difficult to study because of their limited life span. We attempted to extend the life span of WBC, first by using a retrovirus expressing Bmi-1 and hTERT. WBC cells were obtained from buffy coats from CGD carrier donors. Mononuclear cells and granulocytes were isolated by Ficoll paque method. Freshly isolated WBC were prepared for infection with recombinant retroviruses carrying the Bmi-1 and hTERT genes, and then transduced by spin method presence of polybrene. The cells transduced with Bmi-1 and hTERT escaped replication crisis and proliferated continuously. During the following culture, proliferation rate accelerated and the cells became bigger (Fig. 18A). Also, CGD carrier WBC and immortalized (by Bmi-1/ hTERT) WBC were transduced by EF1a and EF1a-p22phox lentiviral vector. Six days after transduction transduction efficiency were compared with FACS (Fig. 18B). Transduction efficiencies of high level WBC $Bmi-1+hTERT$ was >40 % higher than non-immortalized WBC (Fig. 18B). Next, decide to measure the duration of expression of time course. The eGFP expression was detectable at day 3 after transductions (Fig. 18B). The eGFP expression continued for up to 3 weeks and the expression were search to peak at day 16 (Fig. 18B). Since GFP is the indicator for transfection, we tested the augmentation of superoxide production by EF1a-p22phox22 infection. EF1a-p22phox transduced WBC $hTERT+Bmi-1$ at day 6 were analyzed by DHR 123 assay after PMA stimulation. As shown in Figure 18C, CGD carrier derived WBC $hTERT+Bmi-1$ showed a significant difference between PMA stimulated and unstimulated samples; cells showed a

significant shift in fluorescence peak upon stimulation. Upon PMA stimulator number of DHR positive cells increase up to 2-fold (Fig. 18D).

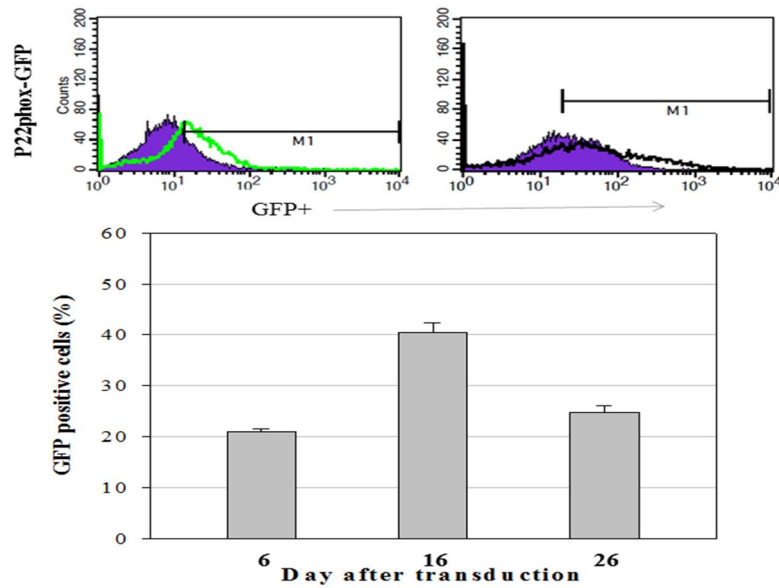
(A)



(B)



(C)



(D)

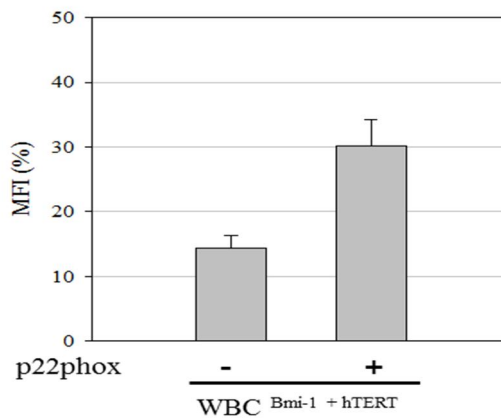


Figure 18. Comparison of transgene expression in WBC (white blood cell) and WBC $hTERT+Bmi-1$ cells. The transduction efficiency of each reaction was determined using fluorescence microscopy or FACS analysis and is typically carried out six days after transduction.

(A) Phase-contrast photographs of the CGD carrier derived WBC $hTERT+Bmi-1$ low density and

high density. **(B)** pLL3.7 EF1a or pLL3.7 EF1a p22phox lentiviral vector in WBC and WBC^{hTERT+Bmi-1}. The WBC are shown compared with transduction efficiency analyzed of flow cytometry. The WBC were transduced using the spin infection method in the presence of polybrene, in combination with the hTERT-Bmi 1 virus. The FACS histogram of the transduced WBC and hTERT-Bmi 1 virus infected WBC. **(C)** EGFP expression was regularly determined by FACS until 26 days after transduction. All the experiments were repeated three times and average values are shown. **(D)** Dihydrorhodamine (DHR) analysis of oxidation in pLL3.7 EF1a p22phox lentiviral vector transduced WBC^{hTERT+Bmi-1} cells. After DHR loading, cells were stimulated for 15 mins with phorbol myristate acetate (PMA) and immediately analyzed by flow cytometry. The results are means \pm SD.

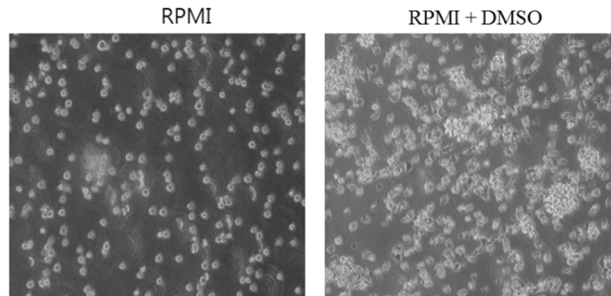
4.5. Analysis of superoxide generation before and after differentiation HL 60 with a pLL3.7 EF1a and pLL3.7 EF1a –p22phox

In a previous studies report on dHL 60 cells, whose differentiation is generally associated with the acquisition of NADPH oxidase, demonstrated much higher levels than ndHL 60 cells, in which small amounts of mRNA transcripts for the gp91phox and p47phox component. NADPH oxidase activation of p22pbhox require the interaction of the p47phox SH3 domains and with the partner of gp91phox (34).

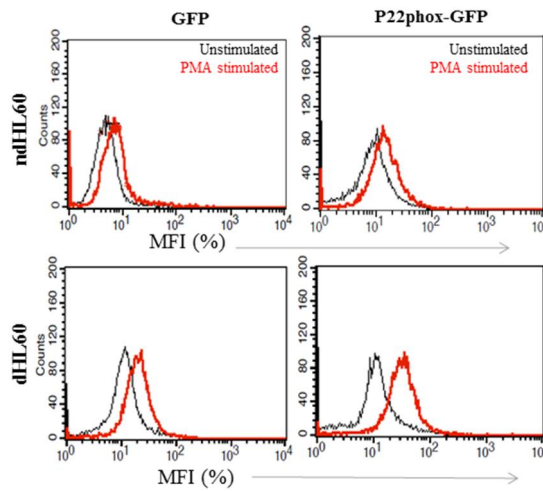
We wanted to determine changes in superoxide release level profiles of these granulocyte like cells. HL60 cells were transduced by spin infection (in presence polybrene) with the GFP- expressing vector pLL37 EF1a and were subsequently differentiated for 6 – 7 days in RPMI supplemented with 1.3 % DMSO. As expected, the exposure to DMSO induced differentiation from cells in suspension into attached cultures forming clumps and adherent (Fig. 19A). Also, the expression persisted in differentiating cells at high levels of about 40 ~ 50 % at least for the observation period of 3 weeks. Taken together, these results indicate that the pLL3.7 EF1a vector allows for efficient gene transfer into ndHL60 and dHL 60 cells using spin infection method, and the EF1a promoter is functional in ndHL60 and dHL60 cells (Fig. 19B). As for the eGFP reporter gene, GFP positive cells were compared to achieve the possible transduction efficiency of ndHL 60 and dHL 60 cells. This cells were transduced by spin method (in presence polybrene) using unconcentrated lentiviral supernatant. Fig. 19C demonstrates PMA-triggered superoxide release of ndHL 60 cells in comparison to dHL 60

cells at a 6 days after transduction. Mean Fluorescence intensity (MFI) of p22phox transduced differentiated HL 60 increased about 10 % than when it was stimulate by PMA (Fig. 19C).

(A)



(B)



(C)

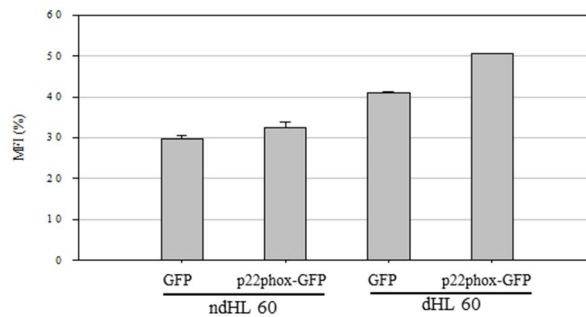


Figure 19. Analysis of superoxide generation before and after differentiation HL 60 with a pLL3.7 EF1a and pLL3.7 EF1a -p22phox. (A) Morphology of ndHL60 and dHL60 cells. Morphological Changes in HL-60 cells induced by DMSO. (B) NADPH oxidase activity measured by intracellular superoxide production in ndHL60 and dHL60 cells in response to 20uM PMA. (C) Average MFI (%) of ndHL 60 and dHL 60 in response to 20 uM PMA. All the experiments were repeated three times and average values are shown. The results are means \pm SD.

5. DISCUSSION

Lentiviral technology represents a powerful method to genetically modify. We chose to use a viral expression backbone driven by the pLL3.7 lentiviral vector (Fig.14A). Lentiviruses have been developed for gene transfer, particularly for applications in gene therapy. These vector systems have also been used of gene function. The popularity of these vectors is in part due to the simplicity of design, ease of production, and efficiency of delivery to various cell types (36-39).

In this study, we choose pLL3.7 (HIV-1) based vector to transduce p22phox gene. pLL3.7 vector is attenuated, self-inactivating (SIN) lentivectors based in human deficiency virus-1 (HIV-1) contained the enhanced green fluorescent protein (eGFP) gene under the transcriptional control of the cytomegalovirus (CMV) immediate-early enhancer/promoter and elongation factor 1- α (EF1 α) promoter for target gene (40) (Fig. 16). The U6 promoter in pLL3.7 (HLV-1 based) replaced by elongation-factor-1-alpha (EF1a) promoter. Activity of the EF1 α promoter was also shown to be high in primary human T lymphocytes isolated from adult peripheral blood. Using the CD34+ hematopoietic precursor cell line KG1a (41), Ramezani and colleagues found that the greatest levels of expression were directed by the EF1 α promoters. The study results showed that HIV-1-derived pLL3.7 EF1a vectors efficiently transduced HeLa cell lines, reaching up to 90% of cells expressing the transgene. . When lentiviral vectors were added at MOI of 10, the percentage of eGFP expressing cells were >90% (Fig. 15A). With regard to transgene expression in general, it has been proposed

that lentiviral vectors, because of their biological property to induce life-long infections, may be less prone to transgene silencing (26). So, lentivirus vectors may have further advantages over other viral vectors in addition to their likely benefit for transduction of more primitive nondividing HSC.

After 6 days incubation with DMSO, 90% of the HL-60 cells became adherent macrophages (fig. 19A). The data in Fig. 6B show that results of DHR 123 assays from oxidation of transduced cells was increased further by 10% upon stimulation of attached cultures with DMSO for 6 days. This result suggests that differentiated macrophagy-like cells have been found to be more permissive than undifferentiated cells for the replication of viruses. Granulocytic differentiation of the HL60 myelocytic cell line provides a useful in vitro model transduced cells efficiency detection and superoxide generation. Because, previous studies report on dHL 60 cells, whose differentiation is generally associated with the acquisition of NADPH oxidase, demonstrated much higher levels than ndHL 60 cells, in which small amounts of mRNA transcripts for the gp91phox and p47phox component. NADPH oxidase activation of p22phox requires the interaction of the p47phox SH3 domains and with the partner of gp91phox (34).

Recent reports have revealed that bmi-1 and hTERT have immortalized BDFCs (bovine dental follicle cells) without affecting their differentiation potential and help to successfully establish a cementoblast progenitor cell line from the immortalized cells (30). To overcome this problem, we attempted to prolong the life span of primary cells and CGD carrier derived WBC immortalized with hTERT and Bmi-1. hTERT and Bmi-1 retrovirus were first used to

transduce granulocyte cells. CGD carrier derived WBC and WBC^{bmi-1+hTERT} cells transduction by pLL3.7EF1a lentiviral vector (Fig. 18). Compared of transduction efficiency higher eGFP expression WBC^{bmi-1+hTERT} than WBC. Furthermore, the eGFP was expressed by more than 60% of the WBC^{bmi-1+hTERT} cells as measured by flow cytometry and WBC^{bmi-1+hTERT} cells were increase in superoxide production by PMA stimulated. These results show that the eGFP expression at high levels over close to 4 weeks in transduced immortalized CGD carrier drved cells and persistent of EF1a driven p22phox expression level up to at least 4 weeks after transduction. We found that the lentiviral transduction high efficiency achieved on the immortalized cell lines. However, the results of the present study establish that lentivirus vectors can be used to superoxide up regulation in CGD carrier derived WBC cells after immortalized indicate that therapeutically sufficient reconstitution of NADPH oxidase activity may be feasible.

This study describes the lentiviral-mediated transduction of CGD carrier driven WBCs in an experimental setting designed to increase gene transfer efficiency and compatibility with clinical constraints. Our results indicate that highly efficient transduction can be achieved nonconcentrated eGFP expressing lentiviral vector stocks following modifications of previously described techniques. Lentiviral vectors efficiently deliver and express eGFP genes for extended periods of 30days.

Indeed, silencing of p22phox transgene expression in the CGD cell line has been reported after gene transfer using a recombinant pLL3.7EF1a lentiviral vector. Studies have therefore been initiated to replace the EF1a promoter by physiologic myeloid-specific regulatory

elements. Further studies *in vitro* and in animal models will be needed to develop and test the best tailored lentiviral vector for CGD gene therapy and a potential system for p22phox gene. Although gene therapy has not yet cured patients with CGD, the field has made significant progress with the demonstration that gene therapy can provide clinical benefit to patients.

V. REFERENCES

Part I.

1. Wientjes FB, Reeves EP, Soskic V, Furthmayr H & Segal AW (2001) The NADPH oxidase components p47phox and p40phox bind to moesin through their PX domain. *Biochem Biophys Res Commun* 289: 382-388.
2. Matute JD, *et al* (2009) A new genetic subgroup of chronic granulomatous disease with autosomal recessive mutations in p40phox and selective defects in neutrophil NADPH oxidase activity. *Blood* 114: 3309-3315.
3. Ellson CD, *et al* (2001) PtdIns (3) P regulates the neutrophil oxidase complex by binding to the PX domain of p40^{phox}. *Nat Cell Biol* 3: 679-682.
4. Ellson CD, *et al* (2006) Neutrophils from p40phox^{-/-} mice exhibit severe defects in NADPH oxidase regulation and oxidant-dependent bacterial killing. *J Exp Med* 203: 1927.
5. Anderson KE, *et al* (2008) CD18-dependent activation of the neutrophil NADPH oxidase during phagocytosis of escherichia coli or staphylococcus aureus is regulated by class III but not class I or II PI3Ks. *Blood* 112: 5202-5211.
6. Tian W, *et al* (2008) FcγR-stimulated activation of the NADPH oxidase: Phosphoinositide-binding protein p40phox regulates NADPH oxidase activity after enzyme assembly on the phagosome. *Blood* 112: 3867-3877.
7. Zhan S, *et al* (1996) Genomic structure, chromosomal localization, start of transcription, and tissue expression of the human p40-phox, a new component of the nicotinamide adenine dinucleotide phosphate-oxidase complex. *Blood* 88: 2714-2721.
8. Moreno-Bueno G, *et al* (2006) Genetic profiling of epithelial cells expressing E-cadherin repressors reveals a distinct role for snail, slug, and E47 factors in epithelial-mesenchymal transition. *Cancer Res* 66: 9543.

9. Wientjes FB, Hsuan JJ, Totty NF & Segal AW (1993) p40phox, a third cytosolic component of the activation complex of the NADPH oxidase to contain src homology 3 domains. *Biochem J* 296 (Pt 3): 557-561.
10. Tsunawaki S & Yoshikawa K (2000) Relationships of p40phox with p67phox in the activation and expression of the human respiratory burst NADPH oxidase. *J Biochem* 128: 777.
11. Hua J, *et al* (2001) Evaluation of the expression of NADPH oxidase components during maturation of HL-60 clone 15 cells to eosinophilic lineage. *Inflammation Res* 50: 156-167.
12. Hasebe T, Someya A & Nagaoka I (1999) Identification of a splice variant mRNA of p40phox, an NADPH oxidase component of phagocytes1. *FEBS Lett* 455: 257-261.
13. Hasebe T, *et al* (2001) Involvement of cytosolic prolyl endopeptidase in degradation of p40-phox splice variant protein in myeloid cells. *J Leukoc Biol* 69: 963-968.
14. Grille SJ, *et al* (2003) The protein kinase akt induces epithelial mesenchymal transition and promotes enhanced motility and invasiveness of squamous cell carcinoma lines. *Cancer Res* 63: 2172.
15. Trachootham D, Alexandre J & Huang P (2009) Targeting cancer cells by ROS-mediated mechanisms: A radical therapeutic approach?. *Nature Reviews Drug Discovery* 8: 579-591.
16. Wang J & Yi J (2008) Cancer cell killing via ROS. *Cancer Biology & Therapy* 7: 1875-1884.
17. Ushio-Fukai M & Nakamura Y (2008) Reactive oxygen species and angiogenesis: NADPH oxidase as target for cancer therapy. *Cancer Lett* 266: 37-52.
18. Yang J & Liu Y (2001) Dissection of key events in tubular epithelial to myofibroblast transition and its implications in renal interstitial fibrosis. *The American Journal of Pathology* 159: 1465.
19. Frey RS, Ushio-Fukai M & Malik AB (2009) NADPH oxidase-dependent signaling in endothelial cells: Role in physiology and pathophysiology. *Antioxidants & Redox Signaling* 11: 791-810.

20. Zhang H, *et al* (1999) Angiotensin II-induced superoxide anion generation in human vascular endothelial cells. *Cardiovasc Res* 44: 215.
21. Radisky DC, *et al* (2005) Rac1b and reactive oxygen species mediate MMP-3-induced EMT and genomic instability. *Nature* 436: 123-127.
22. Sundaresan M, Yu ZX, Ferrans VJ, Irani K & Finkel T (1995) Requirement for generation of H₂O₂ for platelet-derived growth factor signal transduction. *Science* 270: 296.
23. Ambrosone CB (2000) Oxidants and antioxidants in breast cancer. *Antioxidants & Redox Signaling* 2: 903-917.
24. Andoh T, Chock PB & Chiueh CC (2002) The roles of thioredoxin in protection against oxidative stress-induced apoptosis in SH-SY5Y cells. *J Biol Chem* 277: 9655.
25. Nkabyo YS, Ziegler TR, Gu LH, Watson WH & Jones DP (2002) Glutathione and thioredoxin redox during differentiation in human colon epithelial (caco-2) cells. *American Journal of Physiology-Gastrointestinal and Liver Physiology* 283: G1352-G1359.
26. Stamenkovic I (2000) Matrix metalloproteinases in tumor invasion and metastasis 10: 415-433.
27. Okazaki I, *et al* (1997) Difference in gene expression for matrix metalloproteinase-1 between early and advanced hepatocellular carcinomas. *Hepatology* 25: 580-584.
28. Yamamoto H, *et al* (1997) Relation of enhanced secretion of active matrix metalloproteinases with tumor spread in human hepatocellular carcinoma. *Gastroenterology* 112: 1290-1296.
29. Harada T, *et al* (1998) Membrane-type matrix metalloproteinase-1 (MT1-MMP) gene is overexpressed in highly invasive hepatocellular carcinomas. *J Hepatol* 28: 231-239.
30. Storz P (2005) Reactive oxygen species in tumor progression. *Front Biosci* 10: 1881-1896.
31. Batlle E, *et al* (2000) The transcription factor snail is a repressor of E-cadherin gene expression in epithelial tumour cells. *Nat Cell Biol* 2: 84-89.

32. Guaita S, *et al* (2002) Snail induction of epithelial to mesenchymal transition in tumor cells is accompanied by MUC1 repression and ZEB1 expression. *J Biol Chem* 277: 39209-39216.
33. Bolós V, *et al* (2003) The transcription factor slug represses E-cadherin expression and induces epithelial to mesenchymal transitions: A comparison with snail and E47 repressors. *J Cell Sci* 116: 499-511.
34. Matsumoto K, Abiko S & Ariga H (2005) Transcription regulatory complex including YB-1 controls expression of mouse matrix metalloproteinase-2 gene in NIH3T3 cells. *Biol Pharm Bull* 28: 1500-1504.
35. Evdokimova V, *et al* (2009) Translational activation of snail1 and other developmentally regulated transcription factors by YB-1 promotes an epithelial-mesenchymal transition. *Cancer Cell* 15: 402-415.
36. Miettinen PJ, Ebner R, Lopez AR & Derynck R (1994) TGF- β induced transdifferentiation of mammary epithelial cells to mesenchymal cells: Involvement of type I receptors. *J Cell Biol* 2021-2036.
37. Chen XF, *et al* (2011) Transforming growth factor- β 1 induces epithelial-to-mesenchymal transition in human lung cancer cells via PI3K/Akt and MEK/Erk1/2 signaling pathways. *Mol Biol Rep* 1-8.
38. Hensley K, Robinson KA, Gabbita SP, Salsman S & Floyd RA (2000) Reactive oxygen species, cell signaling, and cell injury. *Free Radical Biology and Medicine* 28: 1456-1462.
39. Wang Y & Lou MF (2009) The regulation of NADPH oxidase and its association with cell proliferation in human lens epithelial cells. *Invest Ophthalmol Vis Sci* 50: 2291.
40. Sidhu SS, *et al* (2010) Roles of epithelial cell-derived periostin in TGF- β activation, collagen production, and collagen gel elasticity in asthma. *Proceedings of the National Academy of Sciences* 107: 14170-14175.
41. Buckley ST, Medina C & Ehrhardt C (2010) Differential susceptibility to epithelial-mesenchymal transition (EMT) of alveolar, bronchial and intestinal epithelial cells in vitro and the effect of angiotensin II receptor inhibition. *Cell Tissue Res* 1-13.

42. Sturrock A, *et al* (2006) Transforming growth factor- β 1 induces Nox4 NAD (P) H oxidase and reactive oxygen species-dependent proliferation in human pulmonary artery smooth muscle cells. *American Journal of Physiology-Lung Cellular and Molecular Physiology* 290: L661-L673.
43. Hecker L, *et al* (2009) NADPH oxidase-4 mediates myofibroblast activation and fibrogenic responses to lung injury. *Nat Med* 15: 1077-1081.
44. Seger RA (2011) Advances in the diagnosis and treatment of chronic granulomatous disease. *Curr Opin Hematol* 18: 36.
45. QIAO B & GAO J (2010) Epithelial-mesenchymal transition in oral squamous cell carcinoma triggered by transforming growth factor- β 1 is Snail family-dependent and correlates with matrix metalloproteinase-2 and -9 expressions. *Int J Oncol* 37(3):663-668.
46. McGuire JK, Li Q & Parks WC (2003) Matrilysin (matrix metalloproteinase-7) mediates E-cadherin ectodomain shedding in injured lung epithelium. *The American Journal of Pathology* 162: 1831.
47. SUME S, KANTARCI A, HASTURK H & TRACKMAN P (2010) Epithelial to mesenchymal transition in Gingival Overgrowth. *Matrix Pathobiology* 177(1):208-218.
48. Nannuru KC, *et al* (2010) Matrix metalloproteinase (MMP)-13 regulates mammary Tumor-Induced osteolysis by activating MMP9 and transforming growth factor- β signaling at the tumor-bone interface. *Cancer Res* 70: 3494.
49. Radisky DC, *et al* (2005) Rac1b and reactive oxygen species mediate MMP-3-induced EMT and genomic instability. *Nature* 436: 123-127.
50. Hugo H, *et al* (2007) Epithelial—mesenchymal and mesenchymal—epithelial transitions in carcinoma progression. *J Cell Physiol* 213: 374-383.
51. Kalluri R & Weinberg RA (2009) The basics of epithelial-mesenchymal transition. *J Clin Invest* 119: 1420.
52. Roadcap DW, Clemen CS & Bear JE (2008) The role of mammalian coronins in development and disease. *The Coronin Family of Proteins* 124-135.

53. Dickinson BC & Chang CJ (2011) Chemistry and biology of reactive oxygen species in signaling or stress responses. *Nature Chemical Biology* 7: 504-511.
54. Ueyama T, *et al* (2007) A regulated adaptor function of p40phox: Distinct p67phox membrane targeting by p40phox and by p47phox. *Mol Biol Cell* 18: 441-454.
55. Ueyama T, *et al* (2007) A regulated adaptor function of p40phox: Distinct p67phox membrane targeting by p40phox and by p47phox. *Mol Biol Cell* 18: 441-454.

Part II.

1. Roos D, Kuijpers TW, Curnutte JT. Chronic granulomatous disease. In: Ochs HD, Smith CI, Puck JM, eds, *Primary Immunodeficiency Diseases, a Molecular and Genetic Approach*. New York: Oxford University Press 2007; 525-49.
2. Segal BH, Leto TL, Gallin JI, Malech HL, Holland SM. Genetic, biochemical and clinical features of chronic granulomatous disease. *Medicine (Baltimore)* 2000; 79: 170-200.
3. Lapouge K, Smith SJ, Groemping Y, Rittinger K. Architecture of the p40-p47-p67phox complex in the resting state of the NADPH oxidase, a central role for p67phox. *J Biol Chem* 2002; 277: 10121-8.
4. Heyworth PG, Cross AR, Curnutte JT. Chronic granulomatous disease. *Curr Opin Immunol* 2003; 15: 578-84.
5. Robinson JM, Ohira T, Badwey JA. Regulation of the NADPH-oxidase complex of phagocytic leukocytes. Recent insights from structural biology, molecular genetics, and microscopy. *Histochem Cell Biol* 2004; 122: 293-304.
6. Winkelstein JA, Marino MC, Johnston RB Jr, Boyle J, Curnutte J, Gallin JI, Malech HL, Holland SM, Ochs H, Quie P, Buckley RH, Foster CB, Chanock SJ, Dickler H. Chronic granulomatous disease: report on a national registry of 368 patients. *Medicine (Baltimore)* 2000; 79: 155-69.

7. Hasui M. Chronic granulomatous disease in Japan: incidence and natural history. The study group of Phagocyte Disorders of Japan. *Pediatr Int* 1999; 41: 589-93.
8. Ahlin A, De Boer M, Roos D, Lensen J, Smith CL, Sundin U, Rabbani H, Palmblad J, Elinder G. Prevalence, genetics and clinical presentation of chronic granulomatous disease in Sweden. *Acta Paediatr* 1995; 84: 1386-94.
9. Martire B, Rondelli R, Soresina A, Pignata C, Broccoletti T, Finocchi A, Rossi P, Gattorno M, Rabusin M, Azzari C, Dellepiane RM, Pietrogrande MC, Trizzino A, Di Bartolomeo P, Martino S, Carpinom L, Cossun F, Locatelli F, Maccario R, Pierani P, Putti MC, Stabile A, Notarangelo LD, Ugazio AG, Plebani A, De Mattia D, IPINET. Clinical features, long-term follow-up and outcome of a large cohort of patients with Chronic Granulomatous Disease: an Italian multicenter study. *Clin Immunol* 2008; 126: 155-64.
10. Wolach B, Gavrieli R, de Boer M, Gottesman G, Ben-Ari J, Rottem M, Schlesinger Y, Grisaru-Soen G, Etzioni A, Roos D. Chronic granulomatous disease in Israel: clinical, functional and molecular studies of 38 patients. *Clin Immunol* 2008; 129: 103-14.
11. El Kares R, Barbouche MR, Elloumi-Zghal H, Bejaoui M, Chemli J, Mellouli F, Tebib N, Abdelmoula MS, Boukthir S, Fitouri Z, M'Rad S, Bouslama K, Touiri H, Abdelhak S, Delagi MK. Genetic and mutational heterogeneity of autosomal recessive chronic granulomatous disease in Tunisia. *J Hum Genet* 2006; 51: 887-95.
12. Vowells SJ, Sekhsaria S, Malech HL, Shalit M, Fleisher TA. Flow cytometric analysis of the granulocyte respiratory burst: a comparison study of fluorescent probes. *J Immunol Methods* 1995; 178: 89-97.
13. Rae J, Noack D, Heyworth PG, Ellis BA, Curnutte JT, Cross AR. Molecular analysis of nine new families with chronic granulomatous disease caused by mutations in CYBA, the gene encoding p22 (phox). *Blood* 2000; 96: 1106-12.
14. Yamada M, Ariga T, Kawamura N, Ohtsu M, Imajoh-Ohmi S, Ohshika E, Tatsuzawa O, Kobayashi K, Sakiyama Y. Genetic studies of three Japanese patients with p22-phox-deficient chronic granulomatous disease: detection of a possible common mutant CYBA allele in Japan and a genotype-phenotype correlation in these patients. *Br J Haematol* 2000;

108: 511-7.

15. Ishibashi F, Nunoi H, Endo F, Matsuda I, Kanegasaki S. Statistical and mutational analysis of chronic granulomatous disease in Japan with special reference to gp91-phox and p22-phox deficiency. *Hum Genet* 2000; 106: 478-81.
16. Teimourian S, Zomorodian E, Badalzadeh M, Pouya A, Kannengiesser C, Mansouri D, Cheraghi T, Parvaneh N. Characterization of six novel mutations in CYBA: the gene causing autosomal recessive chronic granulomatous disease. *Br J Haematol* 2008; 141: 848-51.
17. Yu L, Quinn MT, Cross AR, Dinauer MC. Gp91(phox) is the heme binding subunit of the superoxide-generating NADPH oxidase. *Proc Natl Acad Sci USA* 1998; 95: 7993-8.
18. Kim JG, Shin KS, Park JS. Clinical study on chronic granulomatous disease in Korea. *Korean J Immunol* 1999; 21: 271-83.
19. Lee SY, Choi EY, Go SH, Rhim JW, Lee SD, Kim JG. A case of Xlinked chronic granulomatous disease diagnosed in identical twin. *Infect Chemother* 2007; 39: 332-7.
20. Oh HB, Park JS, Lee W, Yoo SJ, Yang JH, Oh SY. Molecular analysis of X-linked chronic granulomatous disease in five unrelated Korean patients. *J Korean Med Sci* 2004; 19: 218-22.
21. De Boer M, De Klein A, Hossle JP, Seger R, Corbeel L, Weening RS, Roos D. Cytochrome b558-negative, autosomal recessive chronic granulomatous disease: two new mutations in the cytochrome b558 light chain of the NADPH oxidase (p22-phox). *Am J Hum Genet* 1992; 51: 1127-35.

Part III

1. Winkelstein JA, *et al* (2000) Chronic granulomatous disease. report on a national registry of 368 patients. *Medicine (Baltimore)* 79: 155-169.

2. Annette Feigenbaum, Robert Moore, Joe Clarke, Stacy Hewson, David Chitayat, (2004) Canavan disease: Carrier-frequency determination in the ashkenazi jewish population and development of a novel molecular diagnostic assay. *Am J Med Genet A* 124A: 142-147.
3. Jurkowska M, Bernatowska E & Bal J (2004) Genetic and biochemical background of chronic granulomatous disease. *Arch Immunol Ther Exp (Warsz)* 52: 113-120.
4. El Kares R, *et al* (2006) Genetic and mutational heterogeneity of autosomal recessive chronic granulomatous disease in tunisia. *J Hum Genet* 51: 887-895.
5. Rada BK, Geiszt M, Hably C & Ligeti E (2005) Consequences of the electrogenic function of the phagocytic NADPH oxidase. *Philos Trans R Soc Lond B Biol Sci* 360: 2293-2300.
6. Roos D, *et al* (2010) Hematologically important mutations: X-linked chronic granulomatous disease (third update). *Blood Cells, Molecules, and Diseases* 45: 246-265.
7. Roos D, *et al* (2010) Hematologically important mutations: The autosomal recessive forms of chronic granulomatous disease (second update). *Blood Cells, Molecules, and Diseases* 44: 291-299.
8. Kim YM, *et al* (2009) Genetic analysis of 10 unrelated korean families with p22-phox-deficient chronic granulomatous disease: An unusually identical mutation of the CYBA gene on jeju island, korea. *J Korean Med Sci* 24: 1045-1050.
9. Broude NE, Zhang L, Woodward K, Englert D & Cantor CR (2001) Multiplex allele-specific target amplification based on PCR suppression. *Proceedings of the National Academy of Sciences* 98: 206.
10. Storm K, Willocx S, Flothmann K & Van Camp G (1999) Determination of the carrier frequency of the common GJB2 (connexin-26) 35delG mutation in the belgian population using an easy and reliable screening method. *Hum Mutat* 14: 263-266.
11. Yamada M, *et al* (2000) Genetic studies of three japanese patients with p22-phox-deficient chronic granulomatous disease: Detection of a possible common mutant CYBA allele in japan and a genotype-phenotype correlation in these patients. *Br J Haematol* 108: 511-517.

Part IV

1. Curnutte J, Orkin S, Dinauer M. Genetic disorders of phagocyte function. In: Stamoyanopoulos G, editor. The molecular basis of blood diseases. 2nd ed. Philadelphia: WB Saunders; 1994; 493-522.
2. Dinauer M. The phagocyte system and disorders of granulopoiesis and granulocyte function. In: Nathan D, Orkin S, editors. Hematology of infancy and childhood. 5th ed. Philadelphia: WB Saunders; 1998; 889-967.
3. Roos D, de Boer M, Kuribayashi F, Meischl C, Weening R, Segal A, et al. Mutations in the X-linked and autosomal recessive forms of chronic granulomatous disease. *Blood* 1996; 87:1663-81.
4. Babior B. NADPH oxidase: an update. *Blood* 1999;93:1464-76.
5. Yu L, Quinn MT, Cross AR, Dinauer MC. Gp91phox is the heme binding subunit of the superoxidegenerating oxidase. *Proc Natl Acad Sci U S A.* 1998;95:7993-7998.
6. Julie Rae, Deborah Noack, Paul G. Heyworth, Beverly A. Ellis, John T. Curnutte, and Andrew R. Cross. Molecular analysis of 9 new families with chronic granulomatous disease caused by mutations in *CYBA*, the gene encoding p22phox. *BLOOD.* 2000;96(3):1106-1112.
7. Roos, D The genetic basis of chronic granulomatous disease. *Immunol Rev.* 1994; 138: 121–157
8. Segal, BH, Leto, TL, Gallin, JI, Malech, HL and Holland, SM. Genetic, biochemical, and clinical features of chronic granulomatous disease. *Medicine (Baltimore).* 2000: 170–200.
9. Holland, SM . Chronic granulomatous disease. *Clin Rev Allergy Immunol.* 2010; 38:3–10.
10. Andrew R. Cross¹, John T. Curnutte, Paul G. Heyworth. Hematologically important mutations: The autosomal recessive forms of chronic granulomatous disease (second update). *Blood Cells, Molecules, and Diseases.* 2010;44(4): 291-299 .

11. Matute, JD, Arias, AA, Wright, NA, Wrobel, I, Waterhouse, CC, Li, XJ et al. A new genetic subgroup of chronic granulomatous disease with autosomal recessive mutations in p40 phox and selective defects in neutrophil NADPH oxidase activity. *Blood*. 2009; 114: 3309–3315.
12. van den Berg, JM, van Koppen, E, Ahlin, A, Belohradsky, BH, Bernatowska, E, Corbeel, L et al. Chronic granulomatous disease: the European experience. *PLoS ONE* . 2009;4: e5234.
13. Seger, RA, Gungor, T, Belohradsky, BH, Blanche, S, Bordigoni, P, Di Bartolomeo, P et al. Treatment of chronic granulomatous disease with myeloablative conditioning and an unmodified hemopoietic allograft: a survey of the European experience, 1985–2000. *Blood*. 2002; 100: 4344–4350.
14. Mardiney M, Jackson S, Spratt S, Li F, Holland S, Malech H. Enhanced host defense after gene transfer in the murine p47phox-deficient model of chronic granulomatous disease. *Blood* 1997;89:2268-75.
15. Young Mee Kim, Ji Eun Park, Jin Young Kim, Hee Kyung Lim, Jae Kook Nam, Moonjae Cho, and Kyung-Sue Shin. Genetic Analysis of 10 Unrelated Korean Families with p22-phoxdeficient Chronic Granulomatous Disease: An Unusually Identical Mutation of the CYBA Gene on Jeju Island, Korea. *J Korean Med Sci*. 2009; 24: 1045-50.
16. Williams D, Lemischka I, Nathan D, Mulligan R. Introduction of new genetic material into pluripotent stem cells of the mouse. *Nature* 1984;310:476-80.
17. Santilli G, Thornhill SI, Kinnon C, Thrasher AJ. Gene therapy of inherited immunodeficiencies. *Expert Opin Biol Ther*. 2008;8(4):397-407.
18. Cavazzana-Calvo M, Fischer A. Gene therapy for severe combined immunodeficiency: are we there yet? *J Clin Invest*. 2007;117(6):1456-1465.
19. Hacein-Bey-Abina S, von Kalle C, Schmidt M, et al. A serious adverse event after successful gene therapy for X-linked severe combined immunodeficiency. *N Engl J Med*. 2003;348(3):255-256.

20. Ott MG, Schmidt M, Schwarzwaelder K, et al. Correction of X-linked chronic granulomatous disease by gene therapy, augmented by insertional activation of MDS1-EVI1, PRDM16 or SETBP1. *Nat Med.* 2006;12(4):401-409.
21. Naldini L, Verma IM. Lentiviral vectors. *Adv Virus Res.* 2000;55:599-609.
22. VandenDriessche T, Naldini L, Collen D, Chuah MK. Oncoretroviral and lentiviral vector-mediated gene therapy. *Methods Enzymol.* 2002;346:573-589.
23. Roos D, Curnutte JT. Chronic granulomatous disease. In: Ochs OD, Smith CIE, Puck FM, eds. *Primary Immunodeficiency Diseases.* New York, NY: Oxford University Press; 1999.
24. Gao Z, Golob J, Tanavde VM, et al. High levels of transgene expression following transduction of long-term NOD/SCID-repopulating human cells with a modified lentiviral vector. *Stem Cells.* 2001; 19:247-259.
25. Gatlin J, Padgett A, Melkus MW, Kelly PF, Garcia JV. Long-term engraftment of nonobese diabetic/ severe combined immunodeficient mice with human CD34 cells transduced by a self-inactivating human immunodeficiency virus type 1 vector. *Hum Gene Ther.* 2001;12:1079-1089.
26. Guenechea G, Gan OI, Inamitsu T, et al. Transduction of human CD34_ CD38_ bone marrow and cord blood-derived SCID-repopulating cells with third-generation lentiviral vectors. *Mol Ther.* 2000;1:566-573.
27. Sirven A, Ravet E, Charneau P, et al. Enhanced transgene expression in cord blood CD34- derived hematopoietic cells, including developing T cells and NOD/SCID mouse repopulating cells, following transduction with modified trip lentiviral vectors. *Mol Ther.* 2001;3:438-448.
28. Woods NB, Fahlman C, Mikkola H, et al. Lentiviral gene transfer into primary and secondary NOD/SCID repopulating cells. *Blood.* 2000;96: 3725-3733.
29. Okamoto T, Aoyama T, Nakayama T, Nakamata T, Hosaka T, Nishijo K, Nakamura T,

Kiyono T, Toguchida J. Clonal heterogeneity in differentiation potential of immortalized human mesenchymal stem cells. *Biochem Biophys Res Commun.* 2002;295:354–361.

30. Masahiro Saito, Keisuke Handa, Tohru Kiyono, Shintaro Hattori, Takamasa Yokoi, Takanori Tsubakimoto, Hidemitsu Harada, Toshihide Noguchi, Minoru Toyoda, Sadao Sato, and Toshio Teranaka. Immortalization of Cementoblast Progenitor Cells With Bmi-1 and TERT. *JOURNAL OF BONE AND MINERAL RESEARCH* . 2005; 20(1): 50-57.

31. Collins, S. J. The HL-60 promyelocytic leukemia cell line: proliferation, differentiation, and cellular oncogene expression. *Blood.* 1987; 70:1233–1244.

32. Collins, S. J., F. W. Ruscetti, R. E. Gallagher, and R. C. Gallo. Terminal differentiation of human promyelocytic leukemia cells induced by dimethyl sulfoxide and other polar compounds. *Proc. Natl. Acad. Sci. USA*1978. 75:2458–2462.

33. Emmendorfer A, Hecht M, Lohmann-Matthes ML, et al. A fast and easy method to determine the production of reactive oxygen intermediates by human and murine phagocytes using dihydrorhodamine 123. *J Immunol Methods* 1990; 131: 269±275.

34. Olga Teufelhofer, Rosa-Maria Weiss, Wolfram Parzefall, Rolf Schulte-Hermann, Michael Micksche, Walter Berger, and Leonilla Elbling, Promyelocytic HL60 Cells Express NADPH Oxidase and Are Excellent Targets in a Rapid Spectrophotometric Microplate Assay for Extracellular Superoxide. *TOXICOLOGICAL SCIENCES.* 2003; 76, 376–383.

35. Kotani, H., Newton, P.B. III, Zhang, S., Chiang, Y.L., Otto, E., Weaver, L., Blaese, R.M., Anderson, W.F., and McGarrity, G.L. 1994. Improved methods of retroviral vector transduction and production for gene therapy. *Human Gene Ther.* 5:19- 28.

36. Roe T, Reynolds TC, Yu G, et al. Integration of murine leukemia virus DNA depends on mitosis. *EMBO J.* 1993; 12: 2099-2108.

37. Sutton RE, Wu HT, Rigg R, et al. Human immunodeficiency virus type 1 vectors efficiently transduce human hematopoietic stem cells. *J Virol* 1998; 72: 5781±5788.

38. Roos D, Curnutte JT. Chronic granulomatous disease. In *Primary Immunodeficiency*

Diseases, Ochs HD, Smith CIE, Puck JM (eds). Oxford University Press: New York and Oxford, 1999; 353-374.

39. Ho CM, Vowels MR, Lockwood L, et al. Successful bone marrow transplantation in a child with X-linked chronic granulomatous disease. *Bone Marrow Transplant* 1996; 18: 213-215.

40. Kim, D. W., Uetsuki, T., Kaziro, Y., Yamaguchi, N., and Sugano, S. Use of the human elongation factor 1 alpha promoter as a versatile and efficient expression system. *Gene*. 1990; 91: 217 – 223.

41. Miyoshi H, Smith KA, Mosier DE, et al. Transduction of human CD34+ cells that mediate long-term engraftment of NOD/SCID mice by HIV vectors. *Science* 1999; 283: 682-686.

42. Somia, N., and Verma, I. M. Gene therapy: trials and tribulations. *Nat. Rev. Genet.* 2000;1: 91 – 99.

VI. 요약문

1. HeLa cell에서 NADPH oxidase 2는 ROS의 증가에 따른 EMT를 유도한다.

Epithelium-to-mesenchyme transitions (EMTs)는 세포들의 형태 및 behavioral 변화를 유도하며, 이 과정 동안 Epithelial marker인 E-cadherin의 발현감소와 mesenchymal marker인 snail, slug 그리고 vimentin의 발현증가를 가져온다. 본 연구에서는 mammary epithelial cell인 HeLa cell을 이용하여 Hela-p40phox model system을 만들어 ROS에 의한 EMT유도과정에 대해 연구하였다. NOX 2 와 NOX5 mRNA증가는 ROS증가를 유도하였으며, 이에 따른 matrix metalloproteinase (MMPs)의 발현증가와 cell migration이 증가를 유도함을 알 수 있었다. 또한 TGF- β 1은 EMT 유도물질로 알려져 있는데, TGF- β 1처리에 의해 EMT 유도과 함께 NOX2의 발현증가와 ROS 생성이 증가됨을 알 수 있었다. 하지만 cell의 형태학적 변화는 없었다. 이는 ROS가 EMT유도에 필요한 switching역할을 하면서도 EMT과정에서의 세포형태의 변화에 필수조건과는 무관하다는 것을 알 수 있다.

2. p22-phox deficient Chronic Granulomatous Disease에 대한 유전적 분석: 제

주도내의 CGD환자는 p22phox 유전자의 동일한 유전적 돌연변이에 의해 발병하는 것임을 알 수 있었다

Chronic granulomatous disease (CGD)는 세균 및 곰팡이의 반복 감염에 의해 발생하는 드문 유전 질환이다. 이는 NADPH 산화 효소의 결함의 결과로 phagocyte에서 reactive oxygen species가 생성되지 못하여 발생된다. CGD는 일반적으로 1,000,000 중 3-4명이 발병하는데 비해 제주도에서는 20.7명으로 높은 발병율을 보인다. 본 연구에서는 제주도내 거주 CGD환자의 유전자를 분석한 결과 CYBA gene 의 exon 1(c.7C>T) 의 동일한 유전적 변이에 의해 발병함을 알 수 있었다. 이것은 제주 지역의 만성육아종질환의 유전 변이가 동일한 유전적인 계보 (proband)에서 유래하였기 때문이라고 여겨져 이에 본 연구는 제주도내 만성육아종질환 보인자의 실태 파악을 해보았습니다. 만성육아종 보인자 실태파악을 위한 방법으로 간단하면서도 빠른 nested PCR방법을 이용한 시스템을 시행하였습니다. Nested PCR에 의한 보인자 조사에는 서귀포지역을 중심으로 모두 704명의 population을 선정하여 조사하였습니다. 제주도 서귀포시 지역거주 704명을 대상으로 specific primers를 이용한 nested PCR 방법을 이용하여 p22phox 결함 CGD환자에 대한 p22phox heterozygote carrier 를 조사한 결과 9명의 p22phox

heterozygote carrier 를 확인할 수 있었는데 이는 100명중 1.3명의 높은 빈도수를 나타내는 결과로 타 지역에 비해 높은 빈도수를 나타냄을 알 수 있었습니다. 단일 유전자의 결함에 의해 생기는 primary immunodeficiency disease인 만성육아종 질환은 자가 조혈모세포를 이용한 유전자 치료가 큰 대안이 될 수 있습니다. 정상과립구의 5-10%에 해당하는 oxidase활성을 가진 보인자의 경우에도 정상적인 생활을 유지할 수 있는 것을 미루어 볼 때 정상과립구의 3-10%에 해당하는 NADPH oxidase 활성을 회복시키더라도 CGD에 대한 근본적인 치료법이 될 수 있다고 생각합니다. 본 연구에 사용된 렌티바이러스 backbone으로 pLL3.7 기본 construct에서 U6 promoter대신 EF1 α promoter로 대체하였으며, 다음에 p22phox 유전자를 넣어 pLL3.7EF1 α -p22phox를 만들어 본 연구에 사용하였습니다. 또한 *in vitro*에서 primary cell line을 이용한 실험을 위해 hTERT와 bmi-1 promoter를 이용한 immortalization 방법도 정립 할 수 있었습니다. 이는 향후 p22phox-Lentiviral vector와 관련한 CGD 환자 cell line을 이용한 실험에 기초자료로 이용될 수 있으리라 사료됩니다.

감사의 글

흔히들 우리가 느끼는 세월의 속도가 사람의 나이와 비례한다고들 말씀하시던데 제가 30대에 느끼는 세월의 속도는 30의 속도가 아닌 아우토파를 달리는 것처럼 정신 없이 달려온 느낌입니다. 엇그제 대학원에 진학한 것 같은데 벌써 졸업을 하게 되었으니..... 서른 넘은 나이에 대학원 과정에 들어와 많은 분들께 도움을 받아 무사히 4년이라는 과정을 마치고 보니 지난 대학원 생활이 주마등처럼 떠오릅니다. 항상 그렇듯 무언가를 마치고 나면 더욱더 최선을 다하지 못한 것에 대한 아쉬움(?)이 남는 것 같습니다. 작년에 누가 드라마에서 그런 것처럼 “이게 최선입니까?” 라고 자문자답을 하게 됩니다. 하지만 이렇게 작게나마 결실을 맺게 된 것은 저에게 많은 도움을 주신 고마운 분들이 있기에 지면으로나마 감사의 마음을 전하고자 합니다. 참으로 부족한 저에게 한결같이 믿는다는 말씀으로 격려해주시고, 항상 신뢰를 주신 조문제 교수님의 은혜에 진심으로 존경과 감사의 마음을 올립니다. 또한 바쁘신데도 불구하고 부족한 저의 논문을 성의껏 심사해주신 박덕배 교수님, 고영상 교수님, 신경수 교수님 그리고 서울대 이정원 교수님께도 감사 드립니다. 그리고 박사과정 4년동안 항상 관심 가져 주시고, 열과 성으로 지도해주신 현진원 교수님, 유은숙 교수님, 강희경 교수님, 은수용 교수님, 김소미 교수님께도 이 자릴 빌어 감사 드립니다.

또 동생들임에도 불구하고 언제나 변함없이 옆에서 할 수 있다는 응원과 격려를 아끼지 않았던 사랑하는 동생님들 희경, 민경, 은진, 정일, 나영에게도 ‘그동안 나이 많은 언니의 말벗이 되어주느라 고생했고 정말 고마웠다’는 말을 전합니다. 그리고 박사 입학동기이자 졸업동기인 미경 언니, 함께 졸업하느라 많은 도움을 주지 못해 항상 미안하던 창희, 같은 실험실에 있어 항상 열심히 모습을 보면 늘 칭찬해주고 싶은 기천에게도 고마움을 보냅니다.

항상 제 옆에서 든든한 후견인이 되어주는 남편 손봉조씨 그 동안 마누라 졸업시키느라 애쓰셨습니다. 뒤늦게 시작한 공부 때문에 제대로 챙겨주지 못해 미안했던, 보고만 있어도 든든하고 뿌듯한 우리 집 기둥이며 좌청룡 우백호인 범석이와 나연이도 고맙다. 항상 죄송스럽고 감사한 우리 어머니, 큰고모, 큰고모부, 작은고모, 작은고모부 하나뿐인 며느리, 올케가 졸업한다고 참 많이 도와주셔서 감사합니다. 마지막으로 절 낳아주시고 늘 사랑과 조용한 관심으로 내 인생 최고의 후원자가 되어주시는 아버지와 어머니, 힘들 때마다 전화해서 폭풍수다를 떨어주며 동생의 스트레스를 저만큼 떨구어주던 언니 그리고 형부, 말을 멋스럽게 못하지만 간간히 전화해서 안부를 챙기는 나의 사랑하는 동생들 창범, 영옥에게도 고마움을 전합니다. 길의 끝은 언제나 또 다른 길의 시작임을 알기에 대학원에서 보고 배우고 느낀 것들을 디딤돌 삼아, 그리고 제 곁에서 힘이 되어주시는 많은 분들이 계시기에 힘을 얻고 다시 새로운 길로 나아가 보려 합니다. 여러분 사랑합니다. 그리고 모두 감사합니다.

2012년 1월

김 영 미